DRYING GRANULAR SOLIDS IN A PACKED BED USING SOLAR ENERGY -A Transient Heat and Mass Transfer Model Specifically Applied to Computer Simulation of Solar Grain Driers

BY

MARC CARL HANSON

A thesis submitted in partial fulfillment of the requirements for the degree of

MASTER OF SCIENCE - CHEMICAL ENGINEERING

at the

UNIVERSITY OF WISCONSIN - MADISON

1978

ABSTRACT

The most common method used to prepare grain for preservation in this country is drying. Accordingly, grain drying is an energy-intensive agricultural operation likely to be increasingly affected by rising costs and reduced supplies of energy. In this country, corn drying alone consumes well over 10^{13} KJ/year of thermal energy. Since many grain drying operations use fairly low temperature heat, solar energy has potential as a thermal supplement to conventional heat sources in grain drying. If solar collection can be added economically, it will likely make at least a modest contribution to conservation of conventional energy supplies.

This study was concerned with computer modeling techniques for investigation of drying grain with solar energy. An infinite NTU equilibrium drying model was derived from the governing, coupled equations for heat and mass transfer between flowing air and porous media. The model is shown to have some unique qualities in its equilibrium approach. It is especially suited for computerized transient simulations of solar supplemented grain drying using actual weather data to determine inlet conditions. Previous grain drying models tend to be more elaborate and heavily concerned with empirical rate measurements and transfer coefficients. The model which is derived and demonstrated in this thesis functions without the need for extensive characteristic

rate and coefficient data on each batch of grain. It is flexible in its application. It is concluded that the new model, compared to other published models, is simpler to apply, is more efficient with respect to computer time (allowing larger time steps and node sizes; involving fewer equations and variables), and is of apparently adequate accuracy for simulating full scale solar grain drying experiments.

The drying model is compared satisfactorily to limited available data and other theoretical presentations. Computer simulations of solar drying systems with various collector sizes and flowrates are presented for a selected bin design and a selected grain utilizing actual hourly weather data from the Madison, Wisconsin "design-year" weather data tabulation. It is tentatively concluded that solar energy has economic potential as a supplemental energy source for grain drying in some cases if the proper design conditions can be determined in advance of collector installation. It is believed that the model (and computer version thereof) and modeling approach presented in this thesis can serve as useful tools in conducting thorough investigations into the economic potential of solar-assisted grain drying and to develop design guidelines for such systems. Several model options intended to provide investigators with increased versatility (e.g., partial recirculation) are also demonstrated and discussed. A course of further study considering a variety of systems designs, grain types, locations, and climatic

data utilizing computer simulation techniques to ultimately determine design guidelines is discussed and recommended.

ACKNOWLEDGEMENTS

I wish to acknowledge the invaluable guidance and suggestions provided by Professors John A. Duffie and John W. Mitchell. Their assistance and patience is sincerely appreciated. I also wish to express appreciation for assistance provided by Dr. D.J. Close and Professor William A. Beckman. I am grateful for the friendship of many fine people whom I met during my association with the University of Wisconsin's Solar Energy Laboratory. I also wish to thank Professor Thomas W. Chapman for consenting to serve on my thesis review committee (with Professors Duffie and Mitchell) and for the academic counselling he provided in previous years when I was earning my B.S. Degree.

This work was partially funded by grants to the University of Wisconsin's Solar Energy Laboratory from the Energy Research and Development Administration (ERDA).

TABLE OF CONTENTS

LIST OF FIGURES

LIST OF TABLES

1. SUMMARY

1.1 Problem Statement

Grain drying is an energy - intensive operation in the United States and other countries. For corn-drying alone it is estimated that 6×10^{13} KJ of thermal energy were expended within this country in 1976 (Foster and Peart, 1976). Considering our decreasing energy resources, it is desirable to reduce the amount of conventional energy utilized to dry grain. Two ways of reducing conventional energy usage are efficiency improvements and utilization of alternate energy sources such as solar energy. Most of the published work in solar grain drying has related to specific trials with little long term simulation design studies. It was felt that published models could not be efficiently applied to computer simulations of long-term, variable input solar drying. The primary goal of this work was to develop a simple yet versatile model of the grain bin drying process which would accept variable inlet conditions necessary to simulate solar grain drying. The model was to be free of the constraints of many drying models which require four, five or more unknowns (for example; air and grain temperatures, moisture content, equilibrium moisture content, humidity and perhaps film temperature and humidity) and a like number of complex equations along with extensive empirical rate data on each batch of grain. That is, the model was to be

more suited than other published models to conducting numerous long-term simulations without requiring extensive computer times. A secondary goal was to demonstrate the applicability of such a model for computer simulations of grain driers using solar energy as a complete or supplemental thermal source and subject to transient conditions. Furthermore, it was desired to tentatively determine the feasibility of solar drying under a selected set of conditions and parameters employing the model.

1.2 Important Results

The most important result of this study was the development of a drying model. An infinite NTU equilibrium drying model was derived from the governing, coupled equations for heat and mass transfer between flowing air and porous media. The model was found suitable for many applications in computer modeling of solar grain drying where it previously would have been necessary to apply more elaborate models concerned with empirical rate measurements and transfer coefficients. This result makes it possible to conduct extensive computer-simulated experimentation with solar supplemented grain drying under various system configurations, conditions and locations. The simulations may employ actual data with variable inputs, be relatively efficient with computer time compared to other drying models, and function without the need for extensive characteristic rate data on each batch.

Another important result was the demonstration of apparent economical potential for solar energy as a supplemental thermal energy source for grain drying. However, this conclusion (based on simulations) should be considered subject to further investigation since this study considered a fairly limited number of designs and conditions using average hourly weather conditions for October in Madison, Wisconsin. Nevertheless, the result is encouraging and should promote further study.

1.3 Conclusions and Recommendations

It is concluded that the new grain drying model, developed and demonstrated as part of this study, is simpler to apply and more efficient with respect to computer time (i.e., allows larger time steps and node sizes and involves fewer equations and variables) than other published models. It is of apparently adequate accuracy for simulating full scale solar grain drying experiments.

It is recommended that the model (and computer version thereof) developed in the course of this work be employed for further and indepth investigations of the economic potential associated with solar energy as a supplement to conventional energy sources for grain drying.

There is a lack of good long-term experimental data available on grain drying in full size bins with variable inlet conditions. Accordingly, the acquisition of such data for full-scale systems subject to transient conditions and suitable for providing more rigorous verification of this model and other models is suggested.

The specific heats of air and of the moist grain and the latent heat of sorption are all expressed in the model as functions. Possibly one or more of these could be expressed as constant average values. As discussed later in this thesis, replacing these functions with constants might further decrease calculational requirements and therefore computer time. Others using the model may wish to consider whether an efficiency im-

provement could be obtained in this manner without significant loss of accuracy.

The computer simulated experiments undertaken to study solar grain drying potential will likely be the most consequential work to utilize the results of this study. A variety of systems designs, grain types, locations, and climatic data should be considered. Special attention should be given to multi-batch operations (that is, two to three batches per season per bin) or those with off-season uses for low-temperature heat. (These have the best potential for favorable economics at the present.) Attention should also be given to the high temperature, rapid drying operations where two or more batches may be processed each day. (These have very high annual energy requirements on a per-unit basis.) Economic analyses of these various systems, all of which may be readily simulated using the model and techniques of this study, should lead to the development of design guidelines and/or criteria. Such guidelines might include suggested type and size of solar collector as a function of bin size, grain type, location, and other system characteristics. (With some modification of the model, it should be possible to also simulate continuous grain counter-flow driers and cross-flow driers to mention a couple.)

With most drying operations the blower is operated continuously. As will be explained later, it is desirable to maintain some minimum aeration level at all times. Some limited simula-

tion work was conducted to observe the results of reducing air flow to minimum levels whenever there is no thermal gain. It would appear that this method of operation might be more energy efficient under some conditions yet more costly under other conditions. Further consideration of this method of operation by experimental simulation might indicate a guideline in this matter.

Some limited simulation work was also conducted to observe the effects of partial recirculation of air exhausted from the drier. Redirecting a portion of exhaust air into the intake to the collector causes the inlet air to the drier to have a higher average humidity. It also causes the inlet air to the drier to be slightly warmer on the average. These humidity and temperature effects work against each other with respect to moisture removal. It appeared that water removal from the grain in the high moisture ranges (of the grain) is more affected by increased temperatures and that water removal in the low moisture ranges is more affected by the increased humidities. Since this is based on a limited amount of inquiry into this area, additional study would be useful to identify the optimum approach. Since low temperature heat is frequently used in grain drying, partial recirculation does not reduce collector efficiency significantly. Perhaps employing recirculation initially when the grain is quite moist, and eliminating recirculation as the grain enters lower moisture ranges could improve the overall efficiency of solar

grain drying. Additional study by experimental simulation could likely answer this question as well as the others which have been raised.

Design and operational guidelines for solar grain drying, it is hoped, may eventually be developed utilizing the modeling concepts and suggestions advanced in this thesis. If solar grain drying can be made to function economically, as it appears from this study, it will be able to reduce consumption of conventional energy supplies. Computerized design studies seem to be an expedient approach for increasing the implementation of solar grain drying.

2.
BACKGROUND

2.1 Introduction

Some method of preservation is used on much of the grain grown in the United States and elsewhere to prevent the development of conditions conducive to mold and/or insect growth. Methods include airtight storage (all oxygen is quickly converted to carbon dioxide), chilled storage, chemical treatment, and probably the most common: drying or dehydration.

Grain drying is an energy intensive agricultural operation likely to be increasingly affected by the rising costs of energy. Consider an example concerning the United States' highest production grain. Corn drying consumes an estimated (in 1976) 6×10^{13} KJ/year (5.6×10^{13} BTU/year) which is equivalent to 2.4×10^{9} l (6.4×10^{8} gal) of LP gas and represents more than half of the total energy equivalent required when considering all phases of corn production (Foster and Peart, 1976). Over 70% of all corn produced is dried in some manner (Peart and Foster, 1975). Approximately one-fifth of all corn produced is dried with relatively low temperature in storage systems utilizing LP gas or natural gas. Some larger installations use fuel oil. The use of electricity for drying operations at individual farms is increasing (Foster and Peart, 1976).

Solar energy as a heat source in grain drying appears to have the most potential in low temperature, in-storage systems rather than in high temperature, high speed systems. Such application would allow the use of small and rather simple solar collectors (for new or existing facilities) which could be quite efficient due to the low temperature rise required. Solar energy could also be used in high temperature, high speed drying applications either as a supplemental or total energy source or as a preheat source. As an example, a large industrial scale operation in Alabama installed 1219 m^2 (13,104 ft^2) of solar collectors designed to supply 6% of the energy requirements for one of the facility's large driers by preheating 756 m^3/min (27,000 ft^3/min) of air (Guinn, 1977). The total installed capital cost for the single glass cover collector system was \$440.00/m^2 (\$41.90/ft^2) (estimated at \$30.00/ft^2 if they hadn't needed elevated construction above a parking lot) (Guinn, 1977). This installation cost provides some illustration of why the lower temperature, small scale systems with simple collectors may have greater potential for utilization of solar energy. Fabrication and construction will be simpler and the installed cost is likely to be less.

Various estimates for the installed cost of complete systems have been published. Some plastic collector systems may be installed for as little as \$21.50/m^2 (\$2.00/ft^2) for the entire system (Schlag, Ray, Sheppard, and Wood 1976). This latter study

discusses inexpensive, user-fabricated systems. (Convenient transmissivity data for plastic covers are also presented.) By incorporating the wall of the grain bin into the collector design, it was estimated (Schoenau and Besant, 1976) that a flat plate collector constructed by the addition of a bare metal plate which creates an air space between the bin and the plate would cost $\$5.65/m^2$ ($\$0.52/ft^2$). Addition of a clear plastic cover would increase the costs to $\$6.60/m^2$ ($\$0.62/ft^2$) while using only the clear cover and the bin wall would result in costs of $\$2.56/m^2$ ($\$0.24/ft^2$). An inflated plastic collector utilized experimentally at Purdue in 1974 had an installed cost of $\$20.00/m^2$ ($\$1.86/ft^2$) at that time (Peart and Barrett, 1975).

The vulnerability to damage and the expected useful life of the collectors must be considered when making long term economic evaluations. Although the inexpensive inflatable plastic systems may be fairly versatile and easily repaired, it is likely that rigid collectors constructed on bin walls or roofs (or as separate units) will provide more years of service.

To be economically feasible, the capital and operating costs of the collector must be offset by the cost of the energy saved. One article (Foster and Peart, 1976) suggested that for designing new systems that do not already include a conventional heat source, it may be worthwhile to consider a collector design sufficiently large to eliminate the need for auxiliary heat. This would allow the collector system costs to be offset by the

costs of the auxiliary heater as well as the cost of the energy saved.

As a final comment in this section, in most cases where grain drying systems might utilize solar energy, drying is carried out only 10 to 20% of the year. Certainly, whatever the merits of solar heat versus conventional heat for grain drying might be, solar heat could be made more attractive for this application if the collector could be used to supply heat for other uses in the remaining 80 to 90% of the year.

2.2 Full Scale Experimentation with Solar Drying

Based on experimental data from 18 successful solar assisted drying tests (15 of which used corn) at 8 locations in 1974 (some continued in 1975 at 6 locations), Foster and Peart (1976) suggest a collector size of 0.27 to 2.0 m^2/m^3 of bin capacity (0.10 to 0.75 ft^2/bushel) for low temperature drying in-storage and 10.6 to 21.2 m^2/m^3 (4 to 8 ft^2/bushel) for batch-in-bin drying where several batches may be dried in one bin during a harvest season. They state the collector should be expected to provide a maximum temperature rise of 3° to 17°C (5° to 30°F) on a clear day at noon and an average temperature rise of 0.5°to 3.5°C (1° to 6°F) when averaged over day and night for the entire drying run. (It should be noted that they are assuming an additional temperature rise of 1.1°C [2°F] due to the blower. They claim this is reasonable in the normal range of blower rates.) For corn, another researcher (Saulnier, 1976) suggests a collector size of 0.5 m^2/m^3 (0.19 ft^2/bushel), an air flow rate of 2 m^3/min per m^3 of bin capacity (2.5 CFM/bushel) and that the optimal temperature rise should be on the order of 5°to 12°C (9°to 22°F). For wheat, Schoenau and Besant (1976) suggested minimum air flow rates of 0.85 m^3/min per m^3 (1.1 CFM/bu). Minimum air flows for corn are often recommended at 1 to 1.75 times higher than for wheat. For corn, Peart and Barret (1975) utilized a flow rate of 1.8 m^3/min per m^3 (2.2 CFM/bu in successful full scale solar drying experiments. Brooker, Bakker-Arkema and Hall (1974) have

suggested minimum air flows of 1.6 to 4.0 m^3/min per m^3 for corn at moisture contents of 22 to 33% (dry basis) respectively.

Eight solar drying tests at the U. S. Grain Marketing Research Center averaged a usable collection of 2.0 KWh/m^2.day (620 BTU/ft^2.day) with inflated plastic collectors (Foster and Peart 1976). South Dakota tests (Peterson and Hellickson, 1976; Peterson, 1977) utilized collectors installed on bin walls (with a 7.6 cm [3 inch] air space). Several designs, e.g., polyethylene cover, translucent corrugated fiberglass cover, and various types of corrugated metal plates with no covers, were used with reasonable success. It is stated by Peterson that some of the tests required no auxiliary energy inputs. Other successful solar drying tests have been described (Peart and Barret, 1975; Peart and Foster, 1975).

2.3 Power Considerations

The pressure drop and power requirements for forced air flow through grain have been empirically developed (Brooker, Bakker-Arkema and Hall, 1974). They indicate that good experimental agreement is observed for the following equation:

$$\Delta P = aQ^2/(\ln(1 + bQ))$$

where Q is the empty tower mass velocity, ΔP is the pressure drop per unit depth and a and b are grain-specific constants given in the reference. The published constants are used with velocity and pressure drop expressed in units of CFM/ft^2 and inches of water respectively. For a flow rate of 4 m^3/min per m^3 of grain (5 CFM/bu) through a bin of corn 5.5 m (18 ft.) in diameter and 3 m (10 ft.) deep, the above equation (with $a = 6.5 \times 10^4$ and $b = 1.56$ for use with English units predicts a pressure drop through the grain of 1.3 KPa (5.3 inches of water). Other pressure drops in a drier system would include the ducts, the sudden expansion from the duct into the sub-floor plenum, and the perforated floor. An example presented by Brooker, Bakker-Arkema, and Hall (1974) showed these may represent an additional pressure drop on the order of 30 to 40% of the drop through the grain. In a solar energy grain drier, the solar collector will also contribute a pressure drop, likely to be negligible in comparison. The addition of large collectors could result in a significant pressure drop through the extra ducts, however. The addition of

a solar collector would generally be the only difference between conventional and solar driers. Given the size of the relative pressure drops, the addition of a collector is not likely to cause an increase in the power consumption of the blower that would be significant with respect to the overall (thermal plus mechanical) energy requirements of the system unless the additional ducts and headers for the collectors were fairly long or did not allow gradual transition between the collector sub-units and the header.

2.4 Selected Agricultural Considerations

2.4.1 OVERDRYING:

Prevention of over-drying is a major concern with in-storage drying. This can occur near the inlet if excessively warm air is utilized for long periods of time. In addition, it should be noted that the heat sensitivity, i.e., maximum allowable kernel temperature, of various grains depends on the intended use of the grain. Brooker, Bakker-Arkema and Hall (1974) indicate approximate guidelines. For in-storage drying, fairly low temperature and flow rates are used since it is desired for the moisture content of all the grain to dry to some maximum level without seriously overdrying the grain near the inlet.

To reduce overdrying of the inlet portion of the grain, it has been suggested to design bins with some type of recirculation or mixing mechanism (Roberts and Brooker, 1975). For batch-in-bin drying in which higher temperatures and flow rates are often used, damage by overdrying is minimized by keeping the length of drying time shorter. When the average moisture content of the bin reaches the desired level, the grain is removed from the drying bin, mixed, and transported elsewhere for storage. It has been reported that such a practice (mixing high and low moisture content layers when the average is at the desired level) will result in each individual kernel equilibrating to within approximately 1% of the average moisture content (White and Ross, 1972). Apparently, adsorption and desorption hysteresis

prevents attainment of the average for all kernels in a batch.

A technique of alternating heated and ambient air has been suggested by one group of investigators as another way to prevent overdrying and to produce a more uniform drying profile through the bed (Browning, Brooker, George, and Browning, 1971). Another has suggested the introduction of air at several locations to provide more uniform moisture profiles (Schove, 1971). Neither of these last two referenced studies discussed whether there was any significant energy penalty over conventional methods.

2.4.2 MOISTURE MIGRATION:

Significant Moisture Migration may occur in a static bin (i.e., one having no air flow). With no air flowing, radial temperature gradients (due to grain respiration and environmental heating or cooling) may develop. The radial temperature gradients generally result in the circulation of convection currents which transport moisture from warmer to cooler areas. Localized wet spots with high spoilage potential may be the net result. This undesirable occurrence may be minimized or eliminated by maintaining at least some minimal air flow through the bin (Brooker, Bakker-Arkema, and Hall, 1974).

2.5 Physical Considerations

2.5.1 EQUILIBRIUM:

An important concept which must be empirically represented in modeling grain drying (and in other applications as well) is that of the equilibrium moisture content. This is the level of moisture which will be obtained if the grain is exposed to air (of a given temperature and humidity) for a sufficient length of time for all driving forces for heat and mass transfer to be eliminated. One of the most convenient relationships to work with is based on the original work of Henderson (1952)

$$We = \left[\frac{-\ln(1 - RH)}{C(T + B)}\right]^{1/n} \div 100$$

where C, B, and n are grain specific constants, RH is the relative humidity in decimal form, and T is the temperature.

2.5.2 SORPTION HYSTERYSIS:

Equilibrium relationships can be adapted to be specific for conditions of desorption or adsorption since there is some hystersis in the moisture content, W (as a function of temperature and relative humidity) depending on which of the above conditions prevails. The amount of hysterysis decreases with increasing temperature (Dunstan, Chung, and Hodges, 1973). Most modeling efforts have included the assumption, however, that the hysterysis effects can be discounted, and that the same empirical constants can be used during either desorption or adsorption.

The hysteresis phenomenon is also discussed by Brooker, Bakker-Arkema, and Hall (1974). A technique for easily approximating the moisture content profile of the grain bed during drying has been advanced based on tapping off samples of flowing air (Gough, 1976). This technique relies on the availability of suitable equilibrium relations.

2.5.3 GRAIN PROPERTIES:

Many other grain properties are functions of temperature and/or moisture content as well as a function of the specific grain. Generally these must all be represented empirically for modeling work. Correlations for various grain properties (e.g. heat capacity, thermal conductivity, diffusivities, void fraction, and latent heat of sorption) are presented for several grains by Brooker, Bakker-Arkema, and Hall (1974). Although it will not be discussed in any detail, it is important to note that the energy requirements for evaporating water bound in grain are greater than those for evaporating free water. This difference, which is primarily a function of the moisture content of the grain, is the latent heat of sorption.

2.5.4 RESPIRATION:

One factor which is generally not considered in most analyses is grain repiration. This phenomenon results in some loss of dry matter, e.g., as carbohydrates are converted to carbon dioxide and water vapor, and a small thermal gain. It is not likely

to be overly important if care is taken not to exceed safe storage times. For example, corn stored longer than four days at 43% moisture content (dry basis) and 23°C (75°F) may approach dry matter losses of 1%; corn stored at 18% moisture content and 15.5°C (60°F) would not likely approach this level of respiration loss for approximately 260 days (Brooker, Bakker-Arkema and Hall, 1974). For most drying conditions, it is reasonable to neglect this in modeling work.

2.6 Survey of Drier Models

A fairly extensive amount of work in modeling the drying process in grain bins has been conducted. Not surprisingly, most of this work has been with respect to agricultural driers and published in the agricultural engineering literature.

2.6.1 NON-EQUILIBRIUM MODELS:

One of the earliest works (Hukill, 1947) considered the analogy between heat and mass transfer. In his study of deep bed drying of corn, Hukill's approach to heat and mass transfer and his development of an explicit solution was in a manner similar to one of the classic studies of heat transfer in porous media (Schumann, 1929). Hukill developed a solution to largely empirical equations and characterized internal temperature and moisture profiles based on "macro-" (rather than "micro-") mass and energy balances with little attention to the more basic phenomena causing them. The unmodified Hukill model* can sometimes provide suitable design data by using published graphical solutions for constant inlet condition cases according to some (Brooker et al., 1974; Young & Dickens, 1975). Some other investigators (Hamdy & Barre, 1970; Barre, Baughman & Hamdy, 1971; Sutherland, 1975) have felt Hukill's unmodified model is not rigorous enough to be applied to a broad set of design simulations.

* Hukill's model and modifications thereof are all generally referred to as the logarithmic model or characteristic logarithmic model.

However, it should be noted that the latter two studies did utilize a slightly modified version of Hukill's model which then required the use of a computer.

Similar models utilizing finite difference and predictor-corrector numerical methods respectively were proposed (Van Arsdel, 1955) to solve the simultaneous, partial differential equations describing the system. A separate determination of the instantaneous rate of drying, R, was necessary. Van Arsdel presented a sound approach and part of his development of the theory served as the starting point for the model developed by this author. This will be discussed in a later section.

Many models in the agricultural engineering literature are not concerned with sensible heat relative to latent heat. Often, however, 12 to 15% of the total heat required may be transferred to the grain as sensible heat (Boyce, 1965). Boyce proposed an empirical model which included sensible heat effects. Accurate empirical drying rate equations and properly measured rate constants were crucial to this model.

Bakker-Arkema et al. published a frequently referenced model which they admitted, however, was more academic than practical (Bakker-Arkema, Bickert, and Patterson, 1967). Their model is quite rigorous and accounts for many of the basic mechanisms. Their model applies only to wet products with all drying occurring in the constant rate period. Constant thermal properties (such as latent heat of vaporization) were assumed. No specific

equation for the medium's moisture content was included. The authors stated that for application to grain drying in general, additional mass and energy balances to account for decreasing moisture content and increasing latent heats would be required. The published model already required four differential equations with four unknowns. A critical analysis of this model (Spencer, 1969) stated there was not satisfactory comparison between theory and experiment.

A three step series was the basis for a model presented by Thompson, Peart, and Foster (1968). Three sequential steps are proposed to represent the simultaneous solution of coupled heat and mass transfer equations. In step 1, an air temperature is calculated based on sensible heat only. This temperature (likely to be overestimated) is then used in conjunction with the inlet humidity and a rate equation to determine the decrease in moisture content and the increase in humidity (likely to be overestimated as well) in step 2. Step 3 reduces the air temperature due to evaporative cooling as based on the amount of moisture removed in step 2 and calculates the grain temperature (which is considered to be different from the air temperature). Apparently, no iterative checks to assure the legitimacy of the solution are performed. It would seem to this author that the model of Thompson et al. would tend to indicate the bed's average moisture to be reduced more quickly than it actually would be. No confirming experimental data were presented; they stated,

however, that unpublished data confirmed the model reasonably well.

An empirical model somewhat similar to that of Boyce (discussed above) was proposed with a different approach to handling the rate equations and constants (Henderson, 1968). Another model based upon coupled partial differential equations and with more concern for the actual heat and mass transfer coefficients than Van Arsdel's model was also presented in 1968 (Myklestad). Spencer (1969) proposed a modified version of the model by Bakker-Arkema et al. which differed primarily by offering a new empirical form for the rate expression in order to handle a broader range of conditions. This model was further extended by Spencer (1972) to account for the variation of latent heat as a function of moisture content and to account for some bed shrinkage as drying progresses. O'Callaghan et al. extended Boyce's model to apply to several novel types of driers (O'Callaghan, Menzies, & Baily, 1971).

A very rigorous model with five partial differential equations in five unknowns was developed for use with a hybrid computer (Hamdy and Barre, 1970). They state that previous theoretical works have not been completely satisfactory because combining descriptions for all of the basic phenomena results in a "complex non-linear mathematical model that does not lend itself well to analytical solutions or to simulation on either a digital or analog computer." They feel that particular strengths

of their model include among other things; consideration of sensible as well as latent heat effects, changes in heat capacity of the medium and of the air as a function of changing moisture contents, ability to handle increasing as well as decreasing moisture contents, and consideration of the latent heat of sorption as a function of moisture content. The practicality of this model for routine simulation is questioned due to its extensive computing requirements.

Two studies by the same researchers (Barre, Baughman, and Hamdy, 1971; Baughman, Hamdy, and Barre, 1971) extended the model of Hukill and simplified the model of Hamdy and Barre. It was noted by the authors that the rigorous Hamdy and Barre model may be simplified to the Hukill model by assuming

(1) The specific heat of moist air is approximately constant with respect to small humidity changes

(2) Sensible heat effects are small compared to latent heat effects

(3) Sensible heat required to raise the evaporated moisture from the grain temperature to the air temperature is negligible

(4) Bulk grain density is independent of moisture content and temperature and

(5) Latent heat of sorption is approximately constant.

The main difference between the various models is the manner of approximating the simultaneous solution of their particular

equation set and the particular rate equation chosen. The various rate equations are generally empirically derived from fitting an equation to observed data and may require as many as 10 or more fitted constants if, as is usually the case, the rate equations require the determination of the equilibrium moisture content.

The references discussed this far represent a thorough survey* of non-equilibrium modeling techniques for simulating conventional deep bed driers as might be employed for grain drying. One common feature to these models is a very critical dependence on accurate drying rate expressions and properly determined rate constants and transfer coefficients. Generally there were at least four unknowns at any given point in time and space (including two temperatures). Any of the models which could conceivably handle variable temperature and humidity inputs appeared to require fairly sophisticating programming and extensive computing. For example, one published application of the model of Bakker-Arkema et al. required two sets of time and distance increments. Within the individual corn kernel, Δr = 0.001 ft (radial) and Δt = 0.003 hr; within the overall 2 ft bed, Δx = 0.005 feet (less than the diameter of a single corn kernel) and Δt = 0.015 hr. (Bakker-Arkema, Evans, & Farmer, 1971). The product of the number of time steps and the number

* Some additional non-equilibrium drier models will also be referenced under a later section on solar drying simulations.

of segments for Van Arsdel's model to reach a length of 3 feet at time 0.08 hours had to be at least 360 for his predictor-corrector method and 60 for his finite difference method. In demonstrating their model, Hamdy and Barre (1970) required a Δx of 0.02 feet and a Δt of 0.002 hrs.

Given the degree of uncertainty which exists in the empirical correlations for drying rate, equilibrium moisture content, other thermal properties, and indeed in the simulated results; and given the uncertainty which may also exist in the models of other units (e.g. solar collector), it would not appear that any of the above models would provide a simple and efficient yet accurate model for the desired purpose of this study.

2.6.2 EQUILIBRIUM MODELS:

A few drier models which are much less dependent upon rate expressions, i.e., equilibrium or near-equilibrium models have also been developed (Bloome and Shove, 1971; Thompson, 1972; Banks, 1972; and Close and Banks, 1972).

Bloome and Shove developed a near equilibrium model for simulation of aerated grain storage employing unheated air and low flow rates. They objected to the inflexibility of other drying models and the critical dependence on the precise determination of rate constants. They noted that the controlling factor in many models was the empirical drying rate equation with mass and energy balances used only to calculate the moisture contents (and temperatures) resulting from the predicted moisture

removal. In their model there are no explicit rate expressions; the drying rate is implicitly governed by the temperature difference between the medium and the fluid. There is some similarity to the previously discussed uncoupled series approach of Thompson (1968). At the beginning of a calculation for a particular segment at a given time, the quantities (T_f-T_s) and $(W-W_e)$ are examined to determine which process(es) will occur (i.e. heating or cooling and drying or condensing). Then the model moves W towards W_e until one of the driving forces based on energy and mass balances is diminished to zero. At any given time and location; the moisture content, the humidity, and the temperatures are not necessarily in equilibrium. The authors stated their model is applicable only to very low flow rates and temperatures. Some confirmation of the model against experimental data was provided. Hourly weather data was utilized for inlet conditions over periods of several days.

Thompson (1972) presented what he considered to be a "simplified version of Bloome's model that...is more accurate and easier to understand." His model was designed for high grain-to-air ratios as found in storage bins of high moisture grain continuously aerated with unheated air. Thompson felt that most drying models (which use much lower grain-to-air ratios) cannot adequately model aerated storage bins. Thompson's model is basically an equilibrium model based on gross rather than differential mass and energy balances and assumes that relative changes

in W and T_s are quite small with respect to relative changes in w and T_f. Thermal properties are assumed to have constant, average values. It is also necessary to include an equation relating changes in grain temperature, T_s, to the heat released by decomposition. With respect to locating a simultaneous equilibrium solution, it is noted that the approach reported by Thompson for his storage model contains some similarities to the approach derived independently from partial differential equations and variable thermal properties by this author.

The following discussion of the development of the Close and Banks model for the general problem of heat and mass transfer is presented in some detail. This background will be needed to understand this author's approach (discussed in later section) in attempting to develop a simplified version of their model for the particular use desired for this study. (For a more detailed discussion the reader should consult the appropriate articles referenced above.)

In the model of Close and Banks, the following assumptions were necessary:

(1) one dimensional fluid flow through a uniform porous medium

(2) diffusion and dispersion in the fluid flow direction are negligible compared to bulk transport

(3) sorption process involves no hysteresis

(4) constant interstitial fluid velocity and pressure

(5) no thermal or mass gradients normal to fluid flow

(6) thermal and sorption equilibrium between fluid and adjacent medium at any given point

(7) no discontinuities in fluid or medium properties in direction of flow

(8) enthalpies h,H, and moisture content W are all functions of temperature T and humidity w only

(9) all mass and energy transfers occur strictly between the fluid and the medium

The energy and mass balance equations are non-linear and are coupled due to the latent heat accompanying sorption and due to the temperature dependence of the sorbate equilibrium relation. Continuing to follow the work of Close and Banks, the equation for the conservation of energy is

$$P(1-\varepsilon)\frac{\partial H}{\partial \theta} + \rho\varepsilon\frac{\partial h}{\partial \theta} + \rho_v\varepsilon\frac{\partial h}{\partial x} = 0 \qquad (1)$$

and the equation for the conservation of mass (sorbate) is

$$P(1-\varepsilon)\frac{\partial W}{\partial \theta} + \rho\varepsilon\frac{\partial w}{\partial \theta} + \rho_v\varepsilon\frac{\partial w}{\partial x} = 0 \qquad (2)$$

These two equations may be transformed into:

$$\frac{\partial F_i}{\partial \theta} + \left(\frac{v}{1+\mu\gamma_i}\right)\frac{\partial F_i}{\partial x} = 0 \qquad i = 1,2 \qquad (3)$$

where F_1 and F_2 are functions of only T and w and are termed characteristic potentials such that F_1 and F_2 satisfy the relations:

$$\left(\frac{\partial F_i}{\partial w}\right)\Big/\left(\frac{\partial F_i}{\partial T}\right) = -\left(\frac{\partial T}{\partial w}\right)_{F_i} = \alpha_i \qquad i = 1,2 \qquad (4)$$

γ_i is termed a characteristic specific capacity ratio since its relationship to F_i is analagous to the relationship between the specific heat ratio and temperature in the special case of heat transfer only. α_i is the slope of a constant F_i line on a T, w plot (e.g. psychrometric chart).

If F_i is replaced by T and $v/(1+\mu\gamma_i)$, the velocity of progration term, is modified to contain the ratio of specific heats instead of γ_i, it is seen that equations 3 are both in the form analagous to the case of only heat transfer. The equations represent the propagation of two waves, or two fronts, through the medium. Changes in F_1 or F_2 propagate through the medium independently of each other and at different velocities. For a system where the equilibrium model is reasonably applicable, coupled heat and mass transfer relationships may be replaced by the uncoupled F_i relationships. If the F_i and γ_i curves as a function of T and w are represented on a T, w plot, the graphical conversion between T and w (and hence h, H, and W) and F_1 and F_2 is straightforward.

By plotting lines of constant F_i on a psychrometric chart, it was shown that for Australian wheat (Banks, 1970) a line of constant F_1 is nearly the same as an adiabatic saturation line and a line of constant F_2 is nearly the same as a line of constant percent moisture. Within suitable ranges a line of constant percent moisture corresponds approximately to a line of constant percent humidity.

Once sufficient data is collected and utilized to generate graphical plots and computerized relationships between $(F_i, \gamma_i)_{i=1,2}$ and (T,w), appropriate for a specific medium (not a trivial task), then routine simulations of drying may be conducted. Practical applications have been demonstrated for beds of silica gel by Close and Banks (1972), and for grain by Sutherland, Banks, and Griffiths (1971) and by Banks (1970). This model was also utilized in a study by Nelson (1976).

2.6.3 COMPARISON OF LOGARITHMIC AND EQUILIBRIUM MODELS:

An Australian study (Sutherland, 1975) compared the performance of the logarithmic model and the "equilibrium (square front) model". The logarithmic model refers to the model derived by Hukill (1947) and further developed by others (Barre, Baughman, and Handy, 1971). The "equilibrium (square front) model" is the Close and Banks model. Sutherland discussed the observation that in deep bed drying, the drying zone quickly travels sufficient distance to reach a steady front velocity and width. Width refers to deviation from a perfect square wave which would have zero width. Width describes the size of the zone of transition between the two distinct values leading and trailing the front. The front velocity of the steady width zone (as developed by the logarithmic model) was found to be identical to the zero width zone (as developed by the equilibrium, square front model). It was concluded that the equilibrium model as advanced by Close and Banks was sufficient for drier simulations under many circum-

stances. However, Sutherland believes that if any portion of the steady width zone would actually exit from the bed during the simulation or if an accurate estimate of the zone width (or internal profile) is desired, then the equilibrium theory would not be sufficient. Sutherland noted that under conditions of low flow rates and high temperatures the steady width zone is decreased in width and the equilibrium model output therefore varies less from the logarithmic model output under these conditions.

2.6.4 SIMULATIONS OF GRAIN DRYING WITH SOLAR ENERGY

There have been several articles on actual drying experiments (discussed elsewhere in this thesis) but only a limited number of studies of experimental simulations of grain drying with solar energy as a heat source have been published. It should be noted of course that some of the models discussed earlier could be modified slightly (or used in conjunction with a solar collector model) to simulate such experiments. One might speculate that the limited amount of published material regarding simulations as compared with that dealing with actual experimentation is because interest in this area is just arising. Alternatively, perhaps it is because of the reasons outlined earlier with respect to suitability of published models for flexible solar grain drying simulations.

Two studies which presented simulations of agricultural

drying with collected solar energy (Akyurt and Selcuk, 1973; Selcuk, Ersay, and Akyurt, 1974) are not particularly applicable to this study. Nevertheless, they are mentioned here as interesting and related applications. Both studies dealt with the mathematical modeling of multishelf driers for fruit. The collector and several independent drying shelves were an integral part of the drier unit. The product on each shelf received some direct solar radiation as well as heat from the air flowing up from below from the main collector. Recently a paper was presented (Osborn, Meinel, and Beauchamp, 1976) indicating that the authors were attempting to provide a mathematical computer model of a solar collector. This model would be designed to use weather data and hopefully interface with existing grain drying models. The idea was that researchers with grain drying models could supplement their computer program with that of Osborn, et al. No further results have been published to the knowledge of this author.

It must be noted here that the Solar Energy Laboratory of the University of Wisconsin's Engineering Experiment Station has for some time made available an extensive and flexible computer program named, TRNSYS, capable of simulating (using actual weather data) a wide variety of solar energy applications (Klein et al., 1974; Solar Energy Laboratory of the University of Wisconsin, 1977). Most valid drying models could be adapted to interface with this program. However, the earlier comments on the

suitability of published models for simulating solar grain drying should be recalled. The development of a simpler but adequate and versatile model to interface with such a program seems desirable.

Rao and Macedo (1976) recently simulated the drying of Brazilian carioca beans with solar energy as the heat source. They employed a mathematical collector model developed at the University of Wisconsin (Duffie and Beckman, 1974) and one of the drying models discussed earlier (Brooker, Bakker-Arkema, and Hall, 1974). Their simulated results were confirmed reasonably well by experimental data. Their drier model includes five equations (including an equilibrium moisture relationship) and five unknowns. The empirical rate equation has three constants which were determined by linear regression of suitable experimental data. The rate equation is also dependent upon an expression for equilibrium moisture content which is a polynomial: 4th order in relative humidity and with eight empirical constants. The controlling equation in the drier simulation therefore requires the experimental determination of over ten constants.

Although the model of Rao and Macedo appeared to perform fairly well, the critical dependence on the above rate expression makes the model somewhat inflexible if it would be wished to simulate the drying another type of product. It is possible that one might even have to experimentally redetermine the three rate constants if this model were to be used to simulate the drying

of the same product from another location or year. The authors make no comment on their opinion of the model's flexibility or of the utility of the model for possible use in extensive modeling and optimization studies. The authors did suggest the possibility of using averaged weather data as inputs but it does not appear that the results of their simulations conducted in this manner adequately match those utilizing hourly inputs of actual data. Their work has also been discussed qualitatively elsewhere (Hammond, 1977).

2.7 Reasons for Initiation of this Study

Based on the survey of published drying models, it was concluded that the development of a simpler but adequate and versatile model to interface with computer simulation programs such as TRNSYS (Klein et al., 1974; Solar Energy Laboratory of the University of Wisconsin, 1977) was desirable. Demonstration of such a model in order to predict the performance and feasibility of solar grain driers under various design conditions also appeared to represent a desired contribution to an expanding area of inquiry.

3.
ACCOUNT OF THIS STUDY

This section of the thesis describes and analyzes the development of the unsuccessful simplified F_1/F_2 model and the development of the successful equilibrium model. Computer programming and execution of the successful model are also discussed.

3.1 Simplified F_1/F_2 Model

An equilibrium model based on infinite heat and mass transfer coefficients has been previously developed (Banks, 1972; Close and Banks, 1972) and applied to heat and mass transfer through grain (Sutherland, Banks and Griffiths, 1971). This model was discussed in detail in an earlier section of this study.

It was suggested (Close, November, 1975) that it might be possible to derive a simpler and approximate model for solar drying from the Close and Banks model. It was envisioned that such a model would not require the preparation of extensive charts for each grain of interest, would require minimal computer time, and would readily accept variable inlet conditions. This suggestion was based in part on the assumption that knowing the average bed conditions at a given time would be more important than the exact axial profiles within the bed. (A similar result with respect to thermal storage in modelling solar energy systems was noted previously (Hughes, Klein, and Close, 1975).)

It was not felt practical to use the rigorous Close-Banks model in conjunction with TRNSYS for modeling solar drying of grain in packed beds. Since grain is highly variable in its properties as a function of such things as grain type, location grown, year grown, etc., a new set of F_1/F_2 and γ_1/γ_2 plots would likely need to be developed for each case. Substantial data and/or experimentation would be required. Once set up, the model does lend itself well to constant inlet conditions with step changes or repeated cycling between design set points. The inlet conditions to a solar drier are rarely so invariant.

3.1.1 DEVELOPMENT:

The following additional assumptions were made to simplify the model of Close and Banks:

(1) The lines of constant F_1 may be adequately approximated by lines of constant wet bulb temperature on a psychrometric chart.

(2) The lines of constant F_2 may be adequately characterized by lines of constant percent humidity.

(3) Within the range of interest it is possible to define constant values for α_1 and α_2 effectively assuming linearized plots of F_1 and F_2.

(4) Within the range of interest, it is possible to choose average values for T and w which are representative of the variable inlet conditions and (knowing initial bed conditions) use those values to define constant values

for γ_1 and γ_2. (This effectively assumes constant average velocities of front propogation.)

(5) A suitable equation for equilibrium moisture content as a function of t and w is available.

Assumptions 3 and 4 are highly suspect from a theoretical point of view, and to some extent, so are assumptions 1 and 2. This was realized, but the goal was a simple model of the average performance versus time.

If the transient condition of the bed is represented approximately by two square fronts passing through the bed, then three (T,w) coordinate pairs are important in this model. Referring to figures 1, 2, and 3; these coordinate pairs represent:

(a) The values in equilibrium with initial bed conditions (which ultimately become the first set of outlet conditions referenced as point 1).

(b) The values representing the inlet air conditions (which ultimately become the third set of outlet conditions referenced as point 3).

(c) The values representing an intermediate point where the air and grain are in equilibrium at some T and w after the passage of the first front and before the passage of the second front. (These values ultimately become the second set of outlet conditions referenced as point 2).

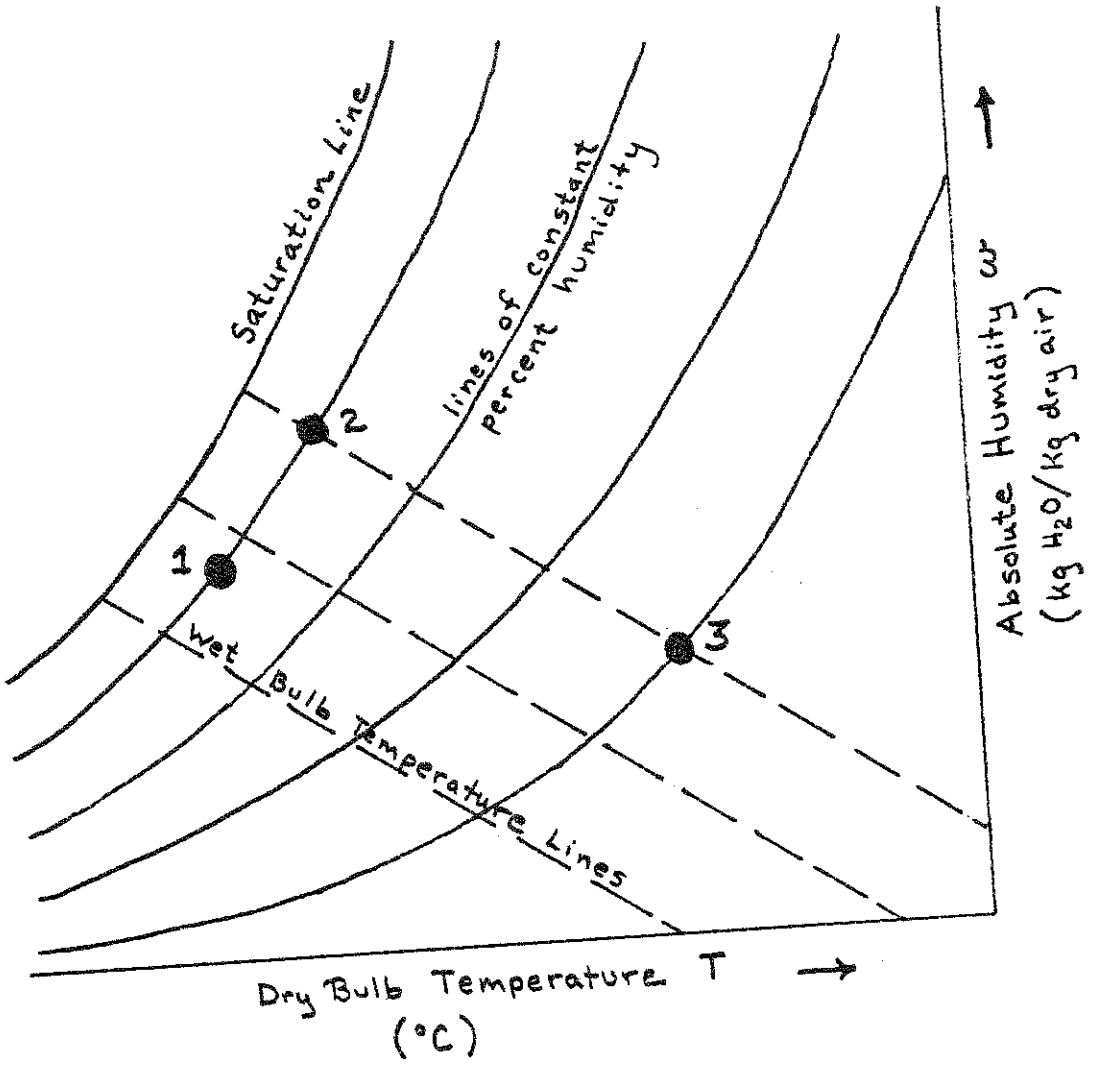

1 ● T and w in equilibrium with initial grain moisture

2 ● intermediate T and w

3 ● T and w of inlet air

Sketch depicting relation of process states on a psychrometric chart

Figure 1

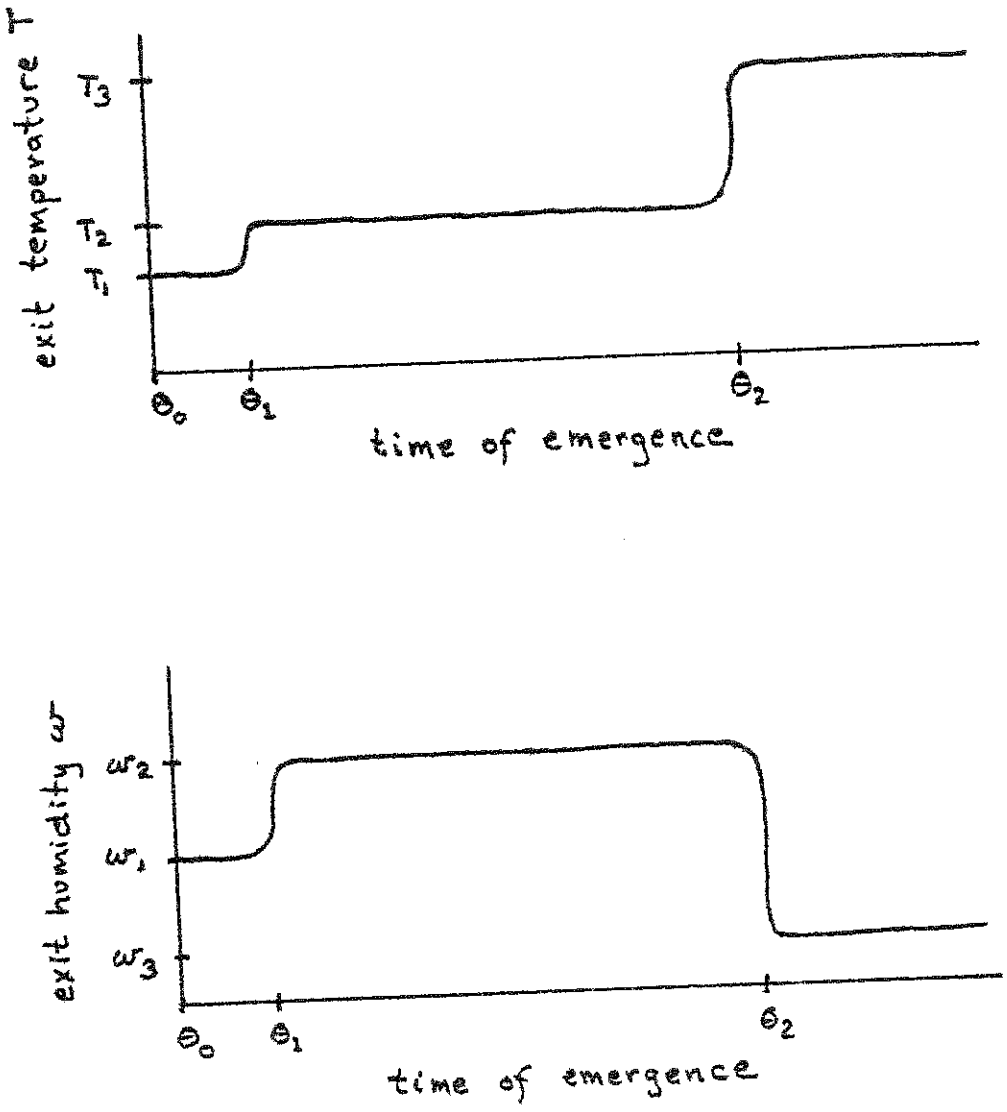

Sketch of exit air conditions versus time of emergence

(Exit air conditions are T_1 and w_1 until time θ_1 when the first front emerges and exit conditions T_2 and w_2 apply until time θ_2 when the second front emerges bringing the inlet air conditions of T_3 and w_3 to the exit.)

Figure 2

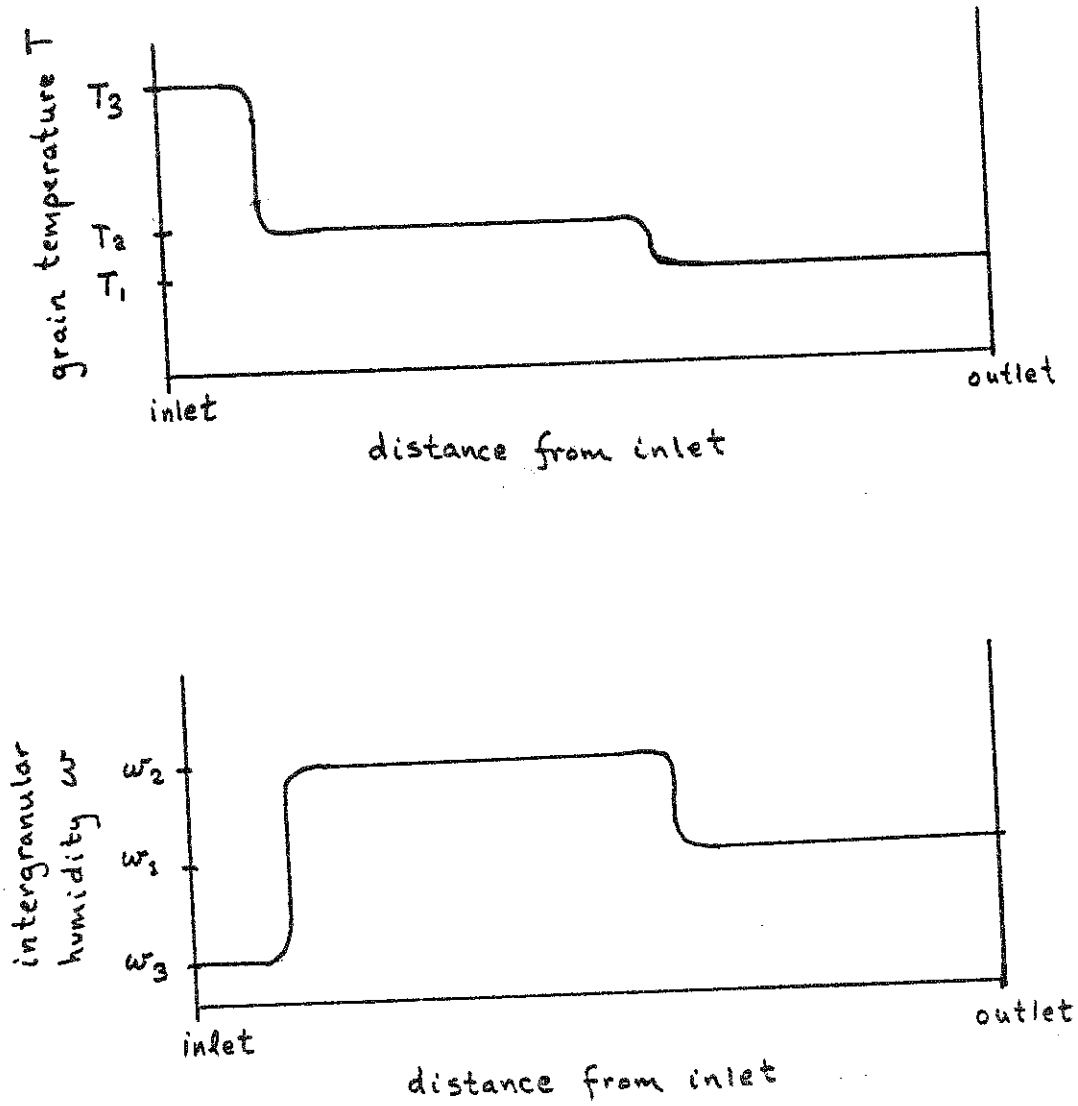

Sketch of internal profiles of temperature and humidity (at a time prior to exit of the first front, i.e., time $< \Theta_1$)

Figure 3

Figure 1 shows a sketch of how these points relate to each other on a psychrometric chart. Figure 2 shows sketches of T and w of the exit air versus time θ and indicates the time of emergence for the respective fronts. Figure 3 is a sketch of the internal profile of T and w versus distance which would exist at some time prior to emergence of the first front, i.e., between time Zero and θ_1. The initial bed state (point 1) and inlet air state (point 3) are known. The intermediate point 2 is assumed to be located at a point found by travelling from the initial state along the constant F_2 line (i.e., constant percent humidity) until intersecting with the constant F_1 line (i.e., the wet bulb temperature of the inlet air). The appropriate equilibrium moisture contents corresponding to these points are known when T and w are known.

It is possible to set up an overall energy balance and an overall mass balance which are valid at the exact time of emergence of the second front.

Letting subscripts 1, 2, and 3 represent the initial, intermediate, and inlet conditions as described earlier, the overall energy balance* is:

$$\dot{m}(h_1-h_3)(\theta_1-\theta_0) + \dot{m}(h_2-h_3)\cdot(\theta_2-\theta_1) = -M_b(H_{final}-H_1) \qquad (5)$$

* note that the balance equations are not dynamic balances applicable at all times but rather expressions of the energy (or mass) changes between time zero and θ_2. At θ_2, the entire bed reaches the final state in equilibrium with the inlet air.

and the gross water balance* is:

$$\dot{m}(w_1-w_3)\ (\theta_1-\theta_0) + \dot{m}(w_2-w_3)\ (\theta_2-\theta_1) = -M_b(W_{final}-W_1) \qquad (6)$$

Assuming $\theta_0 = 0$, the front emergent times are θ_1 and θ_2 respectively. With points 1, 2, and 3 all known, there exist unique front times θ_1 and θ_2 which will satisfy these equations (Close, December, 1975).

Obtaining the front emergent times for this highly averaged system permits the straightforward determination of average front velocities and therefore mean values of $\bar{\gamma}_1$ and $\bar{\gamma}_2$.

The average front velocity is equivalent to the bed length (L) divided by the appropriate front emergence time. From the work of Close and Banks, discussed above, then the instantaneous front velocity may be represented by $v/(1+\mu\gamma_i)$ where v is the intergranular fluid velocity and μ is a ratio of effective media density over effective fluid density. A mean value of $\bar{\gamma}_i$ is defined such that:

$$\frac{L}{\theta_i} = \frac{v}{1+\mu\bar{\gamma}_i} \qquad i = 1,2 \qquad (7)$$

Recalling equations 4, one linear solution would be:

$$F_i = T + \bar{\alpha}_i w \qquad i = 1,2 \qquad (8)$$

where $\bar{\alpha}_i$ may be determined from the slopes of the constant F_1

* Note that the balance equations are not dynamic balances applicable at all times but rather expressions of the energy (or mass) changes between time zero and θ_2. At θ_2, the entire bed reaches the final state in equilibrium with the inlet air.

and F_2 lines (assumed to be linear between points 2 and 3 and between points 1 and 2 respectively). The initial and inlet conditions in terms of T and w can be converted to appropriate initial and inlet values of F_1 and F_2.

To recapitulate, the bed may be assigned the appropriate values of F_{1m} and F_{2m} initially. The inlet air initiates the F_{1f} and F_{2f} wave propogation into the bed at velocities determined by $\bar{\gamma}_1$ and $\bar{\gamma}_2$. (Subscripts m and f represent the medium and the fluid states respectively.) The system is now described by uncoupled, linearized equations which may be solved independently for F_1 and F_2. These may be superposed if desired to convert back into T and w using equations 8, and W may be obtained from an appropriate equilibrium relation.

It is noted that some success was achieved with a somewhat similar linearizing approach to determine initial and boundary conditions for solving the model of an open cycle air conditioner (Nelson, 1976). Significant differences in that study, however, included well defined design points or boundary conditions, step change inlet conditions, and the use of actual F_1, F_2 and γ_1, γ_2 plots rather than repetitive and constant parameter solutions of equations 3.

3.1.2 SOLUTION OF THE MODEL:

The solution of the propagating fronts through the bed over time in this model was based on a finite difference approach to equations 3:

$$\left(\frac{dF_i}{d\theta}\right) = \left(\frac{v}{1+\mu\bar{\gamma}_i}\right)\left(\frac{F_{i_{x-\Delta x}} - F_{i_x}}{\Delta x}\right) \qquad i = 1,2 \qquad (9)$$

Where x represents axial position in the bed and the bed length equals (Δx) (N) where N is some suitable number of segments for the finite difference analysis. A FORTRAN subroutine containing the simplified F_1/F_2 model was developed to interface with TRNSYS. Many of the details in this model subroutine were also used in the more successful model to be discussed later. Therefore, the remaining discussion on this model will concentrate on its particular behavior and problems.

3.1.3 PERFORMANCE OF THE MODEL:

The use of this model to simulate drying of a packed bed produced outlet conditions and internal profiles consistent with the assumed linear, constant F_1 and F_2 lines. That is, values of (T, w) pairs for any point in the bed, when plotted on a psychrometric chart, would trace the progress over time from point 1 to point 2 along the constant percent humidity lines and from point 2 to point 3 along the wet bulb temperature line. Note that perfect square waves (zero width fronts) would jump from point 1 to 2 to 3 without any finite time at intermediate points on the psychrometric chart. Finite width fronts result in portions of the bed spending some finite time at intermediate points.

The model (when compared against limited experimental data) predicted that the final desired average moisture content would

be reached much more quickly than it actually was. This discrepancy was often on the order of 20 to 25% of the actual time requirements depending on the specific parameters of the simulation such as flow rate, inlet conditions, and initial and final bed conditions. A serious lack of closure in the dynamic mass balance was also encountered. The mass balance at any given time θ may be defined as

$$M_b(W_{initial}-W_\theta) = \int_{t=o}^{t=\theta} \dot{m}(w_{out}-W_{in})\,dt \qquad (10)$$

where the W terms are integrated over the entire bed.

For most intermediate times during a simulation, $(W_{initial}-W_\theta)$ was of a magnitude such that for equation 10 to be valid, W_{outlet} would have needed to acquire a value in excess of saturation. The discrepancy was most serious near the beginning of the simulation with a lack of equality in equation 10 well in excess of 50%. This became better as the simulation progressed until finally equality was reached at the time the model finally indicated the complete bed to be in equilibrium with the inlet air.

3.1.4 ANALYSIS OF PROBLEMS:

Both the rapid drying and the lack of mass balance closure are believed related to the model's inability to imitate the square wave propagation which is assumed in part of the derivation. Prior to the time when the second assumed square front should emerge, two things generally occurred. First, there would be a period during which the model calculated the humidity to be

lower and the temperature to be higher than the corresponding square front values for most of the bed. However, the outlet conditions approximately corresponded to the square wave condition. During this time, the model profile for T and w caused unrealistic over-drying conditions in most of the bed which were not reflected by the reasonably realistic outlet humidity. Second, there would be a period during which the model determined much of the bed to correspond to the square wave values except at the outlet where the square wave profile had jumped to a high humidity while the model profile remained at a low humidity. During this time, the model profile for T and w caused realistic drying conditions in much of the bed and an unrealistically low outlet humidity. The sum of all of the above effects appeared to be an indication of too much moisture removed from the grain ($M_b(W_{initial} - W_\theta)$) but too little humidity removed from the bed ($\int \dot{m}(W_{out} - W_{in})dt$).

Note that although the model indicates more rapid drying than it should, its somewhat distorted approximations of square wave forms do not completely emerge as rapidly as the assumed perfect square fronts would have emerged. One other contributing factor may exist. In the work noted earlier (Banks, 1972, Close and Banks 1972) The equilibrium values of W were taken into account over all values of T and w in determining the γ_i and F_i plots. In the model discussed here, equilibrium W was only considered at three specific points in determining $\bar{\gamma}_i$. It is

unlikely that a unit change in T and w along a constant F_i line in this model would necessarily result in the corresponding change in W necessary to satisfy both the mass and equilibrium balances. That is, in determining W, the simplifications in this model carry the implicit assumption that the internal mass balances over a given segment are satisfied when the equilibrium expression for W is invoked. Given the complex dependence of the equilibrium moisture equation on T and w, it is doubted that this implicit assumption is valid. The exact magnitude of its effect compared to the previously discussed problems would be very difficult to determine however.

3.1.5 F_i AS A CONSERVED PROPERTY:

Before concluding the discussion of the simplified F_1/F_2 model, one final observation is worth noting. During the course of this work it was suggested (Mitchell, 1976) that F_i should be conserved properties of the system such that it would be possible to calculate balances analagous to equation 10 for both F_1 and F_2. To show this:

$$\frac{\partial F_i}{\partial \theta} = \left(\frac{v}{1+\mu\gamma_i}\right)\frac{\partial F_i}{\partial x}$$

after dropping the subscript i for clarity and integrating:

$$\int_o^L \frac{\partial F}{\partial \theta}\,dx = \int_o^L \left(\frac{v}{1+\mu\gamma}\right)\frac{\partial F}{\partial x}\,dx$$

$$\frac{d}{d\theta}\left(\int_o^L F\,dx\right) = \left(\frac{v}{1+\mu\gamma}\right)\left(F_L - F_o\right)$$

$$\int_o^{\theta} \frac{d}{d\theta}\left(\int_o^L F dx\right) d\theta = \int_o^{\theta} \left(\frac{v}{1+\mu\gamma}\right)(F_L - F_o)\, d\theta$$

and finally:

$$\left[\int_o^L F dx\right]_{\theta} - \left[\int_o^L F dx\right]_o = \int_o^{\theta} \left(\frac{v}{1+\mu\gamma}\right)\left(F_L - F_o\right) d\theta \qquad (11)$$

Equation 11 says the change in "storage" equals "flow out" minus "flow in". Assuming that the bed conditions can be "assigned" values of F_i representative of the conditions at any given point and that the inlet and outlet air can be thought to "possess" some value of F_i, equation 11 may be used in the following manner. At time θ, the left hand side represents the integrated graphical area between the plots of F_i versus axial distance at time θ and at time zero. The right hand side can be approximated by

$$\left[\sum_{t=o}^{\theta} \left(F_{i_{outlet}} - F_{i_{inlet}}\right)(\Delta t)\right]\left(\frac{v}{1+\mu\gamma_i}\right) .$$

With perfect square wave profiles, equation 11 should close exactly. Equation 11 was checked but once with actual output from the model discussed herein. The lack of closure for ΔF in equation 11 for this one trial was found to be 3.4%. The left hand side of equation 11 deviated from the square wave value by 3.2% and the right hand side by 6.3% (both too low). This discussion of the conservative nature of F_i is obviously by no means conclusive. However, it is postulated, incidental to the other work in this study, that this property could be rigorously shown if it would be of any value to someone employing the Close and Banks model.

3.2 Final Equilibrium Model

Given the difficulties with the simplified F1/F2 model as discussed above it was deemed necessary to develop another approach. It was desired to construct an equilibrium model, assuming that the fluid and the medium are always in complete thermal and sorption equilibrium at any given point in the bed. The basic underlying assumption to this approach is that a model so developed may be used to adequately simulate the average moisture versus time of a drier as a component of a solar simulation. The exact internal profiles of W, w, and T (and indeed, of the temperature of the medium which may sometimes vary slightly from that of the air in real systems) may be of greater significance to someone attempting a very rigorous design of a drier. However, it was anticipated in this study that given the design parameters of an existing drier, the equilibrium model would provide an adequate characterization of performance for determining the feasibility of various solar energy drying schemes.

3.2.1 DEVELOPMENT:

Acknowledgement is given to the importance of an earlier work (Van Arsdel, 1955) as a starting point for the development of this model. The model developed herein starts with heat and mass balances similar in form to those utilized by Van Arsdel and must employ some of the assumptions delineated in his study. Several assumptions (some specific to this model) are necessary in the derivation which follows:

(1) The flow is equally distributed at any given cross section of the uniform porous medium normal to the direction of flow.

(2) Heat and mass transfer through the walls may be neglected.

(3) Interparticle conduction is negligible.

(4) Diffusion and dispersion in the fluid flow direction are negligible compared to bulk transport.

(5) There is no change in the bed dimensions during drying (e.g. no shrinkage)

(6) Changes in thermal properties as function(s) of T, w, and W are small enough to allow those properties to be treated as constants over a small distance segment and small time step.

(7) There are no thermal or mass concentration gradients normal to the direction of flow.

(8) Fluid density is a function of T and w only; interstitial pressure changes may be neglected.

(9) Individual particles may be considered to possess uniform thermal and sorbate distributions, i.e., no internal mass or thermal gradients exist within particles.

(10) In a given segment of the bed, heat and mass transfer between the fluid and all portions of all particles within that segment may be considered instantaneous within the time frame considered (That is, each bed

segment may be lumped and need not be considered as a collection of separate particles).

(11) Hysteresis in the sorption process may be neglected.

(12) The sorbate content in a specific medium is an equilibrium function of only the temperature and sorbate content of the fluid.

(13) The differential terms for the change in air enthalpy over time and for the change in humidity over time are negligible (with respect to the corresponding terms for grain) in the energy and mass balances respectively.

Assumptions 9 and 10 are suspect from a theoretical point of view but are felt not to detract from the suitability of the model for the intended usage.

3.2.2 SOLUTION OF THE MODEL:

The enthalpy of the medium plus sorbate is

$$H_s = C_{ws} (T-T_{ref}) = (C_1+C_2W) (T-T_{ref}) \quad (12)$$

and the enthalpy of the moist air is

$$H_f = C_a(T-T_{ref}) + w\lambda_f$$

$$H_f = (C_{a_1} + C_{a_2}w) (T-T_{ref}) + w\lambda_f$$

$$H_f = C_{a_1} (T-T_{ref}) + \left[C_{a_2} (T-T_{ref}) + \lambda_f\right]w \quad (13)$$

where λ_f is the latent heat of vaporization of free water at the reference temperature. λ_s is the difference between the

latent heat of vaporization of water bound in the medium (λ) and that of free water (λ_f). The variable λ_s may be shown to be reasonably represented by $\lambda_s = (S_1 + S_2 W) \geq 0$ For a system with water as the only sorbate, the differential enthalpy balance may be written as

$$\rho_s (1-\varepsilon) \frac{\partial H_s}{\partial t} + \rho_f \varepsilon \frac{\partial H_f}{\partial t} = - \frac{\dot{m}}{A} \frac{\partial H_f}{\partial x} - \frac{\dot{m}}{A} \lambda_s \frac{\partial w}{\partial x} \qquad (14)$$

and the differential mass balance may be written as

$$\frac{\dot{m}}{A} \frac{\partial w}{\partial x} = - \rho_s (1-\varepsilon) \frac{\partial W}{\partial t} - \rho_f \varepsilon \frac{\partial w}{\partial t} \qquad (15)$$

The equilibrium relationship may be expressed at this time as

$$W = W(T,w) \qquad (16)$$

Assumption 13 allows simplification by deletion of the terms $\partial H_f/\partial t$ and $\partial w/\partial t$. Equation 14 becomes

$$\rho_s (1-\varepsilon) \frac{\partial H_s}{\partial t} = - \frac{\dot{m}}{A} \frac{\partial H_f}{\partial x} - \frac{\dot{m}}{A} \lambda_s \frac{\partial w}{\partial x} \qquad (17)$$

and equation 15 becomes

$$\frac{\dot{m}}{A} \frac{\partial w}{\partial x} = - \rho_s (1-\varepsilon) \frac{\partial W}{\partial t} \qquad (18)$$

It will be noticed that equations 16, 17, and 18 constitute three simultaneous equations with three unknowns (T, w, and W). None of these contain rate expressions or transfer coefficients. A simultaneous solution provides the equilibrium conditions assumed to exist at a given point and given time in accordance with the stated assumptions.

By Euler approximation for a finite difference, equation 17 may be expressed using the first subscript for distance and the second subscript for time as

$$\rho_s(1-\varepsilon)\frac{\partial H_s}{\partial t} = \frac{-\dot{m}}{A\Delta x}\left(Hf_{i,t} - Hf_{i-1,t}\right) - \frac{\dot{m}\lambda_s}{A\Delta x}\left(w_{i,t} - w_{i-1,t}\right) \qquad (19)$$

Before proceeding further, the preference for presentation of scientific work in SI units is acknowledged. However, most of the published correlations for various grain properties are expressed in English units. Therefore, it was decided that completing this derivation for use with SI would increase confusion due to numerous conversion factors and increase opportunity for error. As much as possible, however, the results and other important information have been presented in SI units.

let $T_{ref} = 32^{\circ}F$

λ_f = 1075.8 BTU/lb free water at $T=32^{\circ}F$

C_a = (0.24 + 0.45 w) BTU/lb dry air, $^{\circ}F$

Using equation 13, the above constants, and some algebra, the right side of equation 19 becomes:

$$\left(\frac{-\dot{m}}{A\Delta x}\right)\left\{0.24(T_{i,t} - T_{i-1,t}) + 0.45\left((w_{i,t}\ T_{i,t}) - (w_{i-1,t}\ T_{i-1,t})\right) + (1061.4 + \lambda_s)\ (w_{i,t} - w_{i-1,t})\right\}$$

Using equation 12, an Euler approximation, and some algebra, the left side of equation 19 is rewritten:

$$\rho_s(1-\varepsilon)\ \frac{d}{dt}\left[(C_{ws}\ T) - (C_{ws}\ (32))\right]$$

$$\rho_s(1-\varepsilon)\left[(C_{ws_{ave}})\ \left(\frac{dT}{dt}\right) - 32\left(\frac{d}{dt}C_{ws}\right)\right]$$

and finally,

$$\rho_s(1-\varepsilon)\left\{\left(\frac{C_{ws_{i,t}} + C_{ws_{i,t-1}}}{2}\right)\left(\frac{T_{i,t} - T_{i,t-1}}{\Delta t}\right) - 32\left(\frac{C_{ws_{i,t}} - C_{ws_{i,t-1}}}{\Delta t}\right)\right\}$$

Accordingly, equation 19 may now be written in the form:

$$T_{i,t} = \left(\frac{T_{i,t-1} + \Delta t Z_1 Z_2 + \Delta t Z_1 K(0.24\ T_{i-1,t} + 0.45\ w_{i-1,t}\ T_{i-1,t}) + (1061.4 + \lambda_s)\ (w_{i-1,t} - w_{i,t})}{1 + \Delta t Z_1 K(0.24 + 0.45\ w_{i,t})}\right) \quad (20)$$

where $Z_1 = 2/(C_{ws_{i,t}} + C_{ws_{i,t-1}})$

and $Z_2 = 32(C_{ws_{i,t}} - C_{ws_{i,t-1}})/\Delta t$

and $K = \dot{m}/A\rho_s(1-\varepsilon)\Delta x$

In a similar fashion, with much less algebra, equation 18 may be rewritten as

$$w_{i,t} = w_{i-1,t} + (W_{i,t-1} - W_{i,t})/K\Delta t \qquad (21)$$

An equilibrium expression developed by Henderson (1952) is utilized for the function of equation 16:

$$W = \left(\frac{-\ln(1-R.H.)}{C(T+B)}\right)^{1/n} \Big/ 100 \qquad (22)$$

Where T is in degrees F

and C, B, and n are grain specific constants

and R.H. is the relative humidity in decimal form

Since an air flow equal to Zero is considered undesireable from the standpoint of spoilage, the model does not include equations to describe the case of a perfectly static bed. If a user of this model chooses to allow air flows of Zero at some time in a simulation, the user should be aware that the computer version (discussed in later sections) will make no changes in bed conditions during any time period in which the flow is turned off.

3.2.3 ITERATIVE CONVERGENCE SCHEME:

Equation 20 explicitly contains variables T and w and implicitly contains W if it enters into Cws terms. Equation 21 contains w and W. Equation 22 derives W as a function of w and T. An iterative converge scheme has been developed to find the simultaneous solution, i.e. the values of w, W and T that satisfy all three equations within acceptable tolerances.

The description of the iterative process which follows considers the solution at node i at time t. (The bed is divided into N segments with the outlet conditions from segment i-1, i.e. T_{i-1} and w_{i-1}, assumed to be the inlet conditions to segment i. Bed inlet and outlet are respectively represented by i = 0 and i = N.) To start the process $W_{i,t}$ must be projected for purposes of calculating C_{ws}, Z_1, and Z_2. Generally these parameters will be fairly insensitive to the relatively small changes in W generally occurring between nodes and time steps. $w_{i,t}$ is also projected initially in a manner similar to the $W_{i,t}$ projection, i.e.,

$$\left[W_{i,t}\right]_p - W_{i-1,t} = W_{i,t-1} - W_{i-1,t-1}$$

$$\left[w_{i,t}\right]_p - w_{i-1,t} = w_{i,t-1} - w_{i-1,t-1}$$

where $[\,]_p$ indicates projected value.

At this point, all variables of subscript i-1 and/or t-1 are known, and initial approximations have been made for $w_{i,t}$ and $W_{i,t}$ as discussed above. The iterative loop begins with the projection of $T_{i,t}$ from equation 20. The value for $W_{i,t}$ is then re-calculated from equation 22. Next equation 21 provides a "corrected" value for $w_{i,t}$ with the additional conditions that $w_{i,t}$ may not exceed saturation at the value of $T_{i,t}$ and may not be negative. The corrected value of $w_{i,t}$ is compared to $\left[w_{i,t}\right]_p$.

$$\text{If } \left| \frac{w_{i,t} - \left[w_{i,t}\right]_p}{\left(w_{i,t} + \left[w_{i,t}\right]_p\right)/2} \right| > \sigma$$

then a new projection is made, i.e., $[w_{i,t}]_p$ assumes a new value, and the process cycles back to the point where equation 20 gives new value of $T_{i,t}$. Equation 22 yields a new value of $W_{i,t}$ and equation 21 again provides a newly corrected value for $w_{i,t}$. The process continues until convergence within the specified criterion σ, is obtained.

The particular form that equations 20, 21, and 22 have been manipulated into cause them to interact in an interesting way. Following the iterative scheme above, if $[w_{i,t}]_p$ is too large then $T_{i,t}$ will be too small and $W_{i,t}$ will be too large (all with respect to the simultaneous solution). A value of $W_{i,t}$ which is too large will result in the corrected value of $w_{i,t}$ being too small. Since the converse condition with $[w_{i,t}]_p$ being too small ultimately yields a corrected $w_{i,t}$ which is too large, the solution conditions are always bracketed by $[w_{i,t}]_p$ and $w_{i,t}$. In making the new projection for $[w_{i,t}]_p$, it is not efficient to necessarily set the new value as either $w_{i,t}$ or $([w_{i,t}]_p + w_{i,t})/2$.

The reader may find figure 4 helpful with respect to the following discussion. After the first pass through the iterative loop $[w_{i,t}]_p$ and $w_{i,t}$ have bracketed the solution within some range. The upper limit of the range R_H, assumes the value of the greater of these and the lower limit, R_L, assumes the value of the lesser. The value for $[w_{i,t}]_p$ is reset to the midpoint between R_L and R_H (which for this projection only, also corresponds to the average of $[w_{i,t}]_p$ and $w_{i,t}$, and the second iterative pass

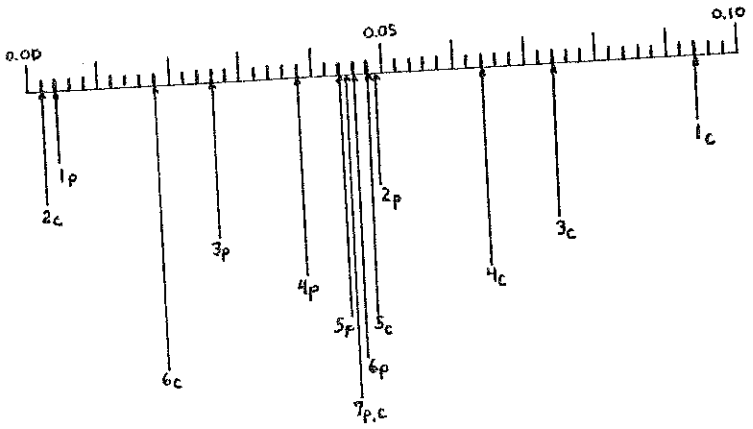

j	guess $[\omega_{i,t}]_p$	$\omega_{i,t}$ which results	Reset R_L to:	Reset R_H to:	$\frac{R_L + R_H}{2}$	case
1	0.004	0.094	0.004	0.094	0.049	II a,b,c
2	0.049	0.002	"	0.049	0.026	III a,b,d
3	0.026	0.074	0.026	"	0.038	II a,b,d
4	0.038	0.064	0.038	"	0.044	II a,b,d
5	0.044	0.048	0.044	0.048	0.046	II a,b,c
6	0.046	0.018	"	0.046	0.045	III a,b,d
7	0.045	0.045	(convergence obtained)			I

Figure 4

Hypothetical example of convergence scheme illustrating the various logic sequences described in the text

Notes

j : number of the iteration

1p : predicted value in first iteration, $[\omega_{i,t}]_p$ (similarly for 2p, 3p, etc.)

1c : corrected value of $\omega_{i,t}$ resulting from 1p (similarly for 2c, 3c, etc.)

R_L, R_H : low and high limits of range (" used where no change was made)

case : number of case illustrated by a given iteration (refer to the text)

is commenced. After any succeeding pass through the iterative loop, $[w_{i,t}]_p$ and the newly corrected value for $w_{i,t}$ are compared to the existing values of R_L and R_H. At this point, either R_L or R_H (or both) must be readjusted as discussed below. Note that prior to this readjustment, $[w_{i,t}]_p$ will still be equal to $(R_L + R_H)/2$. The logic sequence may fall into one of three cases.

Case I $w_{i,t} = [w_{i,t}]_p$

(a) This case would not be processed further since the convergence criteria would have detected this as the solution

Case II $w_{i,t} > [w_{i,t}]_p$

(a) This indicates the solution is greater than $[w_{i,t}]_p$ and less than $w_{i,t}$

(b) since $[w_{i,t}]_p > R_L$ (before readjustment), R_L is adjusted upward to the value of $[w_{i,t}]_p$

(c) if $w_{i,t} < R_H$ (before readjustment), then R_H is adjusted downward to the value of $w_{i,t}$

(d) if $w_{i,t} \geq R_H$ (before readjustment), then R_H is not adjusted

Case III $w_{i,t} < [w_{i,t}]_p$

(a) this indicates the solution is less than $[w_{i,t}]_p$ and greater than $w_{i,t}$

(b) since $[w_{i,t}]_p < R_H$ (before readjustment), R_H is adjusted downward to the value of $[w_{i,t}]_p$

(c) if $w_{i,t} > R_L$ (before readjustment), then R_L is adjusted upward to the value of $w_{i,t}$

(d) if $w_{i,t} \leq R_L$ (before readjustment) then R_L is not adjusted.

Note that each iteration will reduce the range $(R_H - R_L)$ by a minimum of 50% and may possibly reduce it by any amount between 50% and 99+%. After the readjustment of the range limits, the value of $[w_{i,t}]_p$ is reset to the midpoint of the range and the next iteration is commenced.

Experience with using the convegence scheme developed for this model has shown that setting the convergence criterion, σ, at 0.001 usually results in a simulation overall average of between 2 and 10 iterations depending on the other parameters of the system. Less stringent criteria of course reduce this average. Note that in the usual simulation, the humidity values (w) will likely be in the range of 0.01 to 0.10 $\frac{\text{kg } H_2O}{\text{kg dry air}}$. A convergence criterion of $\sigma = 0.001$ then requires convergence of $w_{i,t}$ and $[w_{i,t}]_p$ to within 0.00001 to 0.00010 $\frac{\text{kg } H_2O}{\text{kg dry air}}$.

The range $(R_H - R_L)$ after any iteration will be less than or equal to the width of the original range divided by a factor of 2^j where j is the number of that iteration. For j = 10 (after ten iterations), the range is at most 1/1000 of the original;

for j = 20, at most 1/1,000,000. $\lceil w_{i,t} \rceil_p$ is always the center of the range. Occasionally, however, for a particular node and timestep, this convergence scheme may allow the resultant values of $w_{i,t}$ to repeatedly fall outside the range even as $\lceil w_{i,t} \rceil_p$ closely approaches the (unknown) correct value. In such a case, many unnecessary iterations could be needed before $w_{i,t}$ actually converges to $\lceil w_{i,t} \rceil_p$. Using the previous paragraph's values for humidity range (0.01 to 0.10) and convergence criterion (σ=0.001) $\lceil w_{i,t} \rceil_p$ cannot vary from the (unknown) correct value by more than 0.0008 (in the worst case) after 17 iterations. Even if $w_{i,t}$ and $\lceil w_{i,t} \rceil_p$ have not converged, it can be safely assumed that $\lceil w_{i,t} \rceil_p$ and the (unknown) correct answer are then within the criterion. Such calculations permit one to specify an upper limit for the number of iterations (e.g., 17 for this example) appropriate for a given convergence criterion. This guards against unnecessary computation beyond the required accuracy. A guide for setting the maximum number of iterations ($\#_{max}$) is:

$$(\#_{max}) = (\log \sigma + \log w_{min}) \div (-\log 2) \qquad 23$$

where w_{min} is the minimum value of the expected humidity range. In the above example, σ = 0.001, w_{min} = 0.01, and $\#_{max}$ is calculated at approximately 16.6, i.e., 17 by equation 23. It should be noted that the number of iterations at a particular time and location rarely approaches $\#_{max}$ (if $\#_{max}$ is properly specified). The computer version of the model indicates to the user if and when this happens.

3.3 Computer Programming

The model discussed above has been programmed in FORTRAN IV as a subroutine to interface with the TRNSYS program developed by the Solar Energy laboratory of the University of Wisconsin (1977; Klein et al., 1974). The TRNSYS program was mentioned in an earlier section dealing with solar simulations. The drier subroutine program (and an accompanying subroutine program for solar grain drying controls) may be simply added to any current version of TRNSYS. Simulations of grain drying with solar energy may be routinely performed utilizing actual weather data as inputs by TRNSYS once this has been done.

3.3.1 DRIER SUBROUTINE:

The drier subroutine requires the specification of twenty two parameters, must receive four inputs which are variable over time from other TRNSYS subroutines, and calculates fifteen outputs at each timestep which may serve as the inputs for other subroutines. The TRNSYS drier component configuration is presented below in a format consistent with the TRNSYS manuals. (In presenting these in English units, the reader is asked to recall an earlier discussion explaining the reason for deriving the drier model to function with English units.)

Parameter No.		Description
1	L	- length of grain bed (ft)
2	D	- diameter of drier (ft)

3	N	- number of finite differences into which the model will divide the bed
4	ε	- the porosity or void fraction expressed as a decimal
5	ρ_s	- the density of the grain on a dry weight basis corrected for porosity (lb/ft^3)
6	W_{init}	- initial moisture content of the grain expressed as lb water per lb of dry grain
7	W_{min}	- minimum safe moisture specification (lb water/lb dry grain)
8	W_{ave}	- desired moisture content of grain (lb water/lb dry grain)
9	w_{init}	- initial intergranular humidity (rough approximation is acceptable; lb water/lb of dry air)
10	σ	- Convergence criterion (defined earlier; decimal fraction)
11	$\#_{max}$	- maximum number iterations to be allowed for any one finite segment during a given timestep (discussed earlier; positive integer)
12	C	- first dimensionless constant for Henderson's grain equilibrium moisture equation (Henderson, 1952) discussed earlier
13	B	- second dimensionless constant for Henderson's equation
14	n	- third dimensionless constant for Henderson's equation (exponent; may be non-integer)
15	Print	- time interval for optional internal printer (hours)

16	Δt	- timestep specification; must be same as specified for TRNSYS control statement (hours)
17	T_{init}	- initial (assumed uniform) temperature of the grain (°F)
18	C_1	- constant for heat capacity equation for moist grain $C_{ws} = C_1 + C_2 \cdot W$ (where C_{ws} is the heat capacity of the wet solid in BTU/lb of dry grain, °F and W is the moisture content of the grain in lb water/lb dry grain)
19	C_2	- (see parameter 18)
20	S_1	- constant for equation describing the latent heat of sorption (in excess of the latent heat of free water vaporization) for the particular grain $\lambda_s = (S_1 + S_2 \cdot W) \geq 0$ (where λ_s is the latent heat of sorption in BTU/lb of dry grain and W is the moisture content of the grain in lb water/lb dry grain)
21	S_2	- (see parameter 20)
22	REVERS	- control for choosing flow reversal or recirculation options (hours)

Some additional notes will be useful with respect to parameters 7, 8, 15, and 22. When the average moisture content of the entire grain bed reaches W_{ave} (parameter 8) a message is printed signalling that the desired termination time has been reached; the computer program does not terminate. If parameter 8 is specified as negative, the subroutine takes the absolute value for W_{ave} and assumes the negative sign as an instruction to print the termination message only when <u>both</u> the average moisture content

of the bed and the moisture content of the final segment before the outlet have reached W_{ave}. If the moisture level of any segment drops below W_{min} (parameter 7) a warning message is printed.

Parameter 15 controls the time interval between printings of internal temperature, humidity, and moisture content profiles. Average temperature and moisture content and the average number of iterations is also printed. The internal print commands are inactivated if parameter 15 is specified as negative.

Parameter 22 is an option controller. If it is set larger than the TRNSYS termination time, no option is indicated. If it is set less than the TRNSYS termination time, parameter 22 becomes the time interval between flow reversals. The subroutine switches inlet and outlet location at each flow reversal but internal profile printers continue to be based on position zero being the initial inlet location. If parameter 22 is set between 0 and -1, it signals that the recirculation option is specified. The absolute value of parameter 22 then becomes the recirculated fraction; e.g., a value of -0.4 indicates 40% recirculation.

Input no.		Description
1	T_{in}	- dry bulb temperature of inlet air (°F)
2	T_{wb}	- wet bulb temperature of ambient air (°F)
3	$\dot{m}$	- mass flow rate of inlet air (lb/hr)

4	T_{amb}	- dry bulb temperature of ambient air (°F)

Output no.		Description
1	T_{in}	- same as input 1
2	T_{wb}	- same as input 2
3	$\dot{m}$	- same as input 3
4	$H_{s(I/O)}$	- enthalpy in air entering system (e.g., solar collector inlet) minus enthalpy in drier exhaust air minus latent heat of evaporated moisture (BTU/hr)
5	T_1	- temperature of inlet layer (°F)
6	W_1	- moisture content of inlet layer (lb water/lb dry grain)
7	$T_{B,ave}$	- temperature averaged over entire grain bed (°F)
8	$W_{B,ave}$	- moisture content of grain averaged over entire grain bed (lb water/ lb dry grain)
9	T_n	- temperature of outlet layer (n^{th} segment; °F)
10	w_n	- humidity of outlet air (lb water/ lb dry air)
11	W_n	- moisture content of outlet layer (n^{th} segment; lb water/lb dry grain)
12	$M_{I/O}$	- mass flow of water as humidity out of system minus mass flow of water into system $M_{I/O} = \dot{m}(w_n - w_{in})$; (lb/hr)
13	M_{BED}	- total moisture content of bed minus initial moisture content of bed (lb)

14	$H_{D(I/O)}$	- enthalpy in drier inlet air minus enthalpy in drier outlet air minus latent heat of evaporated moisture (BTU/hr)
15	H_{BED}	- enthalpy of grain bed minus initial enthalpy of grain bed (BTU)

Some additional notes will be useful with respect to the mass and energy balance outputs. A mass balance may be constructed over the drier between times t=o and t=j as follows

$$\sum_{t=o}^{t=j} (M_{I/O} \cdot \Delta t)_t = M_{BED} \tag{24}$$

An energy balance may be constructed over the drier between times t=o and t=j as follows

$$\sum_{t=o}^{t=j} (H_{D(I/O)} \cdot \Delta t)_t = H_{BED} \tag{25}$$

Another energy term is also available to aid the user in formulating an energy balance over the entire system including the solar collector; drier, and auxiliary heater. Between times t=o and t=j the following applies

$$\sum_{t=o}^{t=j} (H_{S(I/O)} \cdot \Delta t)_t + \sum_{t=o}^{t=j} (E_{sol} + E_{aux})_t = H_{BED} \tag{26}$$

Where E_{sol} and E_{aux} represent useful energy inputs to the system from the solar collector and auxiliary heater respectively as obtained from other subroutines. Environmental losses from the drier are not considered.

3.3.2 DRIER CONTROLS SUBROUTINE:

A supplemental subroutine contains control functions for the drier which make it easier to write TRNSYS simulations of solar grain drying.

The drier control subroutine requires the specification of seven parameters, accepts four inputs which are variable over time from other TRNSYS subroutines, and calculates three outputs (control functions).

Parameter no.		Description
1	W_{init}	- the initial moisture content of the grain (same as drier parameter 6)
2	W_{ave}	- desired moisture content of the grain (same as drier parameter 8)
3	t_{max}	- desired target time for termination, i.e., for achieving the final moisture content (in order to avoid spoilage or meet a production or shipping date, etc.)
4	Lag	- the amount (expressed as a decimal fraction) by which actual drying progress may be allowed to fall behind a hypothetical linear schedule from the initial moisture at time zero to the desired moisture at the target time (more on this later)
5	Recalc	- the length of time (hours) between each recalculation of the subroutine's control functions
6	Frac	- minimum allowable blower flowrate expressed as a decimal fraction of the flowrate specified in the simulation (When Frac is set at less than 1.0, the flow reduction option is being selected for periods of no thermal gain.)

7	T_{max}	- maximum desired temperature (°F) of inlet air to the drier (Parameter controls a partial bypass of the collector if necessary to prevent overdrying

Input no.		Description
1	H_T	- incident solar radiation on tilted surface (Output 1 from subroutine type 16 - solar radiation processor)
2	$W_{B,ave}$	- average moisture content of grain bed (Output 8 from drier subroutine)
3	T_{col}	- outlet temperature (°F) of solar collector (Output 1 from subroutine type 1)
4	T_{amb}	- dry bulb temperature (°F) of ambient air (same as input 4 to drier subroutine)

Output no.		Description
1	I_{aux}	- auxiliary heater control (1 is on; 0 is off)
2	OUTCON	- blower fractional flowrate control
3	DAMPER	- fractional bypass control

The value of the auxiliary heater control output is determined as follows. At the frequency determined from Recalc (parameter 5), the subroutine checks the drying progress.

$$(\text{progress}) = \left[\frac{W_{initial} - W_{average}}{W_{initial} - W_{desired}}\right]$$

The elapsed time as a fraction of the target time, t_{max}, is determined:

$$(\text{elapsed time fraction}) = (\text{time} - \text{time zero})/(t_{max})$$

If (progress)$\cdot$(1 + Lag) $<$ (elapsed time fraction) then the auxiliary heater control I_{aux} if set to 1 (or to zero if the opposite is true). In this manner the addition of auxiliary heat may be controlled by the acceptability of drying progress. The first five parameters do not insure that drying to a given level will be accomplished by a given time. They merely determine when auxiliary heat may be needed to keep on schedule. If the fifth parameter is set to some reasonable time (e.g. 6 hours), this procedure would be analagous to a manual control where the operator would check the moisture content, and if behind schedule, could turn on a thermostatically controlled auxiliary heat source. When the auxiliary control function is zero, no auxiliary heat may be added; when the control function is 1, then auxiliary heat may or may not be added according to the auxiliary heater thermostat and the instantaneous energy levels supplied by the solar collector.

A value of the blower control must be determined when the flow reduction option is specified. The control subroutine makes it possible to reduce the flow to minimum aeration levels during periods of no thermal gain. If this option is specified by setting Frac less than 1.0, the control unit sets the blower control function to the specified fraction of the usual flow rate whenever there is a period of no solar radiation and no need for auxiliary supplement. This would be analagous to a manual control where the operator would reduce the flow to minimum levels in the evening and increase the flow to operating levels in the

morning whenever the drier was maintaining adequate progress. If the flow reduction option is not desired, Frac (parameter 6) must be set at 1.0.

The third control function performed by this subroutine is to determine the damper setting (to be used as input 3 to a TRNSYS flow diverter subroutine) for a partial bypass of the collector. When used in conjunction with TRNSYS flow diverter and tee piece subroutines, the control subroutine dictates (via output 3) that ambient air will be mixed with solar heated air as necessary to keep the grain inlet temperature below T_{max} (parameter 7). Total air flow remains constant; the proportions of heated and ambient air are varied.

3.3.3 COMPUTER LISTINGS:

Complete FORTRAN listings of the drier subroutine and of the solar drier control subroutine are included in the appendix. The drier subroutine calls upon an external Real Function to calculate equilibrium moisture contents. This function is also listed in the appendix.

3.4 Use of the Computer Model and Subroutines

The computer version of the drying model is intended to be used with the TRNSYS program of the University of Wisconsin's Solar Energy Laboratory.

3.4.1 TRNSYS SIMULATIONS OF SOLAR GRAIN DRYING:

The basic simulation of a simple grain drier with solar heated air is set up using the following components:

1 card reader (actual weather data input)
2 solar radiation processor (determines radiation on inclinced surface)
3 drier control unit
4 blower
5 flow diverter
6 flat plate collector (air)
7 tee piece
8 auxiliary heater
9 grain drier
10 integrator
11 printer

Figure 5 shows a component diagram and figure 6 shows a TRNSYS block diagram of such a system.

The drier solves all differential equations internally without the aid of the TRNSYS differential equation algorithims.

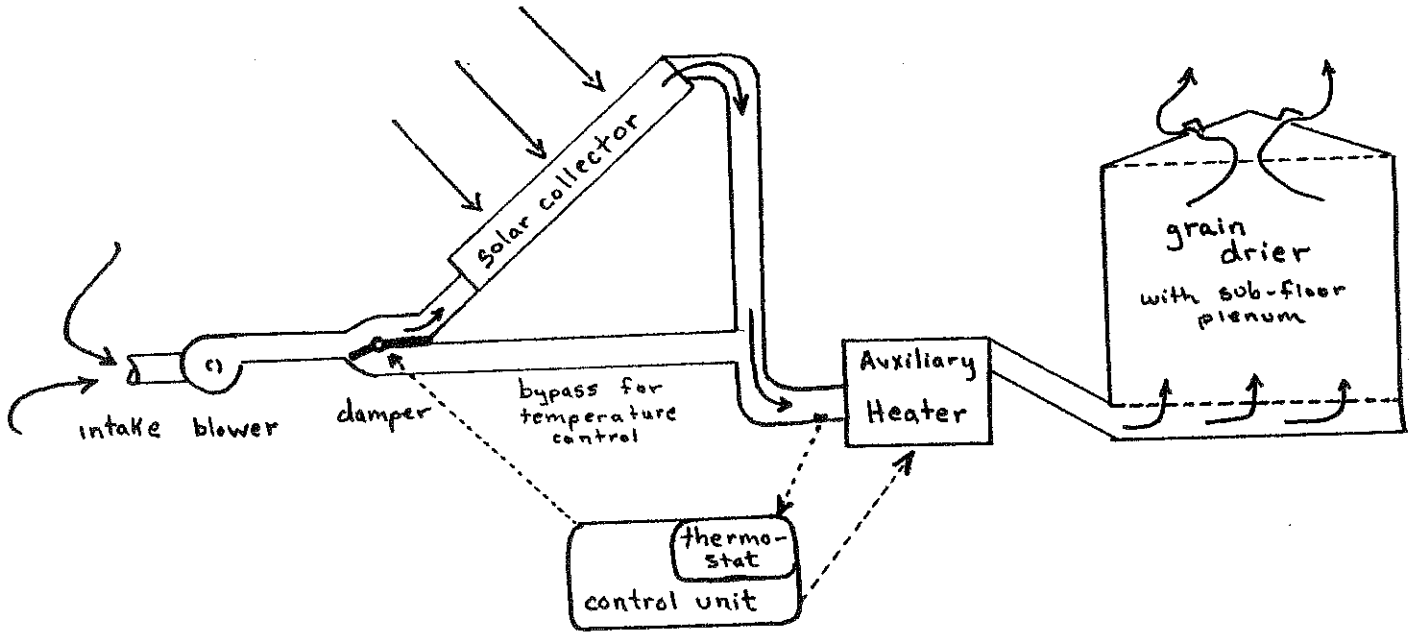

Figure 5 : Simple Solar-Supplemented Grain Drier

Figure 6 - TRNSYS SIMULATION BLOCK DIAGRAM

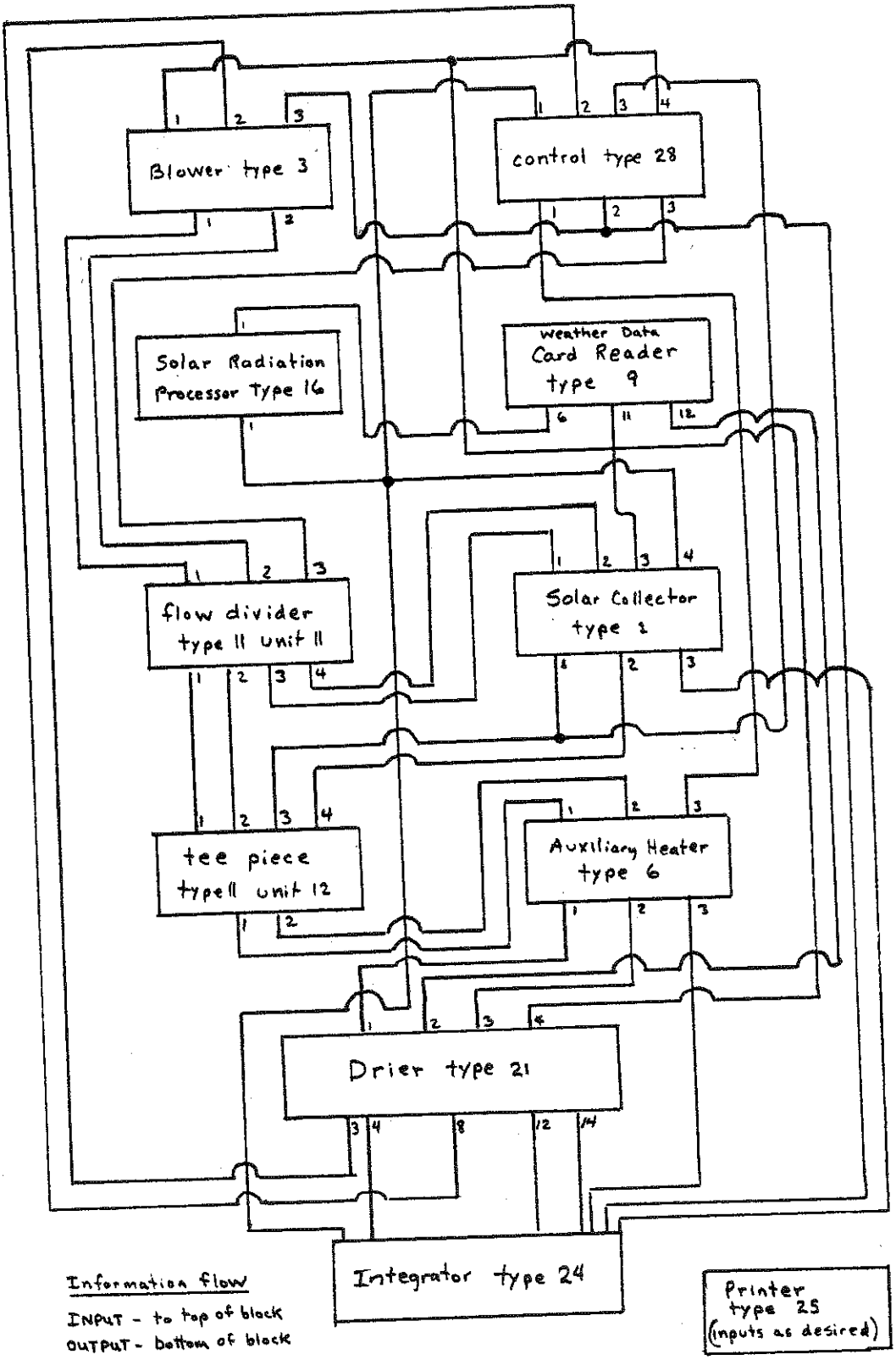

Solving the equations within the drier subroutine allows the use of larger time steps and a smaller number of finite segments or nodes than when using the TRNSYS integrator. The drier's internal solution is computationally more efficient for these particular equations than the TRNSYS integrator's solution and saves computer time. Specification of an unacceptably large timestep or an unacceptably small number of nodes can be detected by poor mass and energy balances.

3.4.2 SPECIFICATION OF TIMESTEP, NODES, AND OTHER OPERATIONAL CRITERIA:

The model accepts any number of finite elements or nodes (N) between 1 and 50 and any value of timestep (Δt). From a study of mass and energy balances closures, it appears that a value for N of 10 to 12 and a value for Δt of 0.10 to 0.20 hours is generally sufficient. TRNSYS error tolerances should be specified between 0.10 and 0.01.

The convergence criterion σ and the maximum iterations parameter $\#_{max}$ were explained in the discussion of the model's derivation. A setting of σ anywhere between 0.001 to 0.010 makes very little or no difference in the results but may affect computing time. The setting of $\#_{max}$ was covered earlier. If the internal profile print option is utilized, the average number of iterations per node per timestep is indicated each time profiles are printed.

Setting the target time and allowable lag for the drier control unit may be fairly straight forward if one employs an auxiliary heater that achieves high output temperatures irrespective of inlet temperatures. More realistically, heaters for agricultural driers have a constant thermal output which increases temperatures to approximately 3°to 11°C (5°to 20°F) over ambient (Brooker, Bakker-Arkema, and Hall, 1974); or according to another investigator, 4°C (7°F) over ambient (Peart and Foster, 1975). In this case the auxiliary supplement may not necessarily be able to get the drying back on schedule if the drying progress lags too far behind. Therefore setting the target time and allowable lag may require some trial and error. Depending on heater capacity, the allowable lag should likely be set somewhat less than the desired target time divided by the absolute maximum tolerable time.

3.4.3 BUILT-IN OPTIONS:

The basic solar grain drying system with various options as it might be simulated was discussed earlier. Options introduced earlier include a thermostatically controlled damper to limit the temperature of inlet air to the drier, a flow reduction option, a flow reversal option, and a flow recirculation option.

Only the recirculation option needs further discussion. The subroutine normally calculates inlet absolute humidity based on ambient dry bulb and wet bulb temperatures. However, in the

recirculation option, the model calculates the inlet absolute humidity as a weighted average (based on the amount recirculated) of ambient air absolute humidity and the drier exit air absolute humidity. To execute a simulation with recirculation, the user must set the final drier parameter as explained earlier (to direct the subroutine to calculate the humidity of the mixed inlet air) and must add a TRNSYS flow mixer component ahead of the blower and collector (to properly determine the temperature of the mixed inlet air to the collector).

4.
RESULTS AND CONCLUSIONS

The computer model of this study allows conducting long term experiments in a short time by simulation. Several sets of simulations were run in each of the various subcategories listed below:

Simulations utilizing only the drier component

a. constant inlet conditions

b. comparison against published experiments

c. comparison against Hukill (1947) logarithmic theory

Simulations of solar grain drying

a. varying collector inclination

b. varying collector area and/or mass flow rate

c. reduction of flow during periods of no thermal input

d. partial recirculation of drier outlet air

e. flow reversal

With the exception of the flow reversal simulations, the other solar grain drying simulations were all very similar in design and in specific grain and drier properties and characteristics. In that manner, the results of changing one or more operating parameters may be better analyzed.

4.1 Non-Solar (Drier only) Simulations

4.1.1 CONSTANT INLET CONDITIONS

The present model generates an equilibrium set of temperature, humidity, and moisture content as a function of distance and time. The process state at any or all points in distance and time can be shown on a psychrometric chart. For the case of constant inlet conditions, all points follow process states along the same path (Figure 7). The initial bed state, point 1, is indicated by a single coordinate pair on the psychrometric chart. The final state of the bed is that in equilibrium with the inlet air, point 3. Point 2 is at the intersection of the line of constant percent humidity which passes through point 1 and the constant enthalpy line which passes through point 3. The drying progress predicted by the computer model follows the humidity line from 1 to 2 and then the enthalpy line from 2 to 3. This type of drying representation has been previously documented and described (Banks, 1970; Banks, 1971; Close and Banks, 1971; and Sutherland, Banks, and Griffiths, 1971).

The model produces two fairly sharp drying fronts for the case of constant inlet conditions and an initially uniform bed. Refer to figures 8 a, b, and c which illustrate front progression at arbitrary times. These figures do not start at time zero; fronts are already established at time t_1. Subscripted ordinate values correspond to points on figure 7. The fronts move through

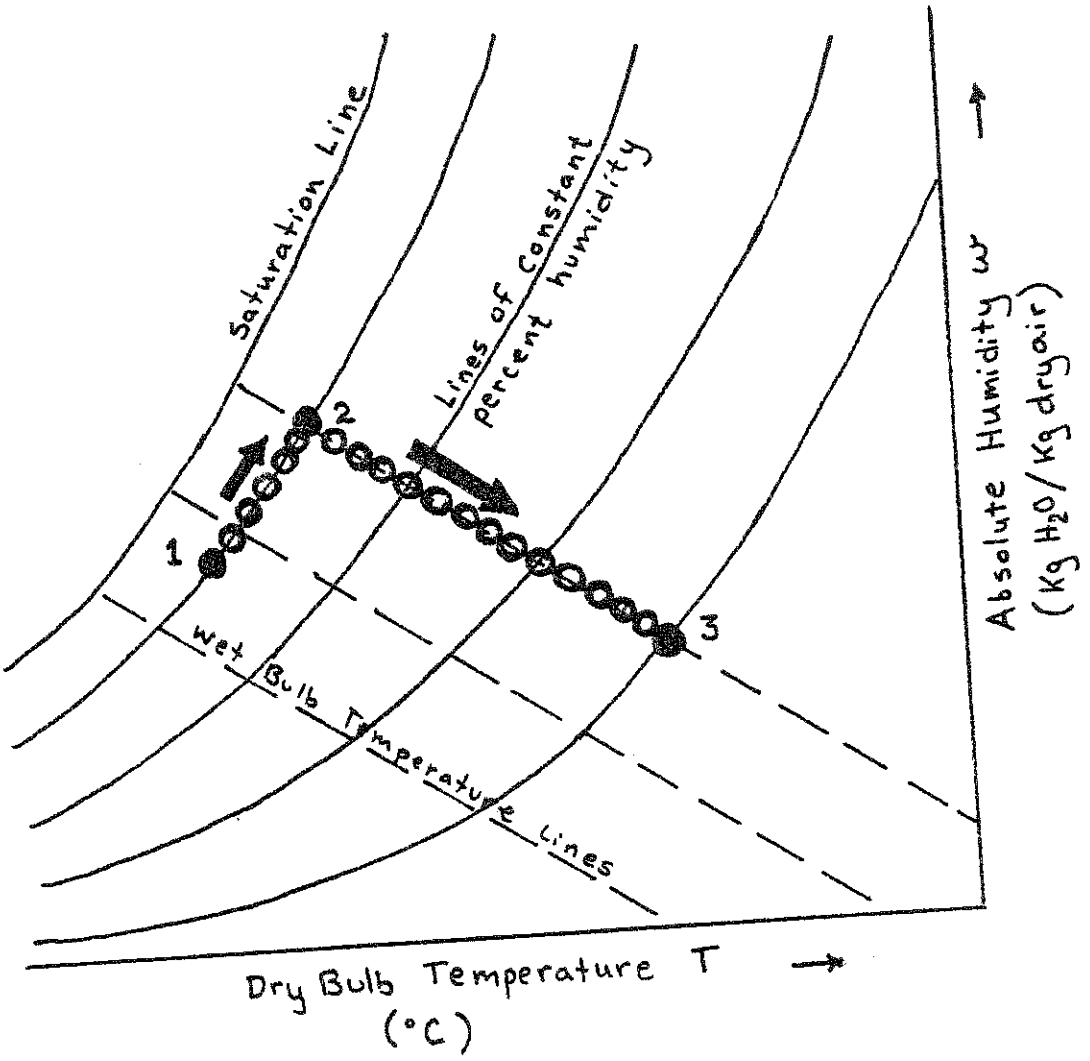

1 ● T and w in equilibrium with initial grain moisture

2 ● intermediate T and w

3 ● T and w of inlet air

Sketch depicting drying progress on a psychrometric chart (in terms of equilibrium temperature and humidity)

Figure 7

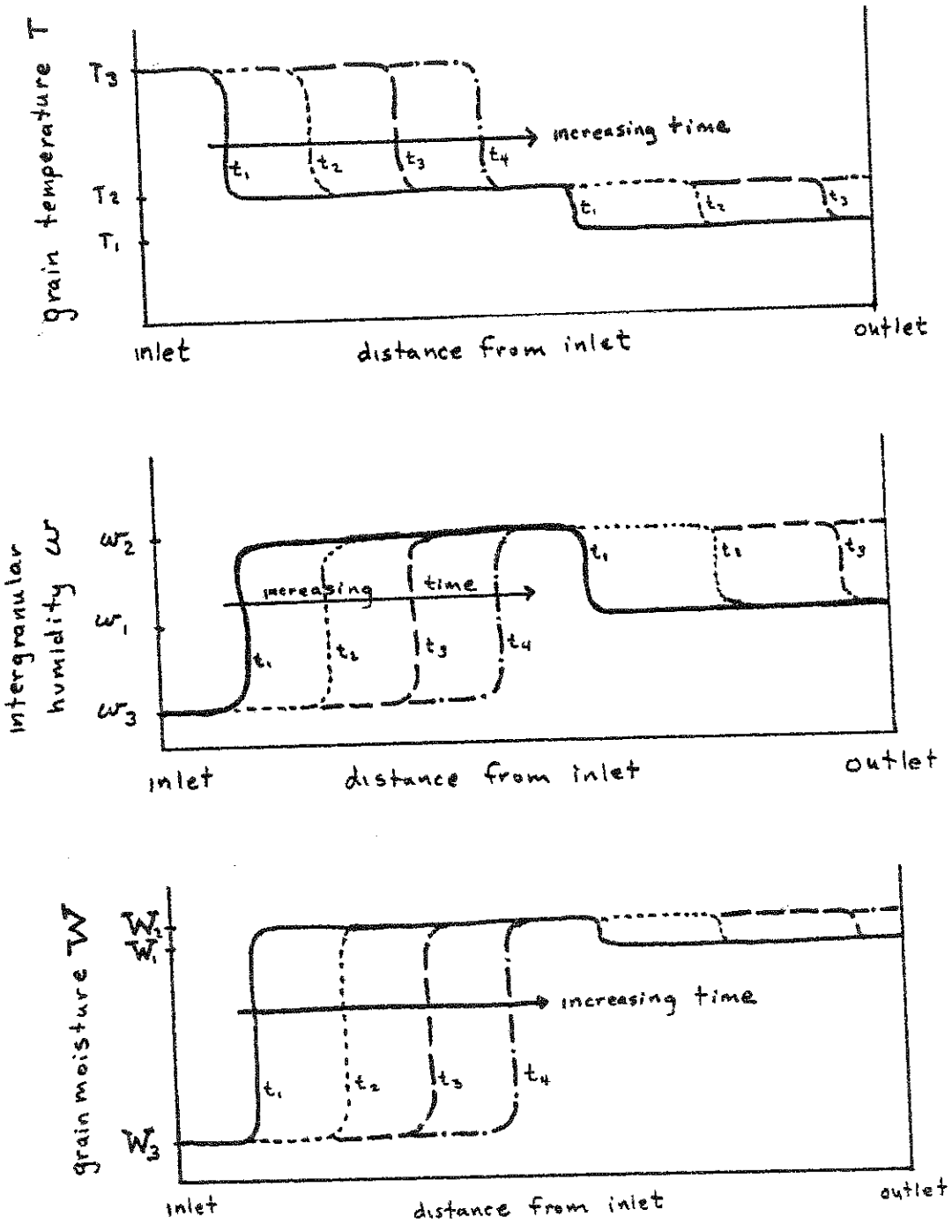

Sketch of internal T, w, and W profiles as a function of distance and time showing movement of two fronts

Figure 8

the bed at different speeds; the first very quickly and often emerges before the second front is completely established. This type of two front behavior has been documented also in the above references. Figure 9 shows temperature data from simulated results in a constant inlet conditions case illustrating the typical even progression of the second front through the bed over time and the steep parallel slopes. The first front proceeds similarly but much faster and had already exited in the case of Figure 9.

4.1.2 COMPARISON AGAINST PUBLISHED EXPERIMENTS:

This section discusses results of simulated drying experiments based on published literature. Few studies present both sufficient input data to allow simulation and output data for meaningful comparison to simulated results. Of those experiments simulated, all of the grain driers were laboratory scale equipment of less than 0.64m (2.0 ft) in length. Length of experiments was less than 8 hours.

In general, the average moisture content versus time is the most important information about drying when full-scale drying operations are considered. Even for those references which lend themselves to simulation, the relationships for equilibrium moisture content, specific heat of moist grain, and the latent heat of sorption for the specific grain were not presented, and were approximated for simulation purposes. Table 1 summarizes the parameters and inputs of those experiments which were

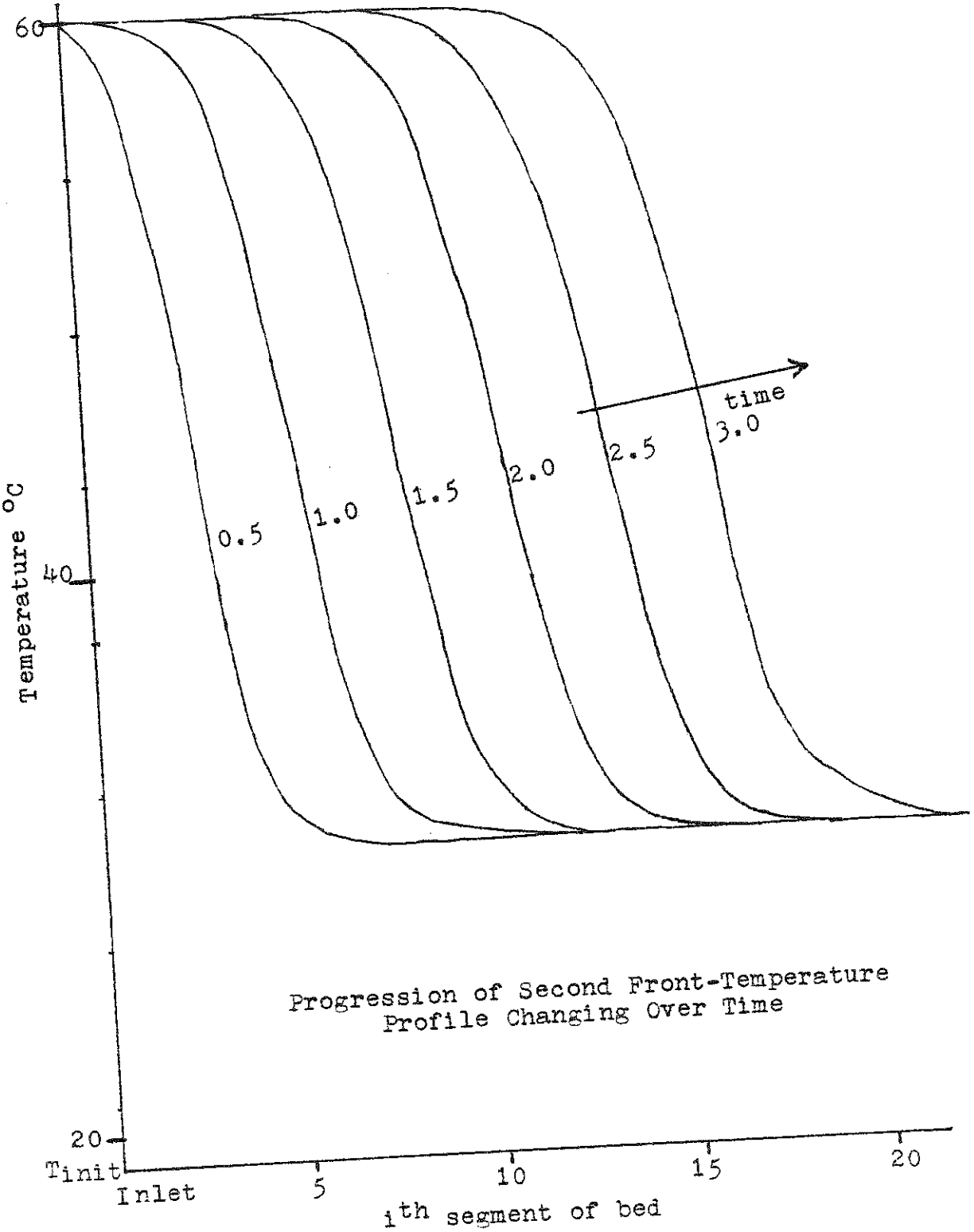

Progression of Second Front-Temperature Profile Changing Over Time

Figure 9

Table 1

Published Laboratory Scale Experiments which were Simulated

Refer to figure	10	11	12	12
Grain	wheat	corn	barley	barley
Bed length (m)	0.62	0.46	0.30	0.30
Cross section (m^2)	0.09	0.09	0.29	0.29
Porosity	0.45	0.45	0.45	0.45
Void free density (kg/m^3)	1140	990	1270	1270
Initial temperature (^oC)	19	29	21	21
Initial moisture fraction	0.247	0.376	0.346	0.342
Mass flow rate (kg/hr)	118	104	185	90
Constant inlet temperature (^oC)	60	50	68	60
Constant inlet humidity (mass ratio)	0.0084	0.022	0.0060	0.0058

simulated (Clark and Lamond, 1968; Woodeforde and Lawton, 1965; Woodeforde and Osborne, 1961; and Boyce, 1965). These experiments employ constant inlet conditions.

Figure 10 compares the experimental and simulated results of drying wheat. The integrated total weight loss is plotted versus time. Both experimental and predicted lines are nearly linear over time; the maximum descrepancy is approximately 2% at the conclusion of the experiment.

Figure 11 is for an experiment drying corn. Agreement is not quite as good here.

Figure 12 shows two experiments in which barley was dried. The lower set of plots is for the experiment with the higher flow rate; the barley dried from 0.346 (dry basis) to 0.145 moisture content in 4.25 hours. The upper set of plots on figure 12 is for the experiment with the lower flow rate; the barley dried from 0.342 to 0.157 in 9.5 hours. Again the drying curves are seen to be linear and very good agreement is obtained.

It has been noted in the literature (Spencer, 1972) that the drying curve of average moisture content versus time is approximately linear for deep bed grain driers over most of the drying time if inlet conditions are constant. When the average moisture content has nearly reached equilibrium with the inlet air, the states asymptotically approach the equilibrium value.

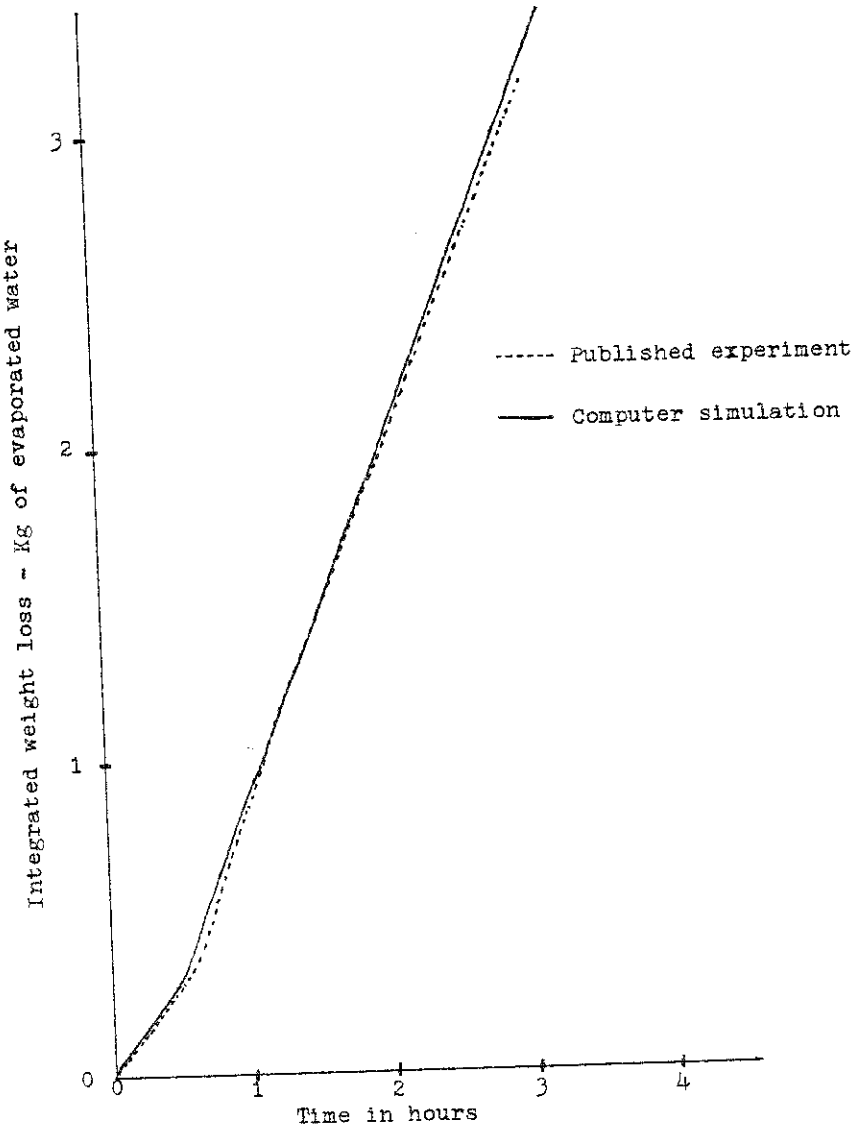

Integrated moisture loss versus time
in laboratory scale drier using wheat
Figure 10

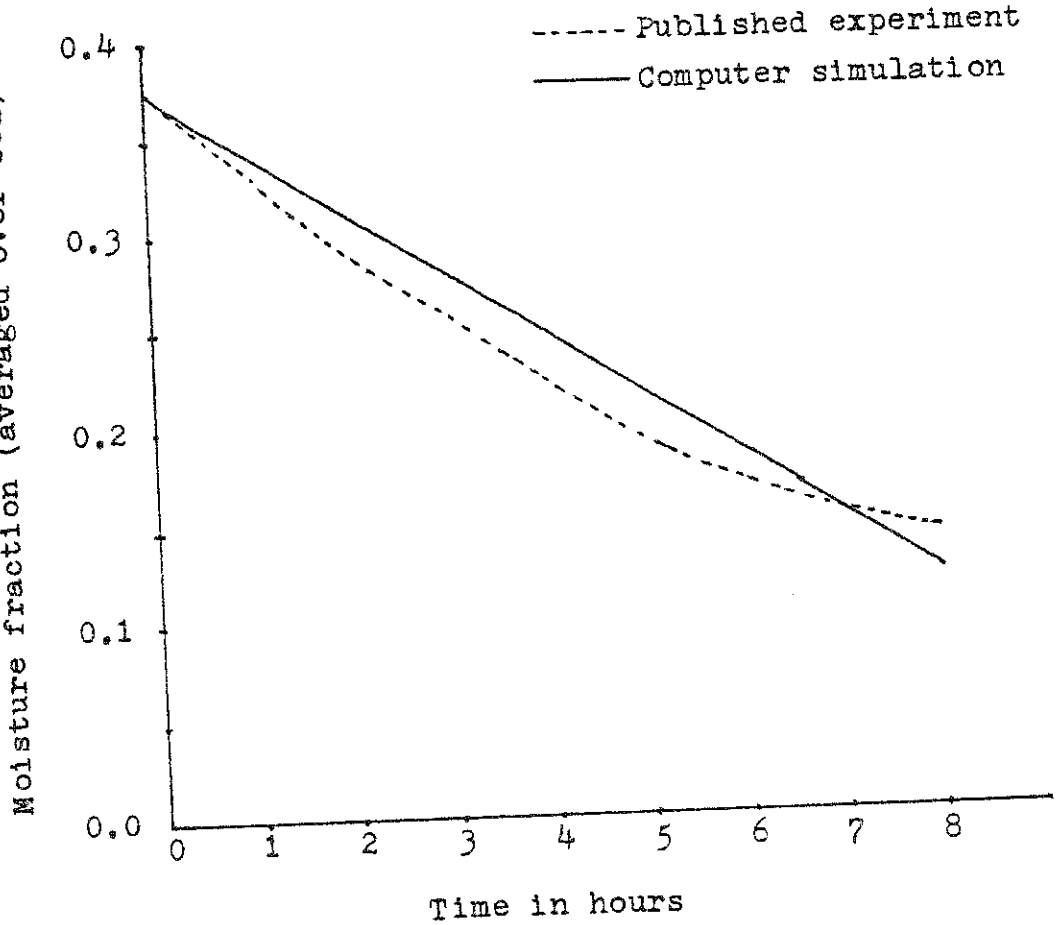

Average moisture content of corn versus time in laboratory-scale drier

Figure 11

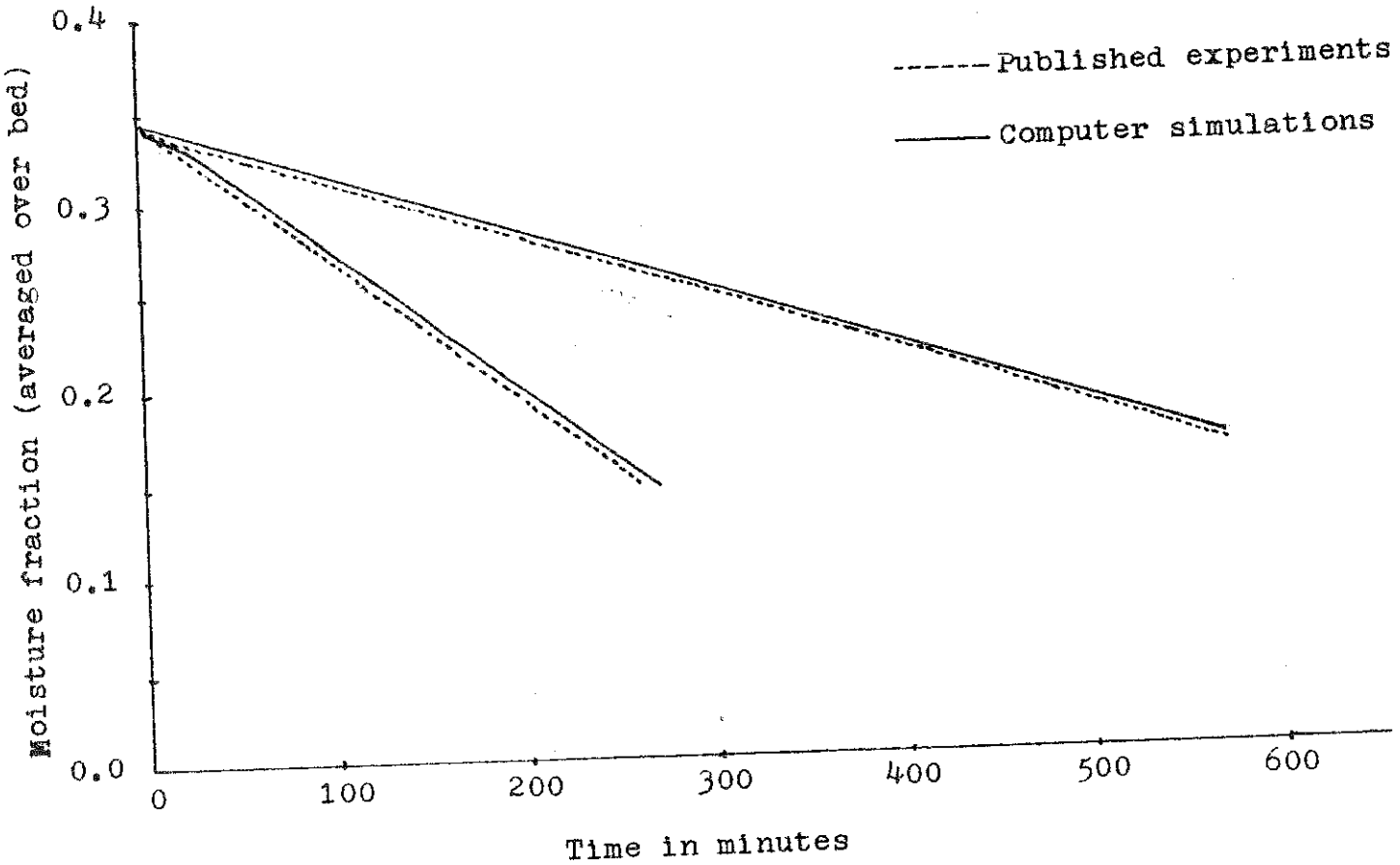

Average moisture content of barley versus time in laboratory-scale drier

Figure 12

4.1.3 COMPARISON AGAINST HUKILL (1947) LOGARITHMIC THEORY:

Hukill's characteristic logarithmic model is based on simplifying assumptions about heat and mass transfer in grain beds which result in a set of equations for which graphical solutions were obtained. For the case of constant inlet conditions and an initially uniform bed, Hukill's graphical solutions may be used for approximate design purposes.

In comparing the internal moisture content profiles generated by the present model with Hukill's graphical profiles, it was seen that the respective fronts of both models, move through the bed at approximately the same speed. (Initially, Hukill's fronts move slightly slower and then speed up to move slightly faster than average at longer times - apparently due to his assumption of constant latent heats; discussed later.) Sutherland, (1975) noted that the respective fronts of an equilibrium model and of the characteristic logarithmic model travel at the same speed despite the differences in slope.

The present model includes the assumption of infinite transfer coefficients while Hukill considered the internal diffusion of moisture in the kernel to be rate-controlling. Consequently, the profiles of the present equilibrium model are more steeply sloped than Hukill's. And Hukill's model results in a wider front than that of the equilibrium model with Hukill's front width dependent upon the assumed rate of internal diffusion.

After a short preliminary time period needed for the trailing edge of the logarithmic model drying front to become completely established within the bed, then each model's profiles of moisture content versus distance for various times tend to intersect at a moisture ratio of $MR=(W_t-W_e)/(W_{init}-W_e) = 0.5$. The integrated areas under the curves are approximately equal for both the present model and Hukill's despite the differences in slope. As shown in fugure 13, the present model predicts essentially the same average moisture content versus time as Hukill's plots. Hukill's solution assumed that the sum of the latent heats of sorption and vaporization is constant. This assumption predicts moisture contents slightly high early in the drying process (when moisture contents are high), most accurate at middle times (when moisture contents are near average of the run), and too low at longer times (when moisture contents are below that averaged over the drying run). Note in figure 13 that Hukill's results are indeed slightly higher than the linear prediction of the present equilibrium model at the earlier times, coincident at the middle times, and slightly lower at longer times.

Average moisture ratio of corn bed versus time
based on Hukill model and present model

Figure 13

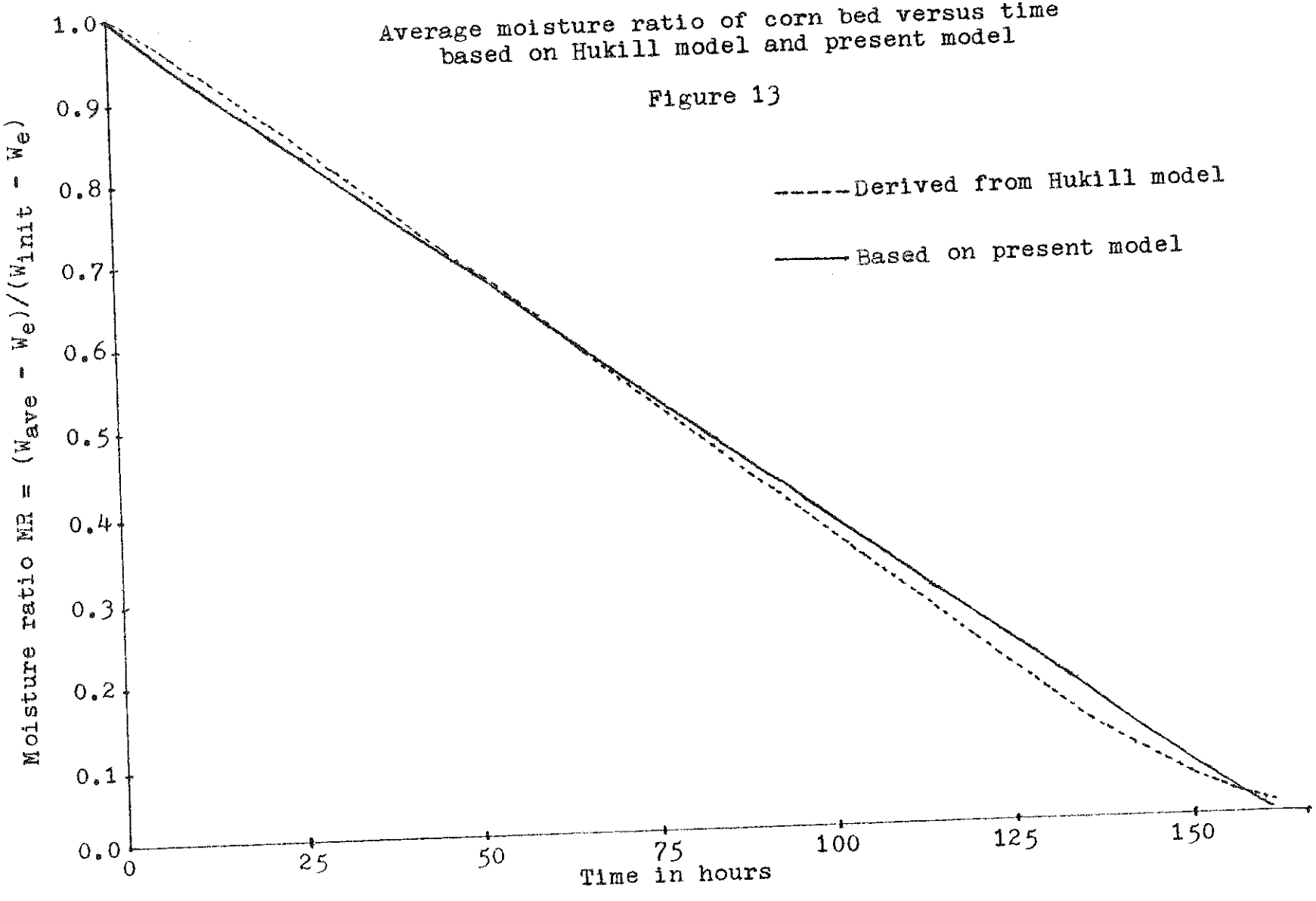

4.2 Simulations of Solar Grain Drying

The accuracy of predictions generated by the model for simulations with variable inlet conditions has not been verified for lack of appropriate experimental data. The simulations of solar grain drying are based on the fact that nothing in the model restricts it to constant inlet conditions.

4.2.1 COMMON PARAMETERS FOR SIMULATIONS OF SOLAR GRAIN DRYING:

The solar grain drying experimental simulations were designed to represent actual practice and to utilize actual weather data. The Madison "design year" (Klein, 1976) consists of those months which most closely match the long term average temperature and insolation. The simulations were based on drying shelled corn initially at 0.40 moisture fraction (dry basis) and 4.4°C (40°F) starting at 6:00 a.m. on October 1 of the Madison design year.

The drying bin was assumed to be 3m (10 ft) deep and 5.5m (18 ft) in diameter. The void free (particle) density of the corn was assumed to be 1102 kg/m^3 (68.78 lb/ft^3) and the void fraction was assumed to be 0.45 (Brooker et al., 1974). The heat capacity of moist corn was represented by

$$C_{ws} = (0.34 + 0.009\ W)\frac{BTU}{lb°F} \times 4.187\ \frac{KJ/Kg\ °C}{BTU/lb°F}$$

(Thompson et al., 1968; Brooker et al., 1974).

The latent heat of sorption (in excess of the latent heat of vaporization of free water) was represented by

$$\lambda_s = (485\text{-}1796\ W)\frac{BTU}{lb} \times 2.326\ \frac{KJ/Kg}{BTU/lb} \text{ and } \lambda_s \geq 0.0$$

based on an analysis of data presented by Brooker et al. (1974).

Based on empirical results published by Thompson et al. (1968) and equilibrium curves published by Brooker et al. (1974), the coefficients for the Henderson equilibrium moisture relationship (equation 22) were taken to be

$C = 0.95 \times 10^{-5}$

$B = 460$

$n = 1.9$

South facing flat plate collectors with single glass covers were used. The collectors were assumed to be constructed of modules each 1m by 2m with a air space of 0.05 m (2 inches) between the glass and the plate. For purposes of determining loss coefficients, F' factors, and pressure losses, it was assumed that the air flow through each collector module would be an equal fraction of the total air flow. Other collector configurations might be better, but they were not studied.

The emissivity of the plate was assumed to be 0.94. Using the methods and equations of Duffie and Beckman (1974), the following values were calculated for the collector design and operating flow rates:

transmissivity = 0.88

$F' = 0.95$

Loss coefficient $U_L = 5.68$ W/m^2 (1.0 BTU/ft^{2}hr°F)

Collector inclination was varied between 0° and 90° (vertical). The collector area was varied between 18 m^2 (200 ft^2) and 204 m^2

(2200 ft^2) and the mass flow rate between 4500 kg/hr (10,000 lb/hr) and 20,400 kg/hr (45,000 lb/hr). These values of air flow and collector area were based on earlier mentioned recommendations for flow and area as functions of bin capacity. In this case, bin capacity was 72 m^3 (2545 ft^3; 2036 bushels).

The auxiliary heater was assumed to be capable of raising the air temperature a maximum of 3.9°C (7°F). Accordingly, the maximum heating rate of the heater was directly proportional to the flow rate.

A timestep of 0.2 hours and 10 finite difference segments were chosen (each segment was 0.3m (1.0 ft)). The TRNSYS tolerances were set at 0.1 and the drier's internal convergence criterion $\mathcal{O}$ was set at 0.01.

The goal was to dry the entire bed to approximately 0.145 moisture fraction within 288 to 366 hours beyond the starting time. The initial and final moisture contents and the desired times were determined based on material presented by Brooker, et al. (1974) and Foster and Peart (1976). Brooker, et al. state that the optimum moisture contents and usual moisture contents of shelled corn at harvest are 0.39 to 0.47 and 0.16 to 0.43 respectively (dry basis). For safe storage of up to one year, shelled corn should be dried to a moisture content of less than 0.15 (dry basis). To prevent over drying, the temperature of solar heated air was limited to 29.4°C (85°F), and the maximum thermostat setting of the auxiliary heater was set at 21°C (70°F).

The pressure drop through each collector module is negligible compared to the drop through the grain and through the ducts. For large collectors, the ducts, headers, and changes in flow direction and velocity between the collectors and headers might produce a significant pressure drop relative to that of the grain bed.

In evaluating systems' performances, it was assumed that the "level of dryness" would be checked by an operator at 6:00 A.M., 12:00 noon, and 6:00 P.M. The termination of an experiment occurred only at one of those times.

This section has summarized the common design basis for the simulations to be discussed in the following sections. All simulations utilized the same parameters inputs and procedures except as otherwise noted in respective sections.

4.2.2 VARYING COLLECTOR INCLINATION:

Simulations were run in which the slope of the solar collector was varied from 0° to 90° (vertical). A collector with $F' = 0.90$, an area of 204 m^2 (2000 ft^2) and a flow rate of 9070 kg/hr (20,000 lb/hr) were used. No auxiliary heat was employed. All such simulations were compared at 180 hours.

Based on integrated collector solar energy, collectors inclined at 30° to 43° (angle of latitude) performed similarly in this test. Of those inclinations tested, 35° collected the most energy although only slightly higher than 30° and 43°.

Refer to table 2.

Many of the collectors used in grain drying have been installed either horizontally on the ground or vertically on the side of a building or bin. This causes a significant energy penalty (in Madison during October). At 0° (horizontal), the incident and collected energy are 82% and 94% respectively of that at 35°. At 90° (vertical), these percentages are only 57% and 78% respectively.

4.2.3 VARYING COLLECTOR AREA AND MASS FLOW RATE:

Simulations were run with collector areas varied between zero and 204 m^2 (2200 ft^2) and with mass flow rates varied between 4500 kg/hr (10,000 lbs/hr) and 20,400 kg/hr (45,000 lbs/hr). Flow rates below 11,340 kg/hr (25,000 lb/hr) were insufficient to dry the grain to the desired 0.145 moisture fraction within 366 hours, and were not considered further. The zero collector area simulations determined a "base line drying response" for non-solar grain drying operations.

4.2.3.1 COMPARISON OF DRYING TIME; AUXILIARY USE; PERCENT SOLAR:

Figure 14 shows the time required for the various mass flow rate and collector area combinations to dry the grain to the desired criterion. Auxiliary-only simulations (zero collector area) required less time than simulations employing a small collector plus auxiliary. This is due to the particular criteria

Table 2

Performance at various collector inclinations at 180 hours

Inclination (degrees)	Integrated incident solar radiation per unit area (GJ/m^2)	Integrated collected solar radiation on 186 m^2 (GJ)	Collector efficiency (%)	Average final bed temperature (°C)	Energy balance closure (%)
0	0.0853	5.93	37	16.6	99.8
30	0.1031	6.30	33	16.7	99.8
35	0.1035	6.31	33	16.9	99.8
43	0.1023	6.26	33	16.8	99.8
50	0.0997	6.18	33	16.7	99.8
90	0.0587	4.94	45	16.5	99.9

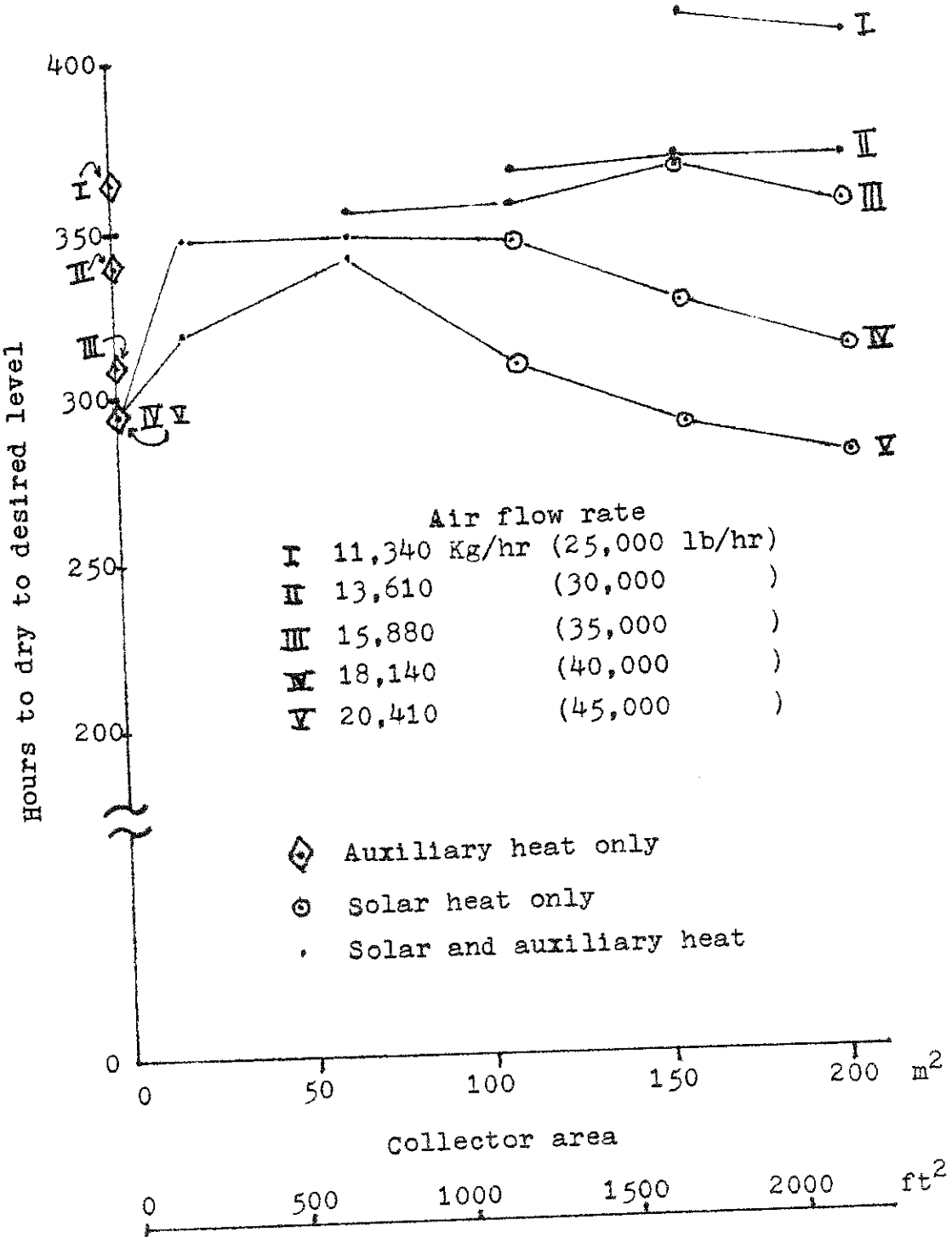

Drying time for various flow rates and collector area combinations

Figure 14

which determine when the auxiliary heater is turned on and off in the solar grain drier. These control criteria (discussed in drier control section) were set to minimize use of the auxiliary rather than to decrease the overall drying time. In auxiliary-only simulations, the auxiliary heat is supplied continuously. This may result in a higher rate of thermal input than with the auxiliary and small collector combination where the auxiliary may frequently be turned off. If a user is willing to accept an energy penalty, it is possible to adjust the control criteria to insure that addition of any size collector will reduce the required drying time.

Figure 15 presents the auxiliary thermal energy required (in addition to solar energy) by the various systems. Some systems required no auxiliary thermal energy. The experiments with a mass flow of 11,340 kg/hr required somewhat longer than the desired drying time but are shown for comparison.

Figures 16 and 17 each present the same information in two different formats. Both show the percentage of the thermal energy requirements which may be supplied by solar energy as a function of collector area and mass flow rate. Of these combinations simulated, eight combinations were capable of achieving 100% of the thermal energy needs from solar energy. For both collector areas 158 and 204 m^2, it might appear from figures 16 and 17 that the same mass flow rate of 15,880 kg/hr is necessary for achieving 100% of thermal energy from solar. It is likely that the

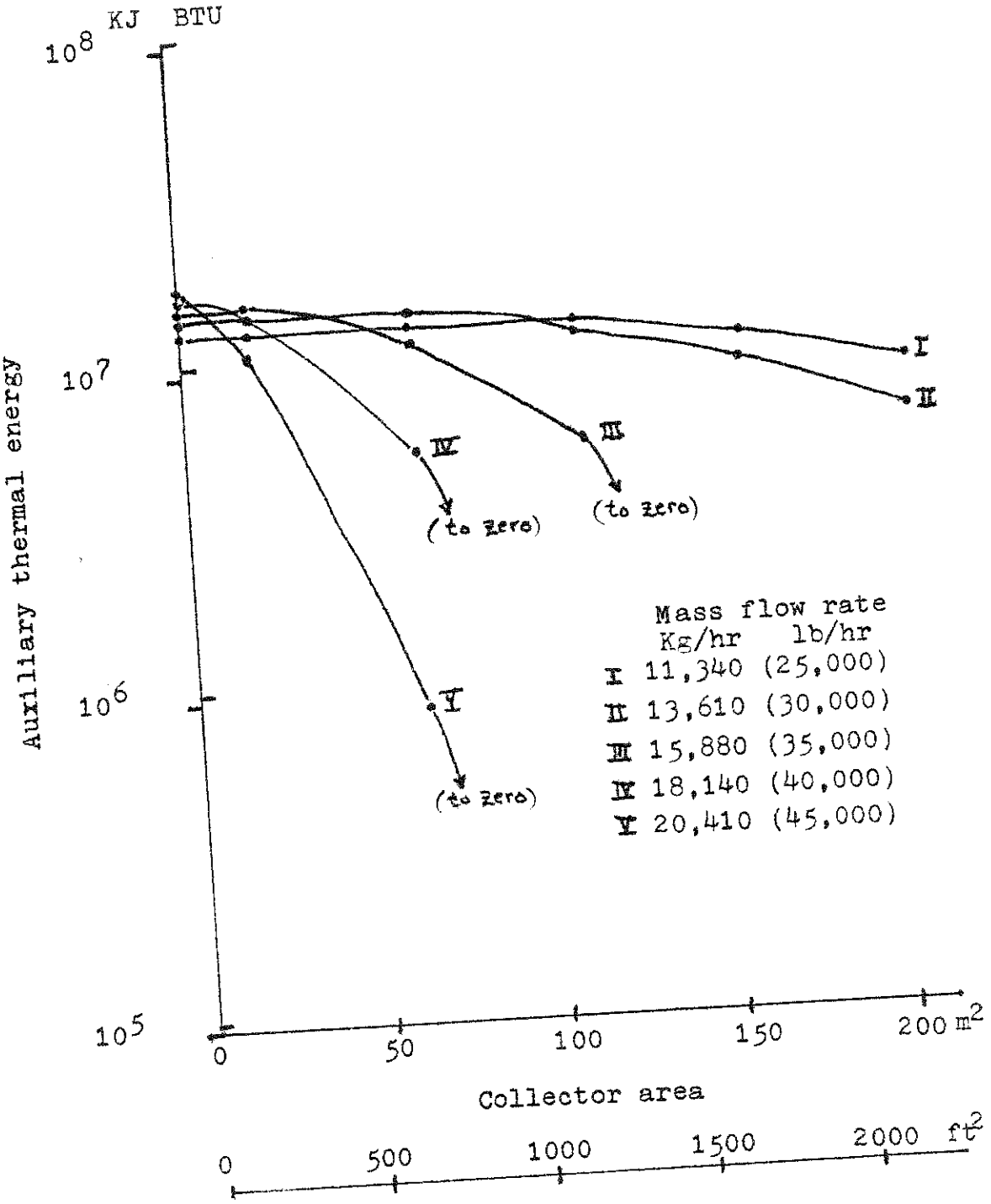

Auxiliary thermal energy requirements for various flow rate and collector area combinations

Figure 15

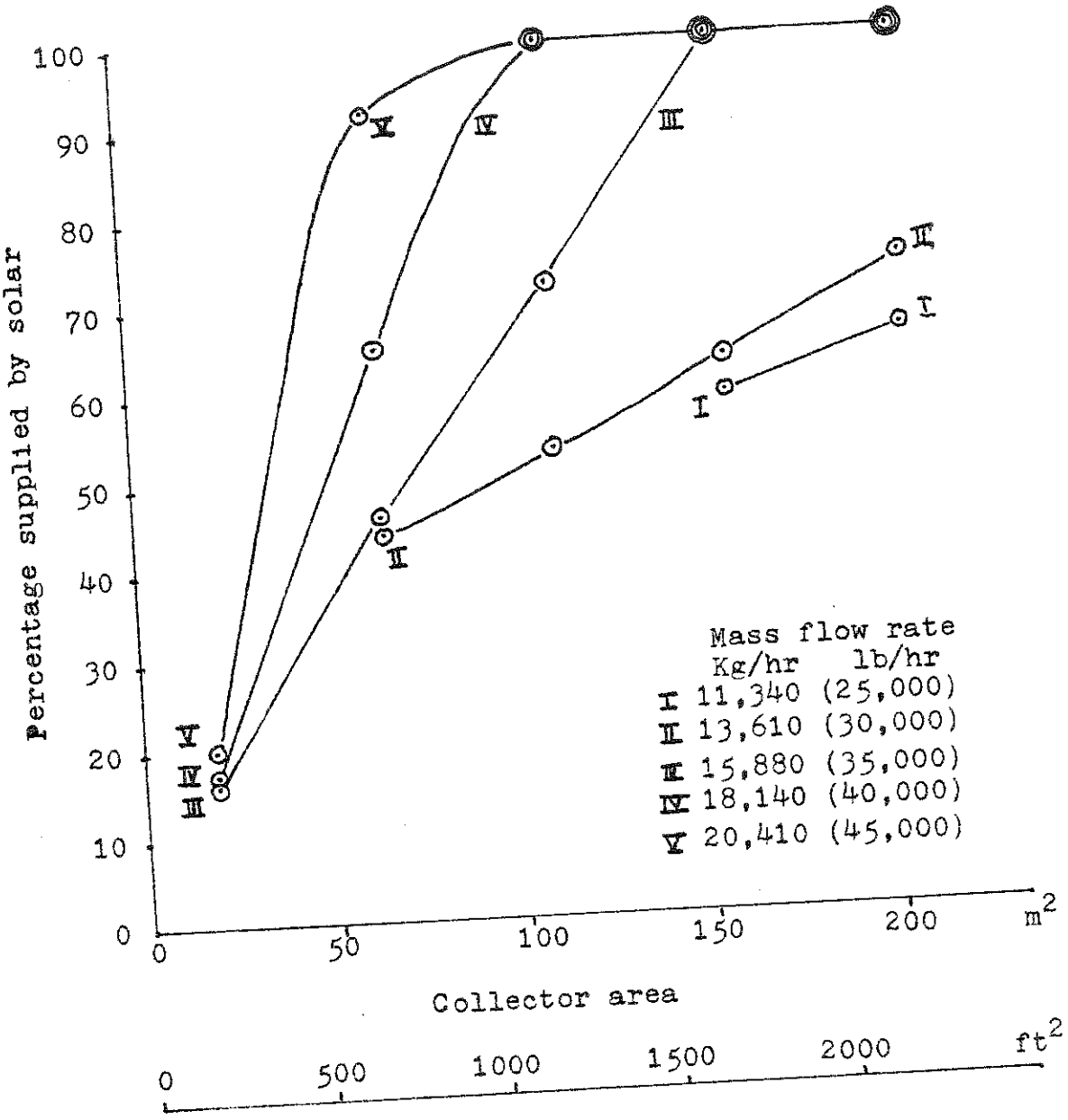

Percentage of thermal energy requirements supplied by solar energy for various flow rate and collector area combinations

Figure 16

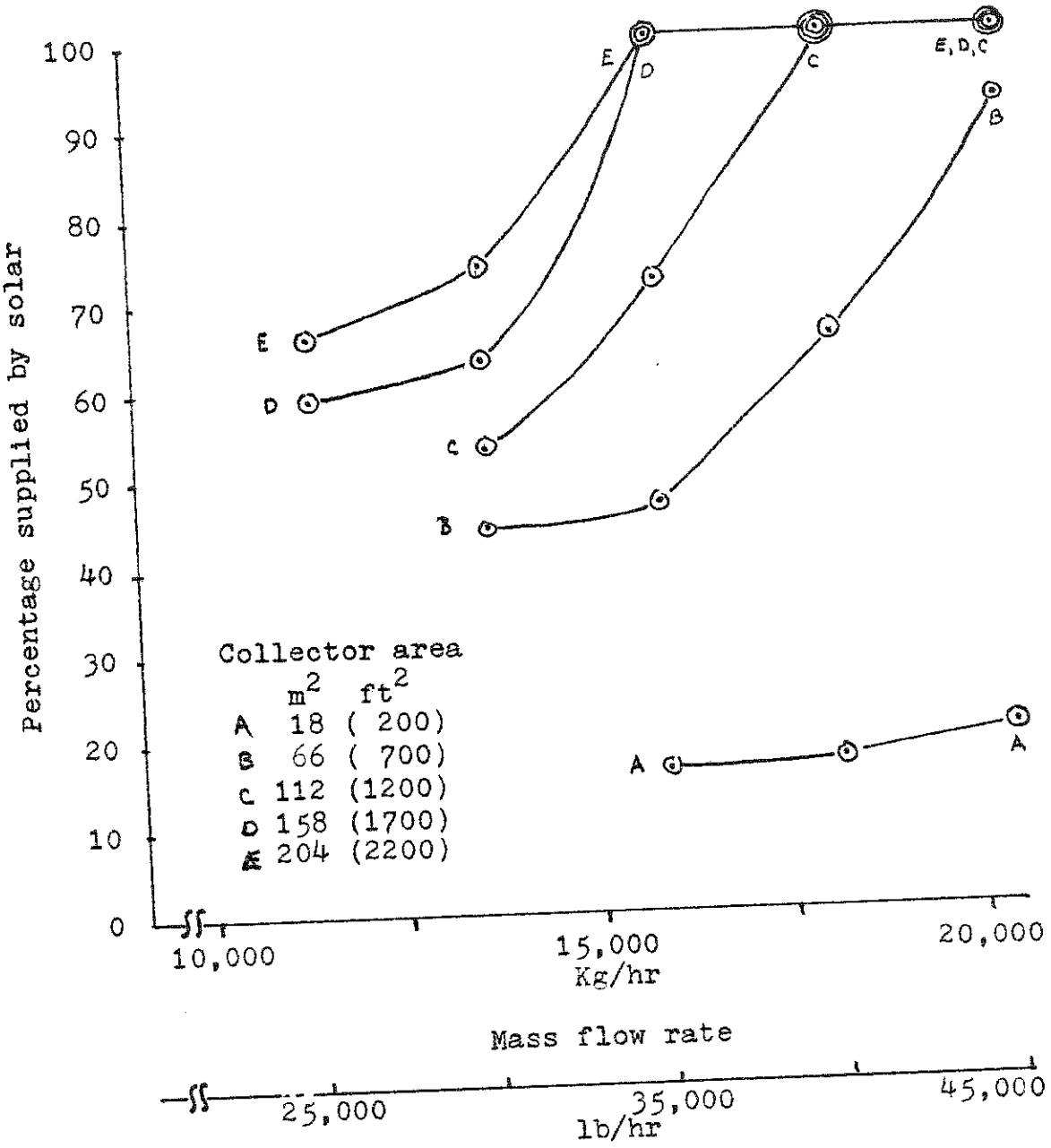

Percentage of thermal energy requirements supplied by solar energy for various flow rate and collector area combinations

Figure 17

204 m^2 collector can supply 100% of thermal needs at a lower flow rate than shown in the figures but no attempt was made to confirm this.

For any application, a large enough flow rate and/or collector area could supply 100% of the thermal energy as solar. However, energy requirements for operating the blower and capital costs for constructing collectors must be considered and the optimum system may not supply 100% of the thermal energy from the sun.

4.2.3.2 COMPARISON OF ENERGY SAVINGS:

Another method for making relative evaluations of these systems with various collector sizes and flow rates is to compare the reductions in auxiliary energy (and the increases in mechanical energy). Such changes in the energy requirements (thermal reductions and mechanical increases) are measured with respect to the "base line case" (which is a non-solar system) at each respective flow rate. For several systems (based on simulation), table 3 presents auxiliary thermal energy requirements and the decrease therein with respect to the appropriate "base line case." Also presented are the mechanical energy requirements (as electricity for the blower) and the increases therein with respect to the appropriate "base line case." (mechanical energy requirements are estimated based on Appendix 6.1.) Figures 18a and b illustrate the auxiliary thermal energy decreases and the

Table 3: Energy Data for various Drying Simulations

1	2	3	4	5	6	7	8	9
Mass flow rate	Collector area	Time at end of run	Aux thermal energy	Thermal saved due to solar	Thermal saved per unit area	Electric energy for blower (total)	Electric increase (due to solar)	Electric increase per unit area
kg/hr	m^2	hours	GJ	GJ	GJ/m^2	GJ	GJ	GJ/m^2
20410	none	300	18.07	-	-	15.66	-	-
20410	18	318	11.64	6.43	0.357	16.85	1.19	0.066
20410	66	342	0.92	17.15	0.260	18.63	2.97	0.045
20410	112	318	0.00	11.64	0.104	17.97	2.31	0.021
20410	158		0.00	11.64	0.074	17.36	1.70	0.011
20410	204		0.00	11.64	0.057	17.25	1.59	0.008
18140	none	300	16.00	-	-	11.64	-	-
18140	18	348	15.04	0.96	0.053	13.79	2.15	0.119
18140	66	348	5.69	10.31	0.156	14.41	2.77	0.042
18140	112	348	0.00	16.0	0.143	15.02	3.38	0.030
18140	158		0.00	16.0	0.101	15.21	3.57	0.023
18140	204		0.00	16.0	0.078	15.23	3.59	0.018
15880	none	318	15.19	-	-	8.76	-	-
15880	66	366	12.20	2.99	0.045	10.89	2.13	0.032
15880	112	366	5.92	9.27	0.083	11.53	2.77	0.025
15880	158	372	0.00	15.19	0.096	12.25	3.49	0.022
15880	204		0.00	15.19	0.074	12.91	4.15	0.020
13610	none	342	14.32	-	-	6.29	-	-
13610	112	366	12.50	1.82	0.016	8.16	1.87	0.017
13610	158	372	9.96	4.36	0.028	8.70	2.41	0.015
13610	204	372	6.54	7.78	0.038	9.49	3.20	0.016
11340	none	366	13.02	-	-	4.41	-	-
11340	158	420	12.08	0.94	0.006	7.15	2.74	0.017
11340	204	414	9.45	3.57	0.017	7.78	3.37	0.017

Column 3 - This is the duration of the drying simulation as determined by drying criteria. All other data are based on the respective time period.
Column 4 - This is the total thermal energy supplied as auxiliary heat.
Column 5 - Based on a comparison to the simulation with the same flow rate but with no collector, this column shows the reduction in auxiliary thermal energy requirements achieved by adding the solar collector.
Column 6 - These data are calculated by dividing the column 5 data by the appropriate collector areas.
Column 7 - This is the total (estimated) electrical energy for the blower.
Column 8 - Analagously to column 5, this column shows the increase in (estimated) electrical requirements due to adding a solar collector.
Column 9 - These data are calculated by dividing the column 8 data by the appropriate collector areas.

1GJ (GigaJoule) = 0.95 million BTU = 278 kWh (kiloWatthours)

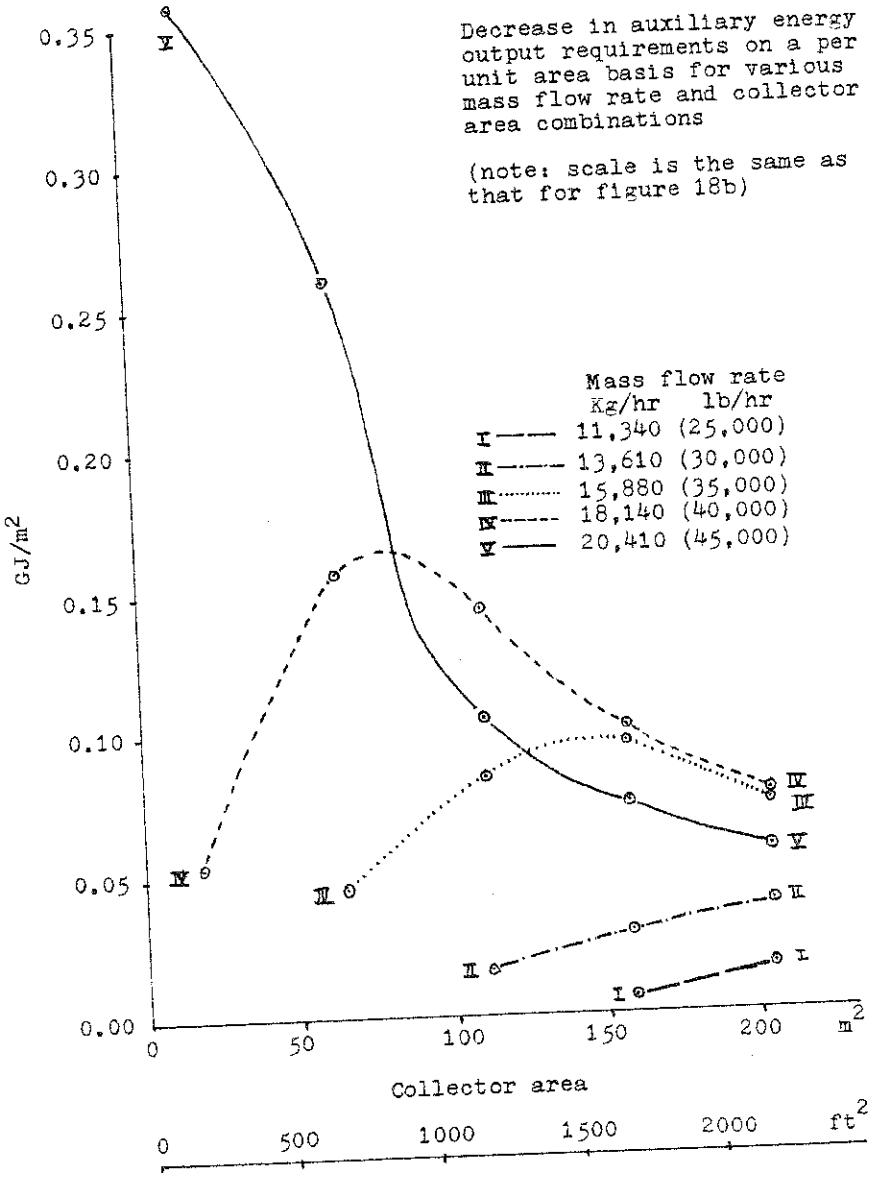
Decrease in auxiliary energy output requirements on a per unit area basis for various mass flow rate and collector area combinations
(note: scale is the same as that for figure 18b)
Mass flow rate
Kg/hr lb/hr
I —— 11,340 (25,000)
II —·— 13,610 (30,000)
III ····· 15,880 (35,000)
IV ----- 18,140 (40,000)
V —— 20,410 (45,000)
GJ/m2
0.35
0.30
0.25
0.20
0.15
0.10
0.05
0.00
0
50
100
150
200
m2
Collector area
0
500
1000
1500
2000
ft2

Figure 18 a

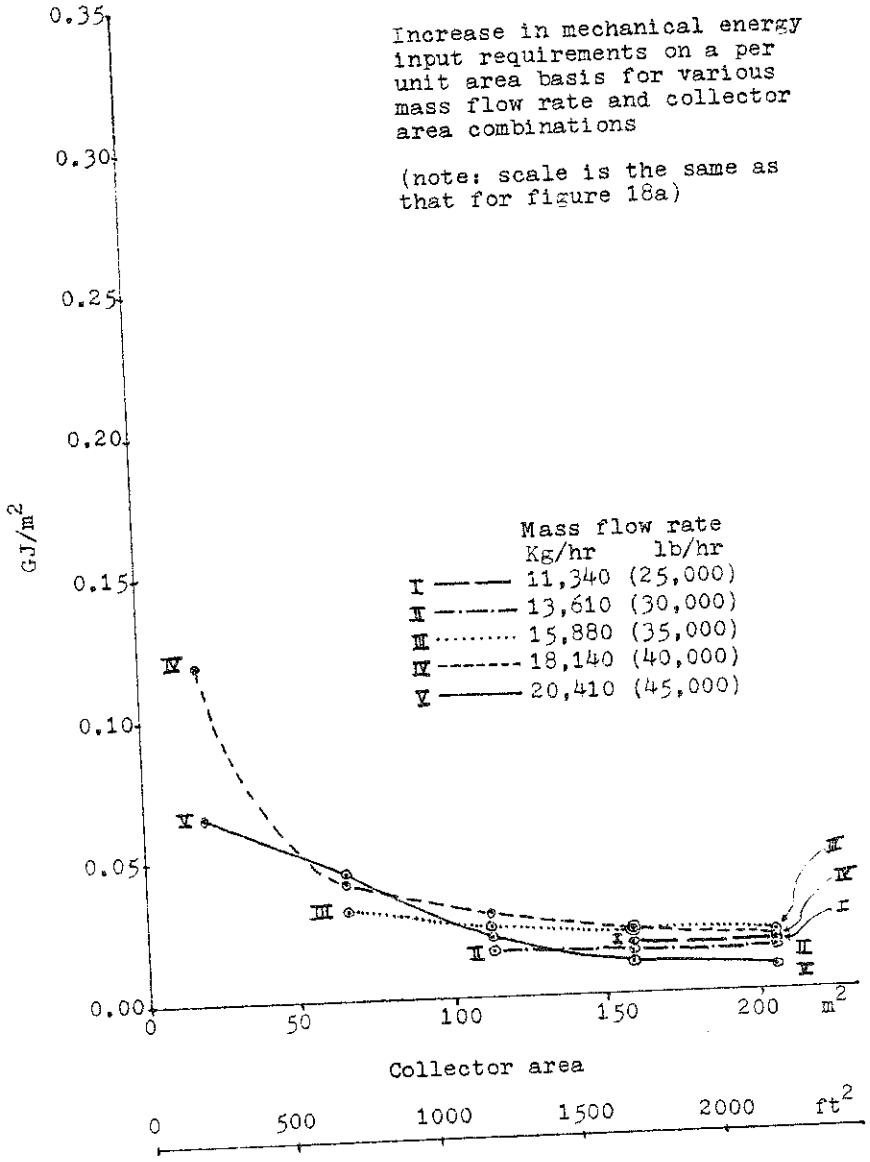
Increase in mechanical energy input requirements on a per unit area basis for various mass flow rate and collector area combinations
(note: scale is the same as that for figure 18a)
Mass flow rate
Kg/hr lb/hr
I —— 11,340 (25,000)
II —·—· 13,610 (30,000)
III ····· 15,880 (35,000)
IV ------ 18,140 (40,000)
V —— 20,410 (45,000)
GJ/m2
0.35
0.30
0.25
0.20
0.15
0.10
0.05
0.00
0
50
100
150
200
m2
Collector area
0
500
1000
1500
2000
ft2

Figure 18 b

mechanical energy increases (per unit area of collector) as a function of mass flow rate and collector area.

The decrease in auxiliary energy use is not simply a function of the total solar energy collected in a particular system. It is also a function of each system's different rate of drying due to differing levels of energy input over time. It is also a function of the different lengths of time needed for obtaining the desired dryness in different systems. And, it is also a function of the significantly different amounts of energy exhausted over time from different systems. For example, if drying progress is insufficient at a given time, the auxiliary heater will be turned on even if solar collection is high. And depending on drying progress and inlet humidity, higher levels of energy input may be primarily manifest as higher levels of energy in the exhaust.

The savings in auxiliary energy usage (due to the addition of a solar collector) increase with increasing collector area. However, the auxiliary energy saved per unit area of collector ultimately decreases as collector area increases. Mechanical energy increases per unit area of collector also decrease with increasing collector area.

4.2.4 ILLUSTRATION OF SELECTED SYSTEM:

Based on the economic analyses of a later section, it appears that of the systems considered in section 4.2.3, the one with a flow rate of 20,410 kg/hr (45,000 lbs/hr) and a collector area

of 66 m^2 (700 ft^2) apparently has the best potential for the exploitation of solar energy. This section illustrates the simulation of that case. 92% of the thermal requirements were satisfied with solar energy. The collector efficiency over 336 hours was 76%.

Figure 19 shows the average moisture fraction as a function of time. Over most of the run, the grain bed is steadily progressing towards achievement of the desired moisture. After time = 300, the rate of decrease of the average moisture fraction levels out; and in this simulation, the remaining drying time was needed primarily to dry the grain near the outlet to the desired moisture fraction.

Figure 20 shows moisture profiles at selected times. The fluctuations observed within the first meter from the inlet are due to fluctuations in inlet temperature and humidity. Note the profile at time = 300, where the average moisture is within the 0.145 moisture criterion but the outlet grain moisture is approximately 0.25.

Figure 21 shows the integrated quantities of delivered solar and auxiliary energy. Note that auxiliary energy was added only between times 168 and 186 hours. The flat portions of the integrated solar plot are indicative of night.

4.2.5 FLOW REDUCTION DURING PERIODS OF NO THERMAL GAIN:

The drier and controls subroutines provide an option of

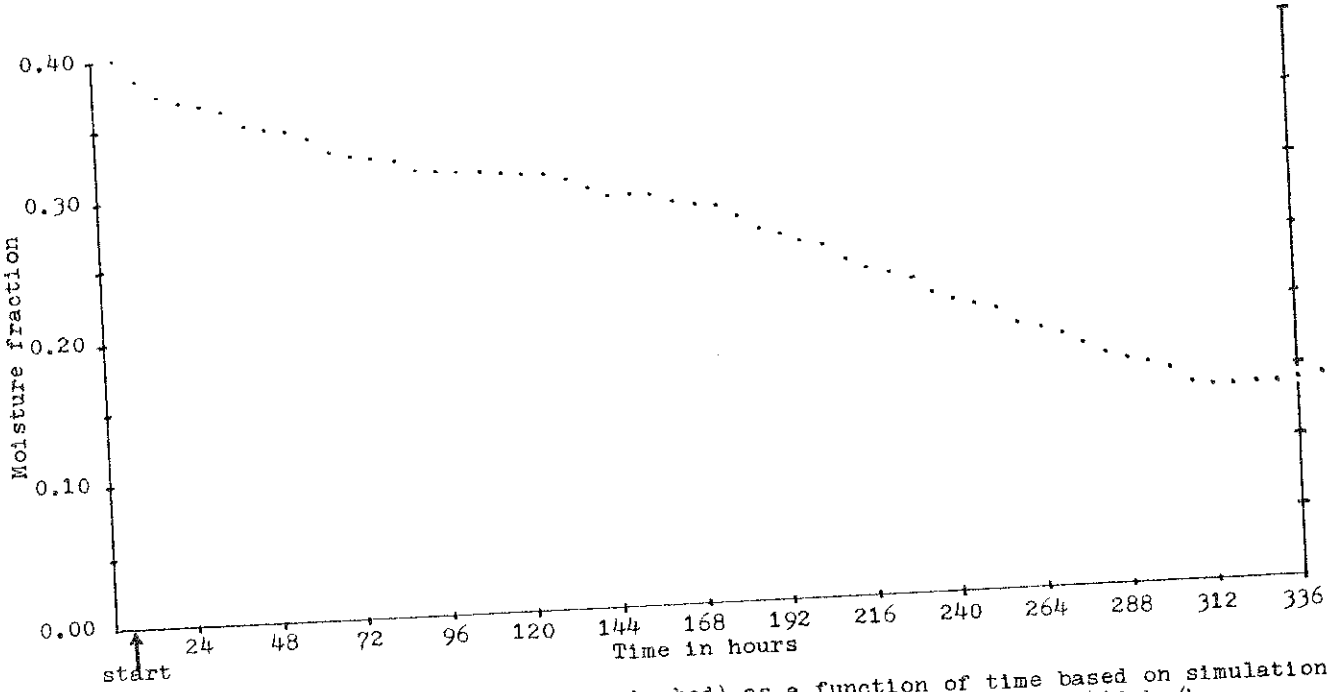

Moisture content (averaged over entire grain bed) as a function of time based on simulation
Collector area = 66 sq m Mass flow rate = 20,410 kg/hr

Figure 19

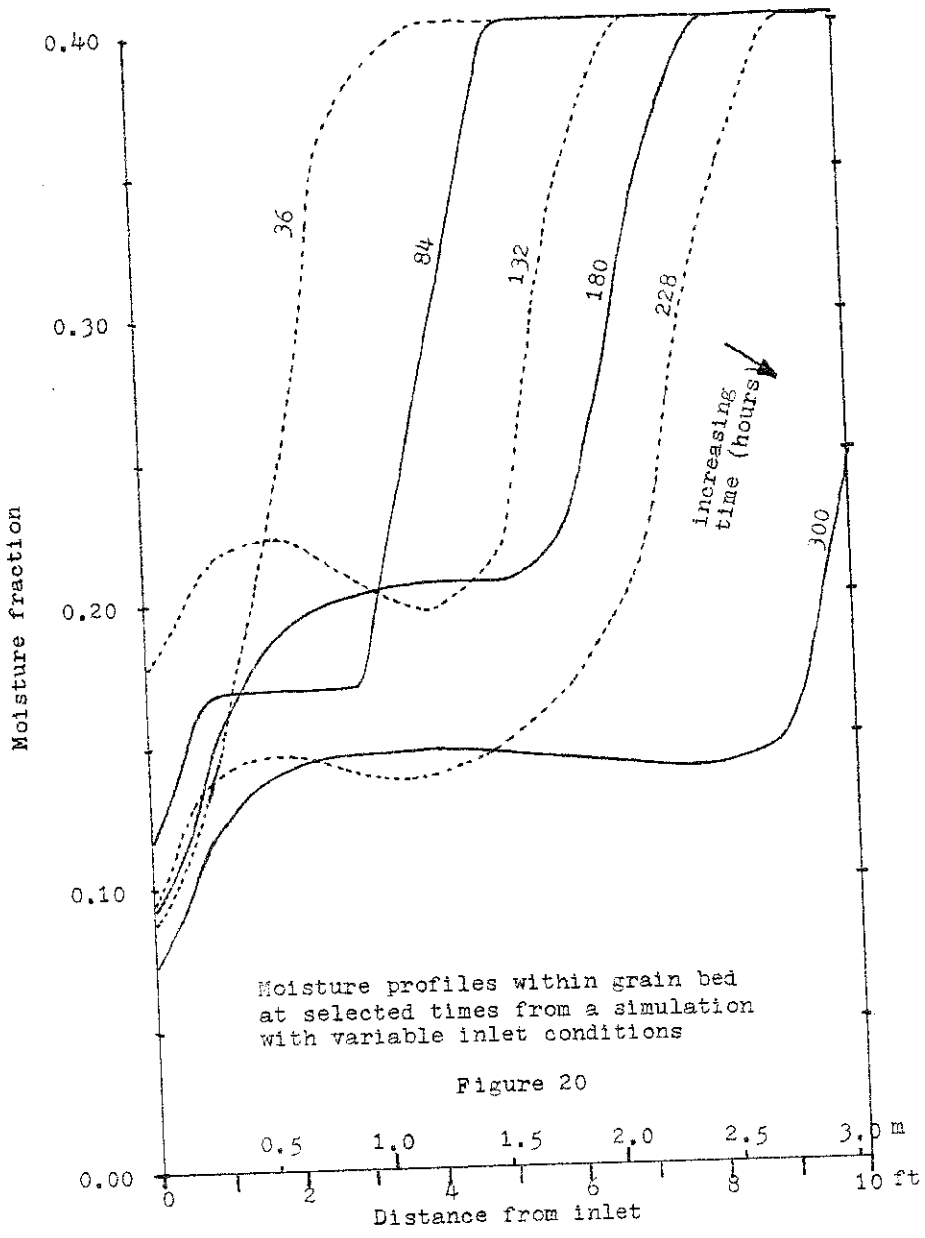

Moisture profiles within grain bed at selected times from a simulation with variable inlet conditions

Figure 20

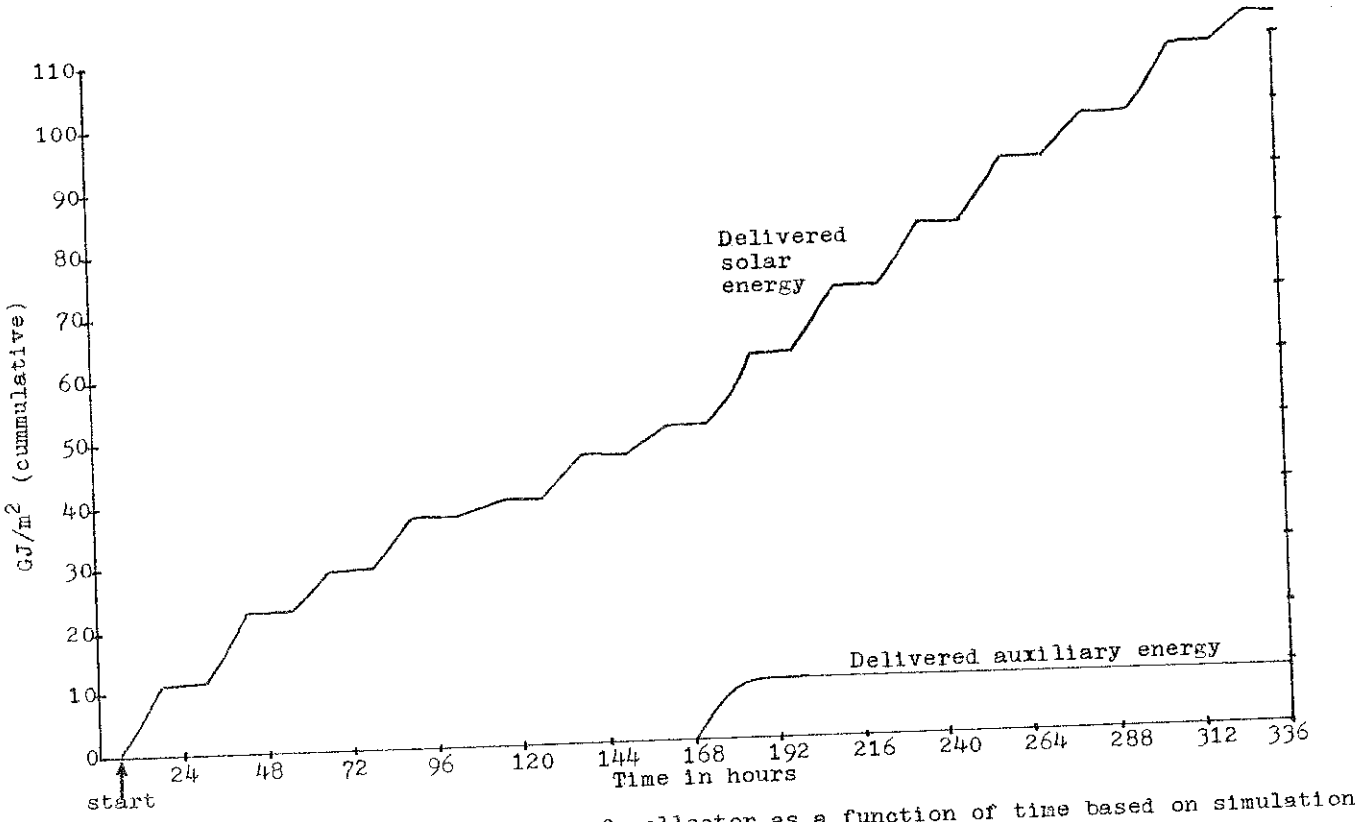

Integrated energy quantities per unit area of collector as a function of time based on simulation

Figure 21

reducing the mass flow. This option permits simulation of the case where the flow would be reduced to some minimum for aeration when there was no solar gain and no need for auxiliary. This section examines the effect of adding the flow reduction option to the system discussed in section 4.2.4. Minimum flow was set at 10%. Figure 22 compares the drying progress with that obtained in the experiment without flow reductions. The drying progress in this experiment lagged slightly behind that of the experiment for which full flow was maintained at all times. The slight difference in drying progress however, caused the drier control to call for over five times as much auxiliary heat during the course of this experiment in an attempt to maintain acceptable progress. This 4.2 GJ increase in auxiliary thermal input was lost in the exhaust air from the drier. That is, the drier exhaust in this experiment carried away 4.2 GJ more energy than in the previous experiment. This indicates the reduced flow drier was less efficient in utilizing applied thermal energy.

The blower operated at full flow for 219 hours and at 10% flow for 153 hours.

Table 4 presents results of the two experiments. The delivered solar energy is higher in the experiment with the flow reduction option only because the operating time is longer. The percent of energy supplied by solar is much lower in this experiment because of the much larger amount of auxiliary energy used. In

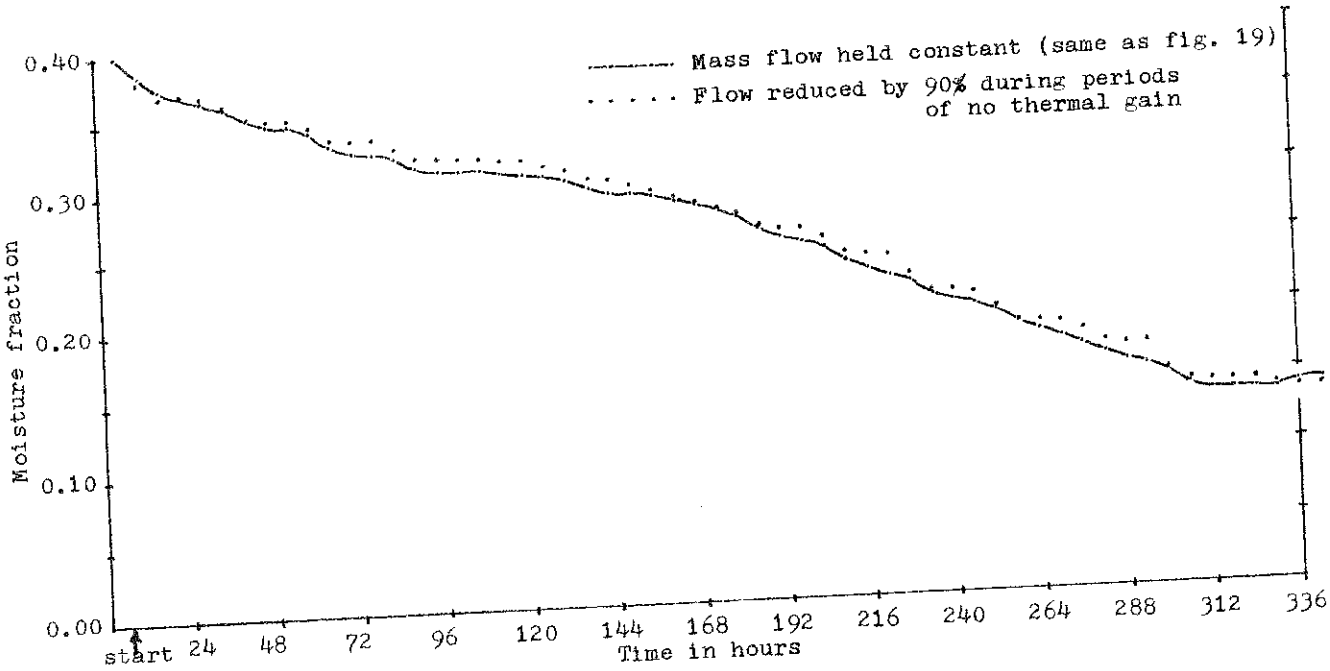

Comparison of average moisture content versus time for simulated drying with and without utilization of flow reduction option

Figure 22

Table 4

Comparison of two simulated drying experiments: with and without the flow reduction option

	Item of comparison	Basic conditions	With flow reduction option
1	Length of operation (hrs)	336	372
2	Delivered solar energy (GJ)	10.60	11.31
3	Collector efficiency (%)	75.7	75.6
4	Thermal needs supplied by solar (%)	92	69
5	Auxiliary energy required (GJ)		
	(a) total	0.92	5.07
	(b) compared to comparable non-solar drier	17.15 (less)	13.00 (less)
6	Estimated electrical* requirement (GJ)		
	(a) total	18.7	13
	(b) compared to comparable non-solar drier	3.0 (more)	2.7 (less)
7	Seasons savings relative to costs of comparable non-solar drier ($/m^2)		
	(a) with LP gas as auxiliary heat	1.14	1.81
	(b) with electricity as auxiliary heat	2.69	2.97
8	Mass balance closure (%)	99.60	99.96
9	Energy balance closure (%)	99.86	99.92

* Mechanical energy (as electricity) for blower operation

the table, "less" and "more" are with respect to the values of the base line case.

The variable flow system is seen to yield larger savings than the basic constant flow system due to significant reductions in mechanical energy consumption which outweighed the increases in auxiliary thermal energy consumption. (Economics will be covered in a later section.)

One disadvantage of the flow reduction option is that the moisture level of the grain near the outlet tends to be higher than in the basic system. This experiment reached the desired average moisture level at approximately the same time as the previous experiment but did not terminate until 36 hours later because the outlet end did not reach the desired dryness as quickly.

The conclusions of this section apply to the comparison made between the two experiments considered. However, the results suggest there is potential for reducing the mechanical energy and demonstrate that simulations can be used to explore such process variables.

4.2.6 PARTIAL RECIRCULATION OF OUTLET AIR:

The drier model provides the option of partially recirculating the flow. This option requires the addition of a flow mixer component subroutine. This section examines the case where half of the drier exhaust air is recirculated to the inlet of the system discussed in section 4.2.4.

Figure 23 compares the drying progress of the recirculating system with that in the experiment without recirculation. Drying progress in this experiment significantly led the progress of the once-through drier experiment during the first eleven to twelve days.

In the moisture range prevalent during the first eleven to twelve days the negative effects on the drying rate due to higher inlet humidities were apparently offset by the positive effects of higher temperatures. This would explain a major observation from figure 23. However as the bed's average moisture content decreased, the humidity effects apparently began to dominate and the drying progress of the recirculation experiment slowed and lagged that of the once-through experiment. Although both experiments reached the average moisture goal at comparable times, the recirculating system required 36 hours more for the grain near the drier outlet to reach the desired moisture. Prior to this experiment's additional 36 hours of operation, both experiments had used very similar quantities of auxiliary and thermal energy. At that time, solar energy had supplied 88% of this experiment's thermal inputs. During the additional operation time, the auxiliary heater was on continuously as the drier control attempted to regain compliance with the drying schedule. This large addition of auxiliary energy caused the percentage of energy supplied by solar to drop to 71.5%. The additional energy input resulted in this experiment losing 3.1 GJ more energy out of

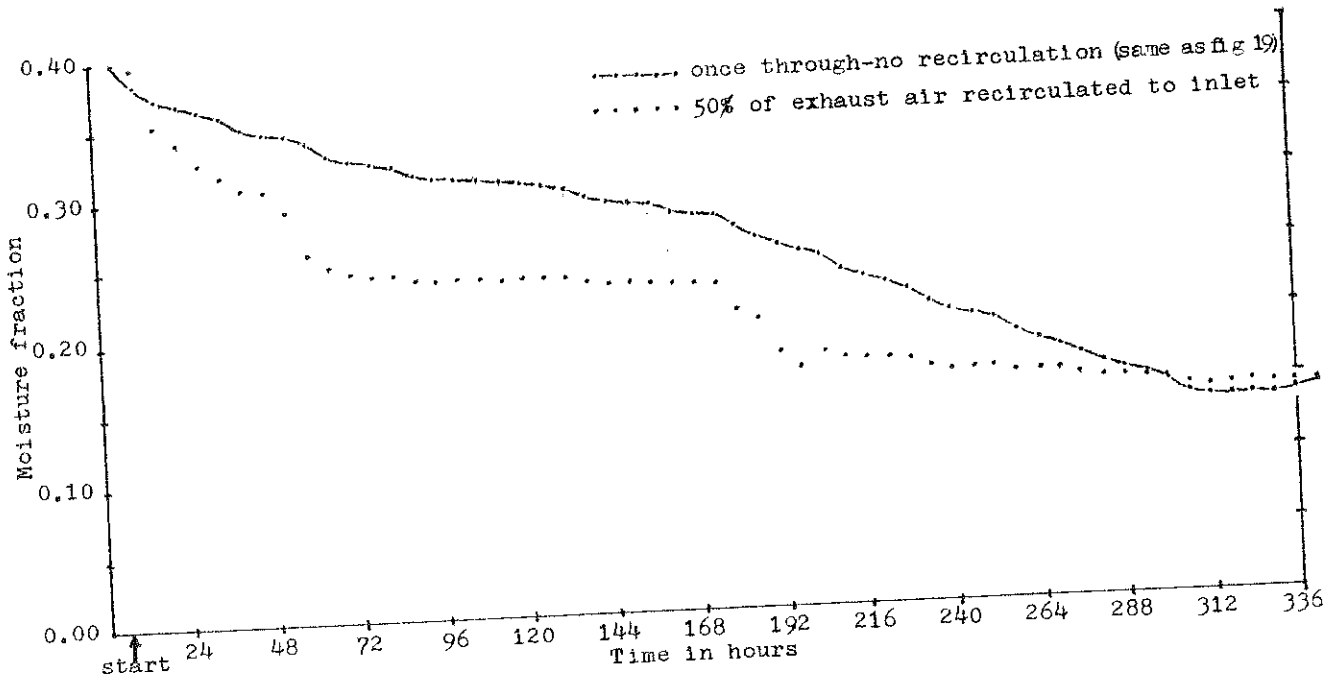

Comparison of average moisture content versus time for simulated drying with no recirculation and with 50% recirculation

Figure 23

the drier exhaust than the once-through experiment. This experiment also required more mechanical energy because it operated longer.

The delivered solar energy and collector efficiencies for the two systems at the end of 336 hours of operation (when the basic system terminated) differ due to the higher inlet and average collector temperatures in the recirculation experiment. Table 5 presents a comparison of the two experiments. Although the conclusions of this section apply to the comparison made between the two experiments considered, the results suggest that advantages exist for employing recirculation in some situations. Varying the amount of recirculation during various operational phases would give increased control over the drying rate and the product quality. This section has also demonstrated that simulation is a valid approach for investigating the effects of recirculation.

4.2.7 FLOW REVERSAL:

The drier model provides the option of reversing the direction of the flow periodically at a frequency specified by the user. Use of this option has shown that the drying zones tend to be pushed back and forth within the bed as the same moisture is repeatedly evaporated and condensed. It was observed that there is a very significant delay in drying when this option is employed (and a large energy penalty).

Table 5

Comparison of two simulated drying experiments: with and without partial recycle

Item of comparison	Basic conditions	With partial recycle
1 Recycle (%)	0	50
2 Length of operation* (hrs)	336	372
3 Delivered solar energy (GJ)		
(a) total	10.60	11.05
(b) within 336 hrs *	10.60	10.47
4 Collector efficiency (%)		
(a) averaged over entire operation	75.7	73.9
(b) averaged over 336 hrs *	75.7	74.8
5 Thermal needs supplied by solar (%)	92	71.5
6 Auxiliary energy required (GJ)		
(a) total	0.92	4.40
(b) compared to comparable non-solar drier	17.15 (less)	13.67 (less)
7 Estimated electrical requirement (GJ) **		
(a) total	18.7	20.7
(b) compared to comparable non-solar drier	3.0 (more)	5.0 (more)
8 Seasons savings relative to costs of comparable non-solar drier ($/m^2)		
(a) with LP gas as auxiliary heat	1.14	0.41
(b) with electricity as auxiliary heat	2.69	1.65
9 Mass balance closure (%)	99.60	99.96
10 Energy balance closure (%)	99.86	90.10

* for comparing collector performances with and without recycled air

** category 7 refers to mechanical energy (as electricity) for blower operation

Consider a case where two experiments differ from each other only in that one drier was subject to flow reversal every 30 minutes. At the time when the one-directional system reached the desired moisture fraction, the flow reversal system had only removed half as much moisture. Overall the flow reversal system required three times as much time to reduce the average moisture to the desired level.

This option might be desired if the user felt that maintaining more uniform drying profiles was of greater importance than minimizing energy consumption or maximizing drying rate.

4.3 Economic Analyses

With respect to the combinations of collector area and flow rate discussed in section 4.2.3, four cases are considered for each combination. These four cases reflect the use of oil, natural gas, LP gas, or electricity as the auxiliary energy source which is being totally or partially offset by solar energy. Mechanical energy for the blower is assumed to derive from electricity. Table 6 presents the reductions in annual operating costs which are achievable by adding solar collection to the grain drying system. The amount of the reduction is being referred to as net dollars saved or solar savings (equals the dollars saved by decreasing auxiliary thermal energy minus the dollars cost for the increased mechanical energy in the blower). Energy to dollars conversion is shown in table 11 of Appendix 6.3. Table 6 is condensed from tables 12 and 13 of Appendix 6.3. It represents annual solar savings assuming one bin of grain per year is dried. Data for systems with oil and electric auxiliary heaters respectively are illustrated in figures 24a and b.

In most cases, criteria for selecting the appropriate design basis* should be based on ecomonic comparisons. There are several common methods of evaluating the economics of solar heating systems. Life cycle economic analysis, which takes into account

* If the solar capability is to be added to an existing system, the air mass flow rate may be already fixed. Optimizing collector area would then be the only criterion. For such a case where the flow is fairly low (e.g. less than 13,600 kg/hr for the systems considered in section 4.2.3) there may be no possibility of economically adding solar capability.

Table 6: Summary of net dollar savings
$Thermal Savings - $mechanical increases = $net savings for replacing or supplementing oil, natural gas, LP gas, or electricity as the thermal source with solar derived from various systems indicated by area and flowrate

flow kg/hr	Area m^2	oil $ total	oil $/$m^2$	natural gas $ total	natural gas $/$m^2$	LP gas $ total	LP gas $/$m^2$	electricity $ total	electricity $/$m^2$
20410	18	21.77	1.21	20.16	1.12	27.37	1.52	65.50	3.64
20410	66	60.63	0.92	56.34	0.85	75.55	1.14	177.25	2.69
20410	112	37.47	0.33	34.56	0.31	47.59	0.42	116.62	1.04
20410	158	45.10	0.29	42.19	0.27	55.22	0.35	124.25	0.79
20410	204	46.47	0.23	43.56	0.21	56.59	0.28	125.62	0.62
18140	18	(-21.41)	(-1.19)	(-21.65)	(-1.20)	(-20.57)	(-1.14)	(-14.88)	(-0.83)
18140	66	24.14	0.37	21.56	0.33	33.11	0.50	94.25	1.42
18140	112	48.95	0.44	44.95	0.40	62.87	0.56	157.75	1.41
18140	158	46.57	0.29	42.57	0.27	60.49	0.38	155.37	0.98
18140	204	46.32	0.23	42.35	0.21	60.24	0.30	155.12	0.76
15880	66	(-9.59)	(-0.15)	(-10.33)	(-0.16)	(-6.99)	(-0.11)	10.75	0.16
15880	112	18.21	0.16	15.89	0.14	26.27	0.23	81.25	0.73
15880	158	42.95	0.27	39.16	0.25	56.17	0.36	146.25	0.93
15880	204	34.70	0.17	30.91	0.15	47.92	0.23	138.00	0.68
13610	112	(-13.01)	(-0.12)	(-13.46)	(-0.12)	(-11.42)	(-0.10)	(-0.63)	(-0.01)
13610	158	(-5.28)	(-0.03)	(-6.37)	(-0.04)	(-1.48)	(-0.01)	24.37	0.15
13610	204	4.35	0.02	2.40	0.01	11.11	0.05	57.25	0.28
11340	158	(-28.89)	(-0.18)	(-29.13)	(-0.18)	(-28.07)	(-0.18)	(-22.50)	(-0.14)
11340	204	(-21.78)	(-0.11)	(-22.67)	(-0.11)	(-18.68)	(-0.09)	2.50	0.01

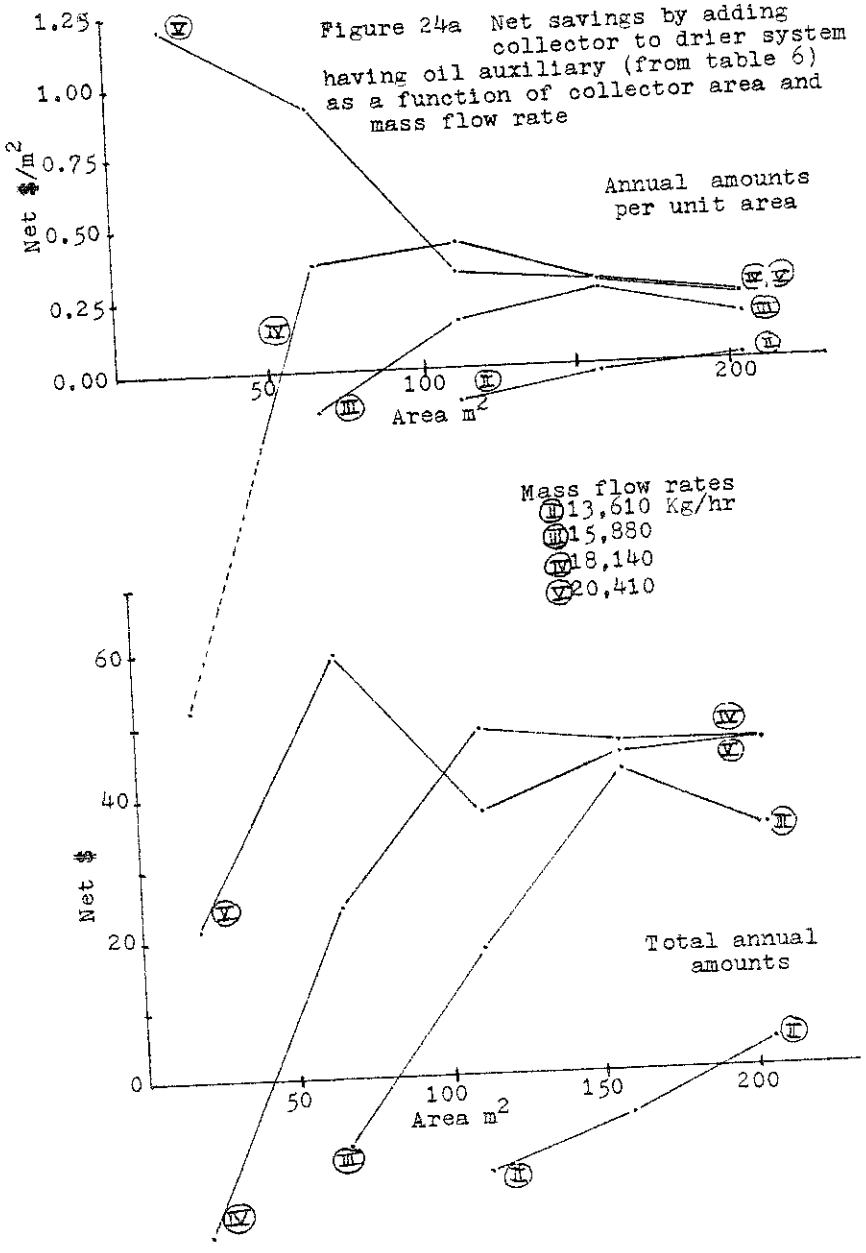

Figure 24a Net savings by adding collector to drier system having oil auxiliary (from table 6) as a function of collector area and mass flow rate

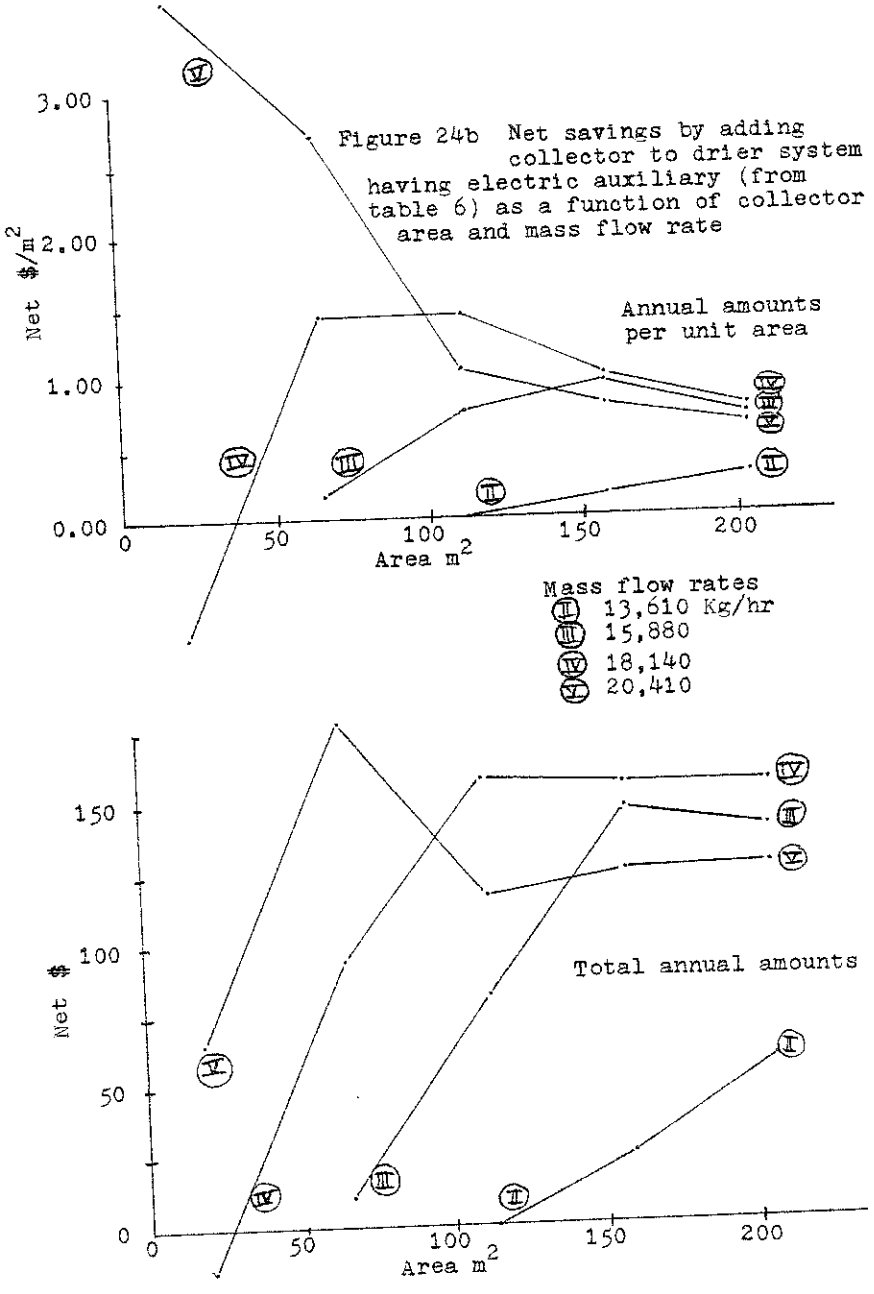

Figure 24b Net savings by adding collector to drier system having electric auxiliary (from table 6) as a function of collector area and mass flow rate

the time value of money, is recommended by Beckman, Klein, and Duffie (1977) who present examples of its use. The technique will be used here also.

Consider the following simple example which examines the previously discussed system (sections 4.2.3 and 4.2.4) having a mass flow rate of 20,410 kg/hr (45,000 lb/hr) and a solar collector area of 66 m^2 (700 ft^2).

Assumptions:

1) collector cost is $10.00 per square meter (see section 2.1)
2) collector life is twenty years (straight line depreciation)
3) ultimate salvage value and any cover replacement costs have been neglected
4) market discount rate is 7%
5) fuel cost inflation rate is 7.75%
6) tax rate is 48%
7) property tax will be unaffected
8) maintenance and insurance costs will not change significantly
9) installation will be paid for without a loan
10) only one bin (of corn) per year will be dried

Refer to table 6 to determine that the annual solar savings (after accounting for parasitic mechanical energy increases) would initially be $60.63 with an oil auxiliary or $177.25 with

an electric auxiliary. The discount and inflation rates conveniently result in a present worth factor of 20.0 for the 20 year period. (That is, in this example the present worth of any future year's fuel savings will be the same as that of the initial year's savings.) Since fuel costs would be a deductible business expense at the 48% rate if they were incurred, the annual solar savings indicated above must be effectively reduced by 48% to $31.53 (oil) and $92.17 (electric). Since the solar savings are now adjusted downward in this manner, the only remaining effect of taxes will be an annual savings due to depreciation:

$$(0.48 \text{ tax rate})(66 \text{ m}^2)(\$10.00/\text{m}^2)/(20 \text{ years}) = \$15.84/\text{year}$$

Since the depreciation rate will not inflate, the present worth factor for the taxes must be taken at 0% inflation or 10.594 for the 20 year period. Then for an oil auxiliary:

present cost of collector = $(66 \text{ m}^2)(\$10/\text{m}^2)$ =	- $660
present worth of tax saved = $(10.594)(\$15.84)$ =	+ $168
present worth of solar savings = $(20.0)(\$31.53)$ =	+ $630
net present worth =	+ $138

With an electric auxiliary, the net present worth would instead be:
(-$660) + (+$168) + (+$1843) = +$1351

An examination of the total dollar returns and the dollar returns per square meter in table 6 indicates that the most favorable economics will belong to either the system with a flow rate of 20,410 kg/hr and a 18 square meter collector or the above system (20,410 kg/hr; 66 m^2). The choice between these two will depend on the type of auxiliary heat in the system and upon the

cost per unit area for installing solar capability. A life cycle analysis has been calculated for these two systems with three possible auxiliaries and with four possible collector costs per unit area. The techniques of the above example were employed; in addition it was assumed for simplicity that all collector costs were area-dependent. Table 7 shows the results of these calculations. Clearly indicated are cases favoring the small collector, cases favoring the large collector, and cases in which both are unfavorable.

The fuel inflation rate could easily exceed the value used in the example. If it were 10% (all else unchanged), the present worth of the example's 66 m^2 system with oil auxiliary (collector @ $10 per sq. m.) would increase (from $138) to $283. With an electric auxiliary, the increase would be (from $1351) to $1776.

The entire analysis has been made assuming that only one bin per year would be dried. Even under this assumption of limited use (approximately 15 days per year), it appears that solar supplemented drying can be economically practical. However, since harvesting frequently lasts longer than six weeks, it might be possible to use one collector to dry two or three bins sequentially. If it was achieveable to dry three bins annually, it is reasonable to assume solar savings would be approximately tripled while collector costs would change very little. With all else unchanged, the present worth of the example's 66 m^2 system with oil auxiliary (collector @ $10 per sq. m.) would increase (from $138) to $1398.

Table 7
Net Present Worth for Various Cases

Area m^2	Type of auxiliary energy	Net present worth in dollars of the various systems at four selected installation costs per m^2 @$5	@$10	@$15	@$20
18	oil	+ 159	+ 92	+ 25	(-42)
66	oil	+ 384	+ 138	(-108)	(-354)
18	LP gas	+ 217	+ 150	+ 84	+16
66	LP gas	+ 540	+ 294	+ 47	(-199)
18	electric	+ 614	+ 547	+480	+412
66	electric	+1597	+1351	+1105	+859

1) mass flow = 20,410 kg/hr

2) system dries only 1 bin per year

With an electric auxiliary the increase would be (from $1351) to $5037. With three bins per year all present worths in table 7 would become more favorable, all entries would be positive (least favorable at -$354 would become +$906), and the 66 m^2 collector would be more favorable than the 18 m^2 collector for all cases considered in table 7.

If the collector was situated reasonably near other buildings (besides the grain bins) solar energy might be utilized for other purposes during the rest of the year. This would increase economic favorability. The federal government and many state governments have been seriously considering offering solar utilization incentives through the tax system. Such incentives would also increase economic favorability.

In addition to presenting favorable economic data, this section has demonstrated the applicability of the present model in conjunction with life cycle economic analyses for purposes of design optimization.

4.4 Conclusions

For the case of drying grain in bins under transient inlet conditions, the governing, coupled equations for heat and mass transfer may be reduced to a model conveniently solved by computer. The basis for the model is instantaneous (within the selected time step) attainment of thermal and sorbate equilibrium between the air and all portions of all particles in each finite difference segment. The model's performance has been verified against limited available data for laboratory scale driers operating under constant inlet conditions. Because of the assumption of instantaneous equilibration, the model is likely limited to grain driers where some function of flow rate over bed length is less than some maximum. This function or maximum limit ratio has not been determined. The model is also limited to cases in which the air flow is never static and is equally distributed over the cross section of a uniformly porous grain column.

This model is simple to apply and is more efficient with respect to computer time than other published models. When interfaced with TRNSYS, it is well suited for computerized simulations and design studies of solar-assisted grain drying under transient inlet conditions. It is especially of utility when fairly large time steps (e.g., 0.2 hrs.) and few finite segments (e.g., 10) are desired in order to limit computer time requirements in the conduct of several long term simulations.

In many cases, and under the proper design conditions, the addition of solar collectors can significantly reduce the auxiliary energy requirements of a drier. Depending on the assumptions and collector cost-

ing data utilized in economic analyses, it is tentatively concluded that solar-assisted grain drying may have positive economic potential. The degree of economic favorability is sensitive to the cost parameters chosen, but in any case may be improved by increasing the number of bins dried. Partial recirculation of exhaust and flow reduction during periods of no energy gain may also improve economic potential.

4.5 Suggested Work

This thesis has described the development of an equilibrium model of grain drying in bins. An efficient iterative convergence scheme has been detailed for solving the model's three basic equations (in three unknowns). Computer subroutines of the model and of controls have been shown to be especially suited for simulations of solar-assisted grain drying utilizing actual (transient) weather data.

The computer subroutines, interfaced with TRNSYS (Klein et al., 1974; Solar Energy Laboratory of the University of Wisconsin, 1977), have been used to simulate several variations in design for a solar corn drying system. In conjunction with this design study, life cycle economic analyses have indicated that (for Madison in October) some designs have positive economic potential. These analyses have also shown that the present worth of such solar drying systems could be further and significantly enhanced if it would be possible to utilize the collector as an aid to drying more than one bin per year.

Simulations of operating options such as partial recirculation and flow reductions during periods of no thermal gain have demonstrated the versatility of the subroutines in studying a number of design possibilities. Such simulations have also indicated that the two options mentioned above may both have potential for increasing economic favorability.

This work could provide a starting point for a number of studies.

It is desireable to provide a more rigorous experimental validation of the model under long term transient conditions, but currently there is a lack of good published data. Such data (with or without solar collectors) would provide a means of thoroughly verifying this and other models.

Further simplification of the model may be possible by utilizing constant values for the heat capacities and heat of sorption now expressed as functions. During the iterative process (as T, w, and W are repeatedly adjusted), their values change. It has been observed that these changes are fairly small and therefore may contribute to increased computing time while only marginally improving accuracy. It may be interesting to determine whether assuming constant values for these (especially for preliminary simulations) could improve computing efficiency without seriously reducing accuracy.

Design studies based on simulation is considered as the most consequential follow up to this work. A variety of system designs, grain types, locations, and climatic data should be considered. Life cycle economic analysis should be used to lead to the development of design guidelines regarding type and size of collectors and mass flow rates; all as a function of bin size, grain type, and geographic location.

Simulated design studies could be expanded to consider types

of solar grain drying systems other than those considered in this thesis. For example, short term, high temperature driers could be readily simulated with the present model. Multiple inlet driers could be simulated by several drier models placed in series together with appropriate flow mixing sub-routines. A rockpile thermal storage unit could be added to the simulated set up. Addition of a heat exchanger would allow investigation of the use of collectors having water as the fluid. Forcing function components combined with several drier components could simulate sequenced batch-in-bin high temperature drying where it might be desired to dry one or two batches of grain per day in the same bin. Annular flow, cross flow, or continuous grain counter flow driers could also be simulated with slight modification to the model.

The development of solar energy as a thermal supplement for grain drying could reduce consumption of conventional energy supplies. Computerized design studies are proposed as the expedient approach for accelerating this development.

5.
NOTATION

A Cross sectional area

a Constant in equation of section 2.3

B Grain specific constant in Henderson equilibrium moisture expression

b Constant in equation of section 2.3

C Grain specific constant in Henderson equilibrium moisture expression

C_a Heat capacity of humid air $C_a = C_{a_1} + C_{a_2}w$

C_{WS} Heat capacity of wet solid (moist grain) $C_{WS} = C_1 + C_2W$

C_1, C_2 See C_{WS}

D Diameter of grain bed (effective inside diameter of drier)

E_{aux}, E_{sol} Thermal energy inputs derived from auxiliary and solar

F' Collector geometry efficiency factor

F_i, F_1, F_2 Characteristic potentials

H Enthalpy of media in F_1/F_2 model

h Enthalpy of fluid in F_1/F_2 model

H_f Enthalpy of fluid in Final Equilibrium Model

H_s Enthalpy of media (solid) in Final Equilibrium Model

$H_{S(I/O)}$, $H_{D(I/O)}$, H_{BED} Enthalpy balance terms calculated by model

i Location subscript

j Number of iterations

K Equation variable defined in conjunction with equation #20

L Total length of grain bed within drier

$\dot{m}$ Mass flow rate of air

M_b Total mass of grain in drier

$M_{I/O}$, M_{BED} Water mass balance terms calculated by model

N Number of finite segments into which grain bed is divided

NTU Number of Transfer Units

ΔP Pressure drop per unit length of grain bed

P Density of media excluding interstices in F_1/F_2 model

Q "Empty-tower" mass velocity (mass per time per cross-sectional area)

R_H, R_L High and low limiting values of range in convergence scheme

RH Relative Humidity in decimal form

Δr Radial distance increment

S_1, S_2 see λ_s

T Temperature (T_f: of fluid, T_s: of solid, T_{ref}: reference, T_{in}: of inlet air, T_{WB}: wet bulb of air, T_{amb}: of ambient air, T_{col}: of outlet air from collector, $T_{B,ave}$: average of bed, $T_{i,t}$: of grain and air at location i and time t)

t Time (also used as subscript)

Δt Increment of time

U_L Collector loss coefficient

v Instantaneous front velocity

W Moisture content (fraction) as mass of water per mass of dry grain (W_e: equilibrium value, W_{init}: initial value, $W_{B,ave}$: average of bed, W_{ave}: desired average of bed, W_{min}: minimum safe value, $W_{i,t}$: value at location i and time t)

w humidity of air (w_{min}: minimum expected value of possible range of humidity values, w_{init}: initial interstitial, $w_{i,t}$: value at location i and time t, $[w_{i,t}]_p$: projected value)

x Axial distance

Δx Axial length increment

Z_1, Z_2 Equation variables defined in conjunction with equation #20

$\alpha_i\ \alpha_1\ \alpha_2$ – Slope of constant F line on psychrometric chart

$\gamma_i\ \gamma_1\ \gamma_2$ – Characteristic specific capacity ratios

ε Void fraction

θ Time (θ_1, θ_2 front emergence times)

λ Latent heat of vaporization (λ_f: of free water, λ_s: of sorbed water, $\lambda_s = S_1 + S_2 W$)

μ Ratio of effective media density over effective fluid density

ρ Density (ρ_f: of fluid, i.e., humid air; ρ_s: of media excluding interstices)

σ Convergence criterion

τ Transmissivity

$\#_{max}$ Maximum iterations

6.
APPENDICES

6.1 Power Requirements for Solar Drying Simulations

Several widely varying flow rates and collector areas were compared for the solar grain drying system discussed in section 4. One should consider whether changes in pressure drop between the various cases will significantly affect the comparison of overall energy requirements. It is not within the scope of this project to make for each simulation a detailed design of the various collector configurations, headers, ducts, etc., which would permit a precise determination of the pressure drop. This appendix, however, estimates the additional pressure drop represented by the addition of the solar collector and necessary ducts. For most systems, these pressure drops should be a small portion of the overall system pressure drop. And since the thermal energy requirements of the system are generally greater than or equivalent to the mechanical energy requirements, it is felt that the following arbitrary technique is not unjustified.

If one assumes that duct size is chosen based on some maximum desired air velocity, a standard size duct may be selected for each given flow rate. If this was a simple case of air flow through a long duct, fixing the velocity and duct size would fix a certain pressure drop per unit length of duct. But this is not such a simple case since the flow velocities will change as

the air from each collector subunit flows into the duct and since there will possibly be expansions and direction changes. Indeed it is possible that the diameter of the duct would be occassionally varied over its length to maintain a desireable flow regime in all sections. It was assumed that the addition of the ducts necessary to utilize solar collectors caused a pressure drop equivalent to twice that of a straight duct having a length equivalent to the long dimension of the collector bank and having a standard cross-section which would yield a velocity of approximately 10 m/sec. The pressure drop through the collector subunits prior to the collection duct is neglected.

Using the formula illustrated in section 2.3 for pressure drop through grain beds and projecting an additional 40% to account for various other pressure losses as per Brooker et al. (1974), table 8 has been constructed. It shows the pressure drop as a function of flow rate for a conventional non-solar drier.

Table 9 indicates for the various flow rates considered, the standard duct size yielding a velocity close to 10 m/sec. The resultant pressure drop per unit length (based on material presented by Brooker et al. (1974)) is also shown.

Table 8

mass flowrate kg/hr (lb/hr; cfm)	pressure drop (ΔP) through grain kPa (in H_2O)	estimated system ΔP with no solar collector kPa (in H_2O)
9070 (20,000; 4500)	0.25 (1.0)	0.35 (1.4)
11340 (25,000; 5700)	0.55 (2.2)	0.77 (3.1)
13610 (30,000; 6800)	0.70 (2.8)	0.97 (3.9)
15880 (35,000; 7900)	0.90 (3.6)	1.2 (5.0)
18140 (40,000; 9100)	1.1 (4.4)	1.5 (6.2)
20410 (45,000; 10200)	1.3 (5.3)	1.8 (7.4)

Table 9

flow rate kg/hr	standard duct size m (in)	pressure drop per unit length Kpa/m	2 x pressure drop per unit length KPa/m (in H_2O/100 ft)
9070	0.51 (20)	0.0025	0.0050 (0.60)
11340	0.56 (22)	0.0020	0.0040 (0.50)
13610	0.61 (24)	0.0018	0.0036 (0.44)
15880	0.66 (26)	0.0016	0.0032 (0.40)
18140	0.71 (28)	0.0015	0.0030 (0.38)
20410	0.76 (30)	0.0013	0.0026 (0.32)

Assuming the collector bank length to be the area in m^2 divided by 2m, and by adding the pressure drop estimates for the solar ducts to the calculated pressure drops for the rest of the drier system at each flow rate the total pressure drop of the entire solar grain drying system is obtained. These data are shown in table 10 as a function of flow rate and collector area.

Given the mass flow rates and the total pressure drop of the system, the power requirements for the blower may be calculated. The blower assumed to have an efficiency of 0.6. The air which is pumped is assumed to be at 21°C (70°F) and have an absolute humidity of 0.01 kgH_2O/kg dry air and a humid density of 1.19 kg/m^3 (0.0735 lbs dry air per ft^3 of moist air). Table 10 also indicates the power requirements for the various systems blowers.

For illustrative purposes, table 10 also shows the percentage of the power requirements which are (in each case) attributable to the addition of the solar collector to the basic non-solar drier system.

Table 10

Mass flowrate kg/hr (lb/hr)	Collector area m^2 (ft^2)	Total ΔP KPa (in H_2O)	Blower power KW (HP)	Percent due to solar %
9070 (20,000)	0 (0)	0.35 (1.4)	1.3 (1.7)	0
9070 (20,000)	18 (200)	0.40 (1.6)	1.4 (1.9)	13
9070 (20,000)	66 (700)	0.50 (2.0)	1.8 (2.4)	30
9070 (20,000)	112 (1200)	0.62 (2.5)	2.2 (3.0)	44
9070 (20,000)	158 (1700)	0.75 (3.0)	2.7 (3.6)	53
9070 (20,000)	204 (2200)	0.85 (3.4)	3.0 (4.0)	59
11340 (25,000)	0 (0)	0.77 (3.1)	3.4 (4.6)	0
11340 (25,000)	18 (200)	0.80 (3.2)	3.6 (4.8)	3
11340 (25,000)	66 (700)	0.90 (3.6)	4.0 (5.4)	14
11340 (25,000)	112 (1200)	1.0 (4.0)	4.5 (6.0)	22
11340 (25,000)	158 (1700)	1.1 (4.4)	4.8 (6.5)	30
11340 (25,000)	204 (2200)	1.2 (4.8)	5.3 (7.1)	35
13610 (30,000)	0 (0)	0.97 (3.9)	5.2 (7.0)	0
13610 (30,000)	18 (200)	1.0 (4.0)	5.3 (7.1)	2
13610 (30,000)	66 (700)	1.1 (4.4)	5.9 (7.9)	11
13610 (30,000)	112 (1200)	1.2 (4.7)	6.3 (8.4)	17
13610 (30,000)	158 (1700)	1.2 (5.0)	6.6 (8.9)	22
13610 (30,000)	204 (2200)	1.3 (5.4)	7.2 (9.6)	28
15880 (35,000)	0 (0)	1.2 (5.0)	7.8 (10.4)	0
15880 (35,000)	18 (200)	1.3 (5.1)	7.9 (10.6)	2
15880 (35,000)	66 (700)	1.3 (5.4)	8.4 (11.3)	7
15880 (35,000)	112 (1200)	1.4 (5.7)	8.9 (11.9)	12
15880 (35,000)	158 (1700)	1.5 (6.0)	9.3 (12.5)	17
15880 (35,000)	204 (2200)	1.6 (6.3)	9.8 (13.1)	21
18140 (40,000)	0 (0)	1.5 (6.2)	11.0 (14.8)	0
18140 (40,000)	18 (200)	1.6 (6.3)	11.2 (15.0)	2
18140 (40,000)	66 (700)	1.6 (6.6)	11.7 (15.7)	6
18140 (40,000)	112 (1200)	1.7 (6.9)	12.2 (16.4)	10
18140 (40,000)	158 (1700)	1.8 (7.2)	12.8 (17.1)	14
18140 (40,000	204 (2200)	1.9 (7.5)	13.3 (17.9)	17
20410 (45,000)	0 (0)	1.8 (7.4)	14.8 (19.8)	0
20410 (45,000)	18 (200)	1.9 (7.5)	15.0 (20.1)	1
20410 (45,000)	66 (700)	1.9 (7.7)	15.4 (20.6)	4
20410 (45,000)	112 (1200)	2.0 (8.0)	16.0 (21.4)	7
20410 (45,000)	158 (1700)	2.0 (8.2)	16.4 (22.0)	10
20410 (45,000)	204 (2200)	2.1 (8.5)	17.0 (22.8)	13

6.2 Example Simulation of Corn Drying

Following are the data cards suitable for the TRNSYS simulation of the system with a collector area of 66 m^2 (700 ft^2) and a mass flow rate of 20410 kg/hr (45,000 lb/hr) which was discussed in section 4. Figures 5 and 6 are also applicable to this example.

```
Simulation 6.0 360.0 0.2
Tolerances 0.1 0.1
Width 132
Unit 9 Type 9 Card Reader
Parameters 11
13 1.0 6 3.69 0.0 11 1.0 0.0 12 1.0 0.0
Unit 16 Type 16 Solar Radiation Processor
Parameters 7
1 244.0 43.0 35.0 0.0 428.0 0.0
Inputs 1
9,6
0.0
Unit 28 Type 28 Drier Simulation Controls
Parameters 7
0.4 0.145 288.0 0.20 6.0 1.0 85.0
Inputs 4
16,1 21,8 1,1 9,11
0 0.4 34.0 34.0
```

```
Unit 3 Type 3 Blower
Parameters 1
4.5E4
Inputs 3
9,11 21,3 28,2
34.0 4.5E4 1.0
Unit 11 Type 11 Flow diverter
Parameters 1
2
Inputs 3
3,1 3,2 28,3
34.0 4.5E4 1.0
Unit 1 Type 1 Collector
Parameters 7
1 700.0 0.95 0.245 0.94 1.0 0.88
Inputs 4
11,3 11,4 9,11 16,1
34.0 4.5E4 34.0 0.0
Unit 12 Type 11 Tee Piece
Parameters 1
1
Inputs 4
11,1 11,2 1,1 1,2
34.0 0.0 34.0 4.5E4
Unit 6 Type 6 Auxiliary Heater
```

```
Parameters 3
7.72E4 70.0 0.245
Inputs 3
12,1 12,2 28,1
34.0 4.5E4 0
Unit 21 Type 21 Drier
Parameters 22
10.0 18.0 10 0.45 68.78 0.4 0.01 -0.145 0.005 0.01 20 0.95E-5 460.0
1.9 6.0 0.2 40.0 0.34 0.009 485.0 1796.0 4.5E4
Inputs 4
6,1 9,12 6,2 9,11
34.0 33.0 4.5E4 34.0
Unit 24 Type 24 Integrator
Inputs 7
16,1 1,3 6,3 21,4 21,14 21,12 28,2
0.0 0.0 0.0 0.0 0.0 0.0 0.0
Unit 25 Type 25 Printer
Parameters 1
24.0
Inputs 9
24,1 24,2 24,3 24,4 21,15 24,5 24,6 21,13 24,7
TS/FT2 TQCOL TQAUX TINOUT ACCUM TAIREN THUMID DMOIST BLOWER
Unit 26 Type 25 Printer
Parameters 1
6.0
```

```
21,6 21,8 21,11 21,1 21,7 21,9
W(1) WAV W(N) TIN TAV T(N)
END
```

6.3 Three Energy Data Tables

Table 11

HEATING FUEL COSTS (1977 IN MADISON)

FUEL	UNIT COST	HEATING VALUE	COST $/GJ	EFFICIENCY	OPERATING COSTS $/GJ
Oil	44¢/gal	140,000 kJ/gal	3.15	0.55	5.70
Natural Gas	30¢/100 scf	1,000 kJ/scf	3.00	0.55	5.45
LP Gas	41¢/gal	96,000 kJ/gal	4.27	0.65	6.57
Electricity (Residential Average)	4.50¢/kwh	3,600 kJ/kwh	12.50	1.00	12.50
(Off Peak)	1.90¢/kwh	3,600 kJ/kwh	5.28	1.00	5.28

Note: 1kJ = 0.95 BTU
1GJ = 0.95 million BTU

Compiled by:

T. Freeman, U.W. Solar Energy Laboratory

Table 12

mass flow kg/hr	col. area m^2	Reduced Thermal GJ total	oil $	natgas $	LPgas $	electric $	Increased Mechanical GJ Total	Cost $
20410	18	6.43	36.65	35.04	42.25	80.38	1.19	14.88
20410	66	17.15	97.76	93.47	112.68	214.38	2.97	37.13
20410	112	11.64	66.35	63.44	76.47	145.50	2.31	28.88
20410	158	11.64	66.35	63.44	76.47	145.50	1.70	21.25
20410	204	11.64	66.35	63.44	76.47	145.50	1.59	19.88
18140	18	0.96	5.47	5.23	6.31	12.00	2.15	26.88
18140	66	10.31	58.77	56.19	67.74	128.88	2.77	34.63
18140	112	16.0	91.20	87.20	105.12	200.00	3.38	42.25
18140	158	16.0	91.20	87.20	105.12	200.00	3.57	44.63
18140	204	16.0	91.20	87.20	105.12	200.00	3.59	44.88
15880	66	2.99	17.04	16.30	19.64	37.38	2.13	26.63
15880	112	9.27	52.84	50.52	60.90	115.88	2.77	34.63
15880	158	15.19	86.58	82.79	99.80	189.88	3.49	43.63
15880	204	15.19	86.58	82.79	99.80	189.88	4.15	51.88
13610	112	1.82	10.37	9.92	11.96	22.75	1.87	23.38
13610	158	4.36	24.85	23.76	28.65	54.50	2.41	30.13
13610	204	7.78	44.35	42.40	51.11	97.25	3.20	40.00
11340	158	0.94	5.36	5.12	6.18	11.75	2.74	34.25
11340	204	3.57	20.35	19.46	23.45	44.63	3.37	42.13

Reduced Thermal: Shown are the total reductions in annual requirements for auxiliary thermal energy and the total economic value of those reductions in terms of various fuels.

Increased Mechanical: Shown are the total increases in annual requirements (estimated) for electrical energy and the cost thereof for blower operation.

Table 13

mass flow kg/hr	col. area m^2	Reduced Thermal					Increased Mechanical	
		GJ/m^2	oil $\$/m^2$	natgas $\$/m^2$	LPgas $\$/m^2$	electric $\$/m^2$	GJ/m^2	$\$/m^2$
20410	18	0.367	2.03	1.95	2.35	4.46	0.066	0.83
20410	66	0.260	1.48	1.42	1.71	3.25	0.045	0.56
20410	112	0.104	0.59	0.57	0.68	1.30	0.021	0.26
20410	158	0.074	0.42	0.40	0.49	0.93	0.011	0.14
20410	204	0.057	0.32	0.31	0.37	0.71	0.008	0.10
18140	18	0.053	0.30	0.29	0.35	0.66	0.119	1.49
18140	66	0.156	0.89	0.85	1.02	1.95	0.042	0.53
18140	112	0.143	0.82	0.78	0.94	1.79	0.030	0.38
18140	158	0.101	0.58	0.55	0.66	1.26	0.023	0.29
18140	204	0.078	0.44	0.43	0.51	0.98	0.018	0.23
15880	66	0.045	0.26	0.25	0.30	0.56	0.032	0.40
15880	112	0.083	0.47	0.45	0.55	1.04	0.025	0.31
15880	158	0.096	0.55	0.52	0.63	1.20	0.022	0.28
15880	204	0.074	0.42	0.40	0.49	0.93	0.020	0.25
13610	112	0.016	0.09	0.09	0.11	0.20	0.017	0.21
13610	158	0.028	0.16	0.15	0.18	0.35	0.015	0.19
13610	204	0.038	0.22	0.21	0.25	0.48	0.016	0.20
11340	158	0.006	0.03	0.03	0.04	0.08	0.017	0.21
11340	204	0.017	0.10	0.09	0.11	0.21	0.017	0.21

Reduced Thermal: Shown are the reductions in annual requirements for auxiliary thermal energy per unit collector area and the economic value of various fuels (also per unit area) that solar energy would replace in each example

Increased Mechanical: Shown are the increases in annual requirements (estimated) for electrical energy and the cost thereof, both on a per unit collector area basis for blower operation

6.4 Mass and Energy Balances

In the simulations of solar grain drying, a mass balance, an internal energy balance, and an overall system energy balance were calculated routinely. The overall system energy balance for which these closures apply is expressed as:

"solar + auxiliary inputs = accumulation + drier output"

where the drier output calculation was referenced to the inlet air state. This overall balance is previous equation 26 rearranged as follows:

$$\sum (E_{sol} + E_{aux})_t = H_{Bed} - \sum (H_{S(I/O)} \Delta t)_t \qquad (26')$$

The internal drier energy balance is expressed as:

"drier input - drier output = drier accumulation"

i.e., equation 25. The mass balance was previously shown in equation 24. (The energy balances account for the fact that the heat capacities of the grain and humid air and the latent heat of sorption vary over time and internal position as a function of variable moisture contents.) Generally the simulations were run for over 300 hours with a timestep of 0.2 hours, 10 finite difference segments, and the internal convergence criterion set at 0.01. The mass balance always closed to within 0.1 to 0.2% The overall system energy balance generally closed to within 0.3 to 0.7%. The internal energy balance on the drier sometimes showed a lack of closure of 4% or higher. The internal energy balance will likely have less closure (on a percentage basis)

than the overall system balance due in part to the algebra. Although similar quantities of energy do affect both, the denominator used for calculating closure is much smaller for the internal balance than for the overall balance (see equations 25 and 26').

Acceptable closure of the mass and energy balance is obtainable in simulations of solar grain drying utilizing the present model in conjunction with very reasonable values for time-step, number of finite elements, and convergence criterion.

6.5 Computer Listings

6.5.1 DRIER:

```
      SUBROUTINE TYPE21(TIME,XIN,OUT,ZZ,ZZZ,PAR,INFO)
C     DRIER SUBROUTINE (NEW VERSION INCORPORATING BASIC EQNS)
C     NO DERIVATIVES REQUIRING TRNSYS INTEGRATOR
C     DIMENSION FOR 50 NODES MAXIMUM
      DIMENSION H(50),W(50)
      DIMENSION HOLD(50),WOLD(50),TOLD(50)
      DIMENSION XIN(4),OUT(15),T(50),PAR(22),INFO(6)
      COMMON /HANSON/ HSAT
      REAL MDOT, LENGTH
      DATA ICT/0/
      IF(ICT).1.1.2
    1 ICT=1
      TIME0=TIME
    2 IF(TIME0.NE.TIME) GO TO 3
      LENGTH=PAR(1)
      DIAM=PAR(2)
      RM=PAR(3)
      VOID=PAR(4)
      PO=PAR(5)
      WINIT=PAR(6)
      WMIN=PAR(7)
      IFIN=0
      IF(PAR(8).LT.0.) IFIN=1
      WAVE=ABS(PAR(8))
C     SET WAVE NEGATIVE FOR TERMINATING BASED ON W(N) INSTEAD OF WAV
      HINIT=PAR(9)
      CHRMAX=PAR(10)
      ICMAX=PAR(11)
      C=PAR(12)
      B=PAR(13)
      EN=PAR(14)
C     PRINT=HOURS BETWEEN PROFILE PRINTS
C     SET PRINT NEGATIVE FOR NO PRINTING
      PRINT=PAR(15)
      DELTIM=PAR(16)
      TINIT=PAR(17)
```

```
37                CP1=PAR(18)
38                CP2=PAR(19)
39          C       CWS EQUALS CP1 + CP2 * W
40                SORB1=PAR(20)
41                SORB2=PAR(21)
42          C       SORB=SORB1-SORB2*W
43                IF(PAR(22).LE.0.0) GO TO 11
44                REVERS=PAR(22)
45          C       REVERS IS # OF HOURS BETWEEN FLOW REVERSALS
46          C       NO REVERSAL IF PAR(22) VERY LARGE
47          C       PAR(22) OF 0.0  IS A LESS DESIREABLE WAY TO INDICATE NO REVERSAL
48                IREMIX=0
49                FMIX=0.0
50                GO TO 12
51          C       NEGATIVE PAR(22) PROVIDES RECIRC OPTION: TYPE 21 CALCULATES M MI
52          C       A TRNSYS TYPE 11 MIXER MUST BE USED TO CALCULATE T MIX
53           11   IREMIX=1
54                FMIX=ABS(PAR(22))
55                REVERS=1.0E6
56           12   N=RN
57                NM=N-1
58                DO 11311 I=1,N
59                T(I)=TINIT
60                H(I)=HINIT
61                W(I)=WINIT
62                TOLD(I)=TINIT
63                HOLD(I)=HINIT
64          11311 WOLD(I)=WINIT
65                HINOLD=HINIT
66                WINOLD=WINIT
67                WAV=WINIT
68                TEMAV=TINIT
69                CTINIT=(CP1+CP2*WINIT)*(TINIT-32.)
70                CT32=CTINIT
71                DELTAX=LENGTH/RN
72                AREA=3.1416*(DIAM/2.)**2
```

```
      CC=PO*(1.-VOID)*AREA*DELTAX
      IAVIT=0
      IITER=0
      IC=0
      ITERM=0
C       INITIALLY SET TIMPRT SO PROFILE PRINTS FIRST TIME
      TIMPRT=-10000
      TIMREV=TIME
      IREV=1
3     CONTINUE
      IF(INFO(7).NE.0) GO TO 14799
C       NOTE THAT INFO(7)=0 FOR FIRST CALL OF EACH TIMESTEP
C       NOTE THAT INFO(7)=-1 AT TIME0
      RCHECK=TIME-TIMREV+0.0001
      IF(RCHECK.GE.REVERS) GO TO 5
      GO TO 4
5     TIMREV=TIME
      IREV=IREV*(-1)
      NN=N-1
      DO 1478 I=1,NN
      J=N-I
      TOLD(I)=T(J)
      HOLD(I)=H(J)
1478  WOLD(I)=W(J)
      TOLD(N)=TIN
      HOLD(N)=HIN
      WOLD(N)=WIN
      HINOLD=H(N)
      WINOLD=W(N)
      GO TO 14799
4     DO 11478 I=1,N
      TOLD(I)=T(I)
      HOLD(I)=H(I)
11478 WOLD(I)=W(I)
      HINOLD=HIN
      WINOLD=WIN
```

```
14799 CONTINUE
C       SKIP CALCULATION FOR UNCHANGED INPUTS AT SUBSEQUENT CALLS
      TINCHK=ABS(2.0*(TIN-XIN(1))/(TIN+XIN(1)))
      TWBCHK=ABS(2.0*(TWB-XIN(2))/(TWB+XIN(2)))
      FLWCHK=ABS(2.*(MDOT-XIN(3))/(MDOT+XIN(3)))
      IF((INFO(7).GT.0).AND.(TINCHK.LE.CHKMAX).AND.(TWBCHK.LE.CHKMAX).AN
     CD.(FLWCHK.LE.CHKMAX)) GO TO 999
      TIN=XIN(1)
      TWB=XIN(2)
      MDOT=XIN(3)
C       TAM IS AMBIENT T INTO SOLAR DRYING SYSTEM
      TAM=XIN(4)
      TCWB=(TWB-32.)/1.8
      PSATWB=10.**(8.10765-(1750.29/(235.+TCWB)))
      HSATWB=0.622*PSATWB/(760.-PSATWB)
      VAPWB=1094.5-0.581*TWB
      HIN=HSATWB-0.227*(TAM-TWB)/VAPWB
      IF(IREMIX.EQ.1) HIN=(1.-FMIX)*HIN+FMIX*HOLD(N)
      IF(MDOT.LE.0.0001) GO TO 791
C       THIS RESULTS IN NO CHANGE SINCE IT IS ASSUMED THAT MDOT OF 0.0
C       DURATION WILL BE VERY SMALL AS MDOT=0.0 IS UNDESIREABLE
      WIN=WG1(TIN,HIN,C,B,EN)
      C1=CC/(MDOT*DELTIM)
      C2=MDOT/CC
C       PROJECTION OF T,H,W
      IF(TIME.EQ.TIME0) GO TO 791
      CT32=0.0
      TEMAV=0.0
      WAV=0.0
      DO 78 I=1,N
      IFLAG=0
      ICOUNT=0
      RLOW=0.0
      RHIGH=100.0
C       PROJECT H AND W FROM PREVIOUS TIMESTEP
      IF(I.NE.1) GO TO 70
```

```
145         H(1)=HIN+(HOLD(1)-HINOLD)
146         W(1)=WIN+WOLD(1)-WINOLD
147         GO TO 711
148      70 H(I)=H(I-1)+(HOLD(I)-HOLD(I-1))
149         W(I)=W(I-1)+WOLD(I)-WOLD(I-1)
150   C        BEGIN INTERNAL ITERATIVE LOOP*********
151   C     PROJECT W FROM EQUILIB EQN
152   C     W01 IS AN INTERNAL FUNCTION TO CALCULATE W (MOISTURE)
153   C        W01 FUNCTION ALSO CALCULATES HSAT (COMMUNICATED VIA COMMON)
154     711 IF(H(I).GE.HSAT) H(I)=HSAT
155   C        AT THIS POINT IN PROGRAM, HSAT IS SAT HUMIDITY FOR (I-1)
156         IF(H(I).LE.0.0001) H(I)=0.0001
157   C        HEAT CAP OF WET SOLID IS CWS
158         CWSOLD=CP1+CP2*WOLD(I)
159      71 CWS=CP1+CP2*W(I)
160         CWS1=2./(CWS+CWSOLD)/DELTIM
161         CWS2=32.*(CWS-CWSOLD)/DELTIM
162         Z1=DELTIM*CWS1*C2
163         Z2=DELTIM*CWS1*CWS2
164         SORB=SORB1-(SORB2*(W(I)+WOLD(I))/2.)
165         IF (SORB.LE.0.) SORB=0.
166   C        SORB IS DIFF BETWEEN LATENT HEAT OF VAP FOR FREE & BOUND WATER
167         IF(I.NE.1) GO TO 77
168         DTW=TIN*(.244+.45*HIN)+(1061.+.45ORB)*(HIN-H(1))
169         GO TO 781
170      77 DTW=T(I-1)*(.244+.45*H(I-1))+(1061.+.45ORB)*(H(I-1)-H(I))
171     781 DENOM=1.+Z1*(.244+.45*H(I))
172         T(I)=(TOLD(I)+Z2+Z1*DTW)/DENOM
173   C        IFLAG WILL BE SET TO 1 WHEN ITERATION IS OVER SO THAT
174   C        CONTROL IS REDIRECTED THROUGH THE TEMP CALC FOR FINAL
175   C        UPDATE OF CWS & T. IFLAG THEN SKIPS CONTROL TO CT32 CALC
176         IF(IFLAG.EQ.1) GO TO 72
177         W(I)=W01(T(I),H(I),C,B,END)
178   C        TRY TO CORRECT H TO HC USING MASS BALANCE
179         IF(I.NE.1) GO TO 72
180         HC=HINTIA*WOLD(1)-W(1)
```

```
181             GO TO 73
182       72    HC=H(I-1)+C1*(WOLD(I)-W(I))
183       73    IF(HC.GE.HSAT) HC=HSAT
184       C       AT THIS POINT IN PROGRAM, HSAT IS SAT HUMIDITY AT T(I)
185             IF(HC.LE.0.0001) HC=0.0001
186       C       ABOVE STATEMENT PREVENTS NEGATIVE HUMIDITIES
187             CHECK=ABS(2.*(HC-H(I))/(HC+H(I)))
188             IF(HC-H(I)) 101,76,102
189       101   IF(H(I).LE.RHIGH) RHIGH=H(I)
190             IF(HC.GE.RLOW) RLOW=HC
191             GO TO 103
192       102   IF(H(I).GE.RLOW) RLOW=H(I)
193             IF(HC.LE.RHIGH) RHIGH=HC
194       103   RCHECK=(RHIGH-RLOW)/H(I)
195             H(I)=0.5*(RLOW+RHIGH)
196       C       NEW PROJECTION FOR W(I) FROM MASS BALANCE
197             IF(I.NE.1) GO TO 401
198             W(1)=WOLD(1)+(HIN-H(1))/C1
199             GO TO 402
200       401   W(I)=WOLD(I)+(H(I-1)-H(I))/C1
201       402   IF((CHECK.LE.CHKMAX).OR.(RCHECK.LE.CHKMAX)) IFLAG=1
202       C     SETTING IFLAG=1 ALLOWS FOR FINAL UPDATE OF T & CWS AFTER
203       C       CONVERGENCE IS OBTAINED. AFTER UPDATE, CONTROL WILL BE
204       C       SENT TO STATE # 76
205             ICOUNT=ICOUNT+1
206             IF(ICOUNT.GE.ICMAX) GO TO 74
207             GO TO 71
208       C       END INTERNAL ITERATIVE LOOP **********
209       74    WRITE(-,-) TIME,I,H(I),HC,HSAT,RLOW,RHIGH,ICOUNT
210       C       CT32 WILL EVENTUALLY REPRESENT BED AVERAGE OF CWS*(T-32)
211       76    CT32=CT32+CWS*(T(I)-32.)
212       C       TEMAV WILL EVENTUALLY REPRESENT BED AVERAGE TEMPERATURE
213             TEMAV=TEMAV+T(I)
214       C       WAV WILL EVENTUALLY REPRESENT BED AVERAGE MOISTURE
215             WAV=WAV+W(I)
216             IF(I.NE.1) GO TO 61
```

```
217                SORTOT=SORB4(HIN-H(I))
218                GO TO 62
219             61 SORTOT=SORTOT+SORB4*(H(I-1)-H(I))
220             62 CONTINUE
221                IC=IC+ICOUNT
222                ITER=ITER+1
223             78 CONTINUE
224              C    CHECK FOR SAFE MOISTURE MINIMUM AT TOP OF DRIER (NODE # 1)
225                IF(W(1).LE.WMIN) WRITE(6,22) W(1),WMIN,TIME
226             22 FORMAT(1X,F10.3,17HIS DRIER THAN MIN,F10.3,8HAT TIME=,F10.3)
227              C    CALCULATE  AVERAGE MOISTURE AND TEMPERATURE
228                TEMAV=TEMAV/RN
229                WAV=WAV/RN
230                CT32=CT32/RN
231              C    PROFILE PRINTERS
232            791 IF((INFO(7).GT.0).OR.(PRINT.LT.0.))GO TO 202
233                PCHECK=TIME-TIMPRT+0.0001
234                IF(PCHECK.GE.PRINT)GO TO 307
235                GO TO 202
236            307 TIMPRT=TIME
237                IF(TIME.NE.TIMEO) IAVIT=IC/ITER
238                WRITE(6,40) TIME                TIME=,F10.3,4X,8H********)
239             40 FORMAT(1X,///,23X,17H********
240                WRITE(6,45) IAVIT
241             45 FORMAT(23X,36HAVE # ITERATION/N/STEP SINCE TIMEO=,14)
242                IF(IREV.EQ.-1) GO TO 14
243                WRITE(6,41) TIN, (T(I),I=1,N)
244             41 FORMAT(1X,11HTEMPERATURE/1X,F10.3,/(1X,10F10.1))
245                WRITE(6,42) HIN, (H(I),I=1,N)
246             42 FORMAT(1X,8HHUMIDITY/1X,F10.4,/(1X,10F10.4))
247                WRITE(6,43) WIN,(W(I),I=1,N)
248             43 FORMAT(1X,14HSOLID MOISTURE/1X,F10.3/(1X,10F10.3))
249                GO TO 1021
250             14 WRITE(6,46)
251             46 FORMAT(1X,35HREVERSE FLOW OCCURRING AT THIS TIME)
252                WRITE(6,41) (T(I),I=N,1,-1), TIN
```

```
253              WRITE(6,42) (H(I),I=N,1,-1), HIN
254              WRITE(6,43) (W(I),I=N,1,-1), WIN
255        1021  WRITE(6,44) ,TEMAV,,WAV
256        44    FORMAT(1X,10HAVERAGE T=,F10.3/1X,11HAVERAGE W= ,F10.4)
257        202   IF((IFIN.EQ.0).AND.(WAV.LE.(1.003*WAVE)).AND.(ITERM.LE.3))GO TO 35
258              IF((IFIN.EQ.1).AND.(WAV.LE.(1.003*WAVE)).AND.(ITERM.LE.3).AND.(W(N
259             C).LE.1.003*WAVE)) GO TO 35
260              GO TO 200
261        35    ITERM=ITERM+1
262              WRITE(6,222)
263        222   FORMAT(1X,52H**********************************************************)
264              WRITE(6,201)TIME,WAV
265        201   FORMAT(1X,5HTIME=,F10.3,28HDRIER TEMNINATION*AVERAGE W=,F10.4)
266              IF(IFIN.EQ.1) WRITE(6,2011)TIME,W(N)
267        2011  FORMAT(1X,5HTIME=,F10.3,23HDRIER TERMINATION*W(N)=,F10.4)
268        200   CONTINUE
269        C       ENTHALPY AND MASS BALANCE TERMS
270              DHUMID=MDOT*(H(N)-HIN)
271              DMOIST=(CC*RN)*(WINIT-WAV)
272              DBEDEN=(CC*RN)*(CT32-CTINIT)
273              DAIREN=MDOT*(.24*(TIN-T(N))+.45*(HIN*TIN-H(N)*T(N))+1061.4*(HIN-
274             CH(N))+SORTOT)
275        C       SUM OF (DHUMID*DELTIM) SHOULD = DMOIST
276        C       SUM OF (DAIREN*DELTIM) SHOULD = DBEDEN
277        C       DAIREN IS IN-OUT-LATENT FOR DRIER SUBUNIT
278        C       SINOUT IS IN-OUT-LATENT FOR ENTIRE SOLAR SIMULATION
279              SINOUT=MDOT*(.24*(TAM-T(N))+.45*(HIN*TAM-H(N)*T(N))+1061.4*(HIN-
280             CH(N))+SORTOT)
281        999   OUT(1)=XIN(1)
282              OUT(2)=XIN(2)
283              OUT(3)=XIN(3)
284              OUT(4)=SINOUT
285              OUT(5)=T(1)
286              OUT(6)=W(1)
287              OUT(7)=TEMAV
288              OUT(8)=WAV
```

```
289             OUT(9)=T(N)
290             OUT(10)=H(N)
291             OUT(11)=W(N)
292             OUT(12)=DHUMID
293             OUT(13)=DMOIST
294             OUT(14)=DAIREN
295             OUT(15)=DBEDEN
296             RETURN
297             END
```

The above listed subroutine, "Drier," calls external REAL FUNCTION WG1 frequently during its execution. Therefore REAL FUNCTION WG1, which is listed in section 6.5.3 of this appendix,must be included in any TRNSYS compilation that is to include the Drier subroutine.

6.5.2 CONTROLS:

```
      SUBROUTINE TYPE28(TIME,XIN,OUT,T,DTDT,PAR,INFO)
C      CONTROLLER FOR GRAIN DRIER
      DIMENSION XIN(4),OUT(3),PAR(7),INFO(8)
      DATA ICT/0/
      IF(ICT) 1,1,2
    1 ICT=1
      TIMEO=TIME
    2 IF(TIMEO+NE+TIME) GO TO 3
C      INITIAL MOISTURE CONTENT
      WINIT=PAR(1)
C      DESIRED FINAL MOISTURE CONTENT
      WAVE=PAR(2)
C      MAX HOURS DESIRED (TO PREVENT SPOIL)
      HRMAX=PAR(3)
C      ALLOWABLE LAG BEHIND SCHEDULE (DECIMAL FRACTION)
      SOLLAG=PAR(4)
C      W IS DETERMINED EVERY FREQ NUMBER OF HOURS T
      FREQ=PAR(5)
C      MINIMUM BLOWER SPEED DECIMAL FRACTION OF ROOT MAX
      FRACM=PAR(6)
C      MAX DESIRED TEMP INPUT TO GRAIN
      TMAX=PAR(7)
      WCHECK=TIMEO
      TAUX=0
      DAMPER=1.0
      DAMP=1.0
    3 CONTINUE
C      HSOL=SOLAR RABIATION ON COLLECTOR
      HSOL=XIN(1)
C      CURRENT AVERAGE MOISTURE
      WAV=XIN(2)
C      COLLECTOR OUTPUT TEMP
      TCOL=XIN(3)
C      AMBIENT TEMP
      TAMB=XIN(4)
      IF((TIME-WCHECK+0.0001),LT,FREQ) GO TO 11
```

```
      WCHECK=TIME
      IAUX=0
      PROGRS=(WINIT-WAV)/(WINIT-WAVE)
      TIMING=(TIME-TIME0)/HRMAX
      IF((PROGRS*(1.+SOLLAG)).LT.TIMING) IAUX=1
11    CONTINUE
C      IAUX OF 1 SAYS AUX MUST AUGMENT SOLAR IF NECESSARY TO MEET TSET
C      IAUX OF 0 SAYS AUX OFF UNDER ALL CONDITIONS
C      HSOL >0.0 INDICATES COLLECTOR HAS A SOLAR GAIN (I.E.SUN SHINING)
C      OUTCON PROVIDES 1.0 OR FRACM AS CONTROL FOR BLOWER SPEED
C      OUTCON MUST BE 1.0 IF EITHER IAUX=1 OR HSOL > 0.0
C      OTHERWISE OUTCON=FRACM INDICATING NO SOLAR GAIN & AUX UNNEEDED
      IF((IAUX.EQ.1).OR.(HSOL.GT.0.0)) GO TO 13
      OUTCON=FRACM
      GO TO 14
13    OUTCON=1.0
C      CONTROL FOR PARTIAL COLLECTOR BYPASS (PREVENT GRAIN OVERDRY)
C      GIVE DAMPER LAGTIME OF 1 TIMESTEP BY USING LAST STEP'S VALUE
14    IF(INFO(7).LE.0) DAMPER=DAMP
C      DAMP SET TO FRACTION OF FLOW ALLOWED INTO COLLECTOR
      DAMP=(TMAX-TAMB)/(TCOL+1.0-TAMB)
      IF(DAMP.GE.1.0) DAMP=1.0
C      CONTROL FOR AUX HEATER
      OUT(1)=IAUX
C      CONTROL FOR BLOWER
      OUT(2)=OUTCON
C      CONTROL FOR BYPASS
      OUT(3)=DAMPER
      RETURN
      END
```

The controller subroutine listed above is very useful for TRNSYS simulations which employ subroutine, "Drier," for solar grain drying experiments. "Drier" can function without the controller subroutine.

6.5.3 MOISTURE FUNCTION:

```
      REAL FUNCTION WG1(TF,H,C,B,EN)
C       CALCULATE SOLID EQUILIBRIUM MOISTURE CONTENT
        COMMON /HANSON/ HSAT
        TC=(TF-32.)/1.8
        IF(TC.LE.60.)GO TO 17
C         SATURATION PRESSURE IN MM HG
        PSAT=10.**(7.96681-(1668.2/(228.+TC)))
        GO TO 18
17      PSAT=10.**(8.10765-(1750.29/(235.+TC)))
18      PVAP=H*760./(0.622+H)
C         RELATIVE HUMIDITY=PVAP/PSAT
        RH=PVAP/PSAT
C         ASSUME RH ALWAYS < OR = .99 BECAUSE OF ALOG CALCULATION
        IF(RH.GE.0.99)RH=0.99
        HSAT=0.622*PSAT/(760.-PSAT)
        IF(EN.LE.0.0) GO TO 19
        WG1=((-(ALOG(1.-RH))/(C*(TF+B)))**(1./EN))/100.
        RETURN
19      WG1=(0.25*RH)+0.0774
        RETURN
        END
```

This function, although external to subroutine, "Drier," is an integral part of the computer model.

7.
REFERENCES

In the following compilation some abreviations have been employed:
TRANS ASAE - Transactions of the American Society of Agricultural Engineers
J.Ag.Eng.Res. - Journal of Agricultural Engineering Research
ISES - International Solar Energy Society

Akyurt, M., and Selcuk, M.K., "A Solar Drier Supplemented with Auxiliary Heating Systems for Continuous Operation," Solar Energy, 14(3), 1973, 313-320.

Bakker-Arkema, F.W., Bickert, W.G., and Patterson, R.J., "Simultaneous Heat and Mass Transfer during the Cooling of a Deep Bed of Biological Products under Varying Inlet Air Conditions," J.Ag.Eng.Res., 12(4), 1967, 297-307.

Bakker-Arkema, F.W., Evans, T.W., and Farmer, D.M., "Simulation of Multiple Zone Grain Drying," Trans ASAE, 14(5), September-October 1971, 935-938.

Banks, P.J., "Combined Heat and Moisture Transfer in Air Flow through Porous Beds - Prediction by Analogy with Heat Transfer," a paper reprinted from I.I.R. Commission II,IV,V, and VII (Leningrad) Meeting, Vol 1, 1970, 39-45.

Banks, P.J., "Coupled Equilibrium Heat and Single Adsorbate Transfer in Fluid Flow through a Porous Medium - I: Characteristic Potentials and Specific Capacity Ratios," Chemical Engineering Science 27(5), May 1972, 1143-1155.

Barre, H.J., Baughman, G.R., and Hamdy, M.Y., "Application of the Logarithmic Model to Cross-Flow Deep-Bed Grain Drying," Trans ASAE, 14(6), November-December 1971, 1061-1064.

Baughman, G.R., Hamdy, M.Y., and Barre, H.J., "Analog Computer Simulation of Deep-Bed Drying of Grain," Trans ASAE, 14(6), November-December 1971, 1058-1060.

Beckman, W.A., Klein, S.A., and Duffie, J.A., Solar Heating Design by the f-chart method, New York: John Wiley and Sons, 1977.

Bloome, P.D., and Shove, G.C., "Near Equilibrium Simulation of Shelled Corn Drying," Trans ASAE, 14(4), April 1971, 709-712.

Boyce, D.S., "Grain Moisture Changes with Position and Time during Through-Drying." J.Ag.Eng.Res., 10(4), 1965, 334-341.

Brooker, D.B., Bakker-Arkema, F.W., and Hall, C.W., Drying Cereal Grains, AVI Publishing, Connecticut, 1974.

Browning, C.W., Brooker, D.B., George, R.M., and Browning, C.E., "Batch-in-bin Drying by Alternating Heated and Unheated Air," Trans ASAE, 14(1), January-February 1971, 193-194.

Clark, R.G., and Lamond, W.J., "Drying Wheat in Two Foot Beds; I: Rate of Drying," J.Ag.Eng.Res., 13(2), 1968, 141-148.

Clark, R.G., and Lamond, W.J., "Drying Wheat in Two Foot Beds; II: Exhaust Air Humidity," J.Ag.Eng.Res., 13(4), 1968, 323-331.

Close, D.J., personal communication, November 1975.

Close, D.J., personal communication, December 1975.

Close, D.J., and Banks, P.J., "Coupled Heat and Mass Transfer in Fluid Flow through a Porous Medium - II: Predictions for a Silica-Gel Air-Drier Using Characteristic Charts," Chemical Engineering Science 27(5), May 1972, 1157 +.

Close, D.J., and Pryor, T.L., "The Behavior of Adsorbent Energy Storage Beds," Unpublished paper.

Duffie, J.A., and Beckman, W.A., Solar Energy Thermal Processes, New York: John Wiley and Sons, 1974.

Dunstan, E.R., Chung, D.S., and Hodges, T.O., "Adsorption and Desorption Characteristics of Grain Sorghum," Trans. ASAE, 16(4), July-August 1973, 667-670.

Foster, G.H., and Peart, R.M., Solar Grain Drying-Progress and Potential, bulletin issued by the Agricultural Research Service in cooperation with the Cooperative State Research Service and the State Agricultural Experiment Stations of the USDA (supported by ERDA), November 1976, Supt of Documents, U.S. Gov't Printing Office, Washington, D.C.

Freeman, T.L., "Heating Fuel Costs (1977 in Madison)," U.W. Solar Energy Laboratory, 1977.

Hammond, A.L., "Unconventional Energy Sources: Brazil Looks for Applications," Science, vol. 195, March 4, 1977, 862.

Gough, M.C., "Remote Measurement of Moisture Content in Bulk Grain using an Air Extraction Technique," J.Ag.Eng.Res., 21(2), June 1976, 217-219.

Guinn, G.R., "Soybean Drying using Heat from Solar Energy," Proceedings of the 1977 Annual Meeting of the ISES, Volume 1, Section 32, Session K.2.

Hamdy, M.Y., and Barre, H.J., "Analysis and Hybrid Simulation of Deep-Bed Drying of Grain," Trans ASAE, 13(6), November-December 1970, 752-757.

Henderson, J.M., and Henderson, S.M., "A Computational Procedure for Deep-Bed Drying Analysis," J.Ag.Eng.Res., 13(2), 1968, 87-95.

Henderson, S.M., "A Basic Concept of Equilibrium Moisture," Agricultural Engineering, 33(1), January 1952, 29-32.

Hughes, P.J., Klein, S.A., and Close, D.J., "Packed Bed Thermal Storage Models for Solar Heating and Cooling Systems," paper to be submitted to Solar Energy Journal (1975).

Hukill, W.V., "Basic Principles in Drying Corn and Grain Sorghum," Agricultural Engineering, 28(8), August 1947, 335-338, 340.

Klein, S.A., "A Design Procedure for Solar Heating Systems," Ph.D. Thesis, University of Wisconsin - Madison, 1976.

Klein, S.A., et al., "A Method of Simulation of Solar Processes and its Application," Solar Energy, 17(1), 1974, 29-37.

Mitchell, J.W., Personal Communication, 1976.

Myklestad, O., "An Analysis of Transient Flow of Heat and Moisture During Drying of Granular Beds," Int. J. of Heat and Mass Transfer, 1968, 11(4) 675 +.

Nelson, J.S., "An Investigation of Solar Powered Open Cycle Air Conditioners," unpublished M.S. Thesis from the University of Wisconsin Solar Energy Laboratory, 1976.

O'Callaghan, J.R., Menzies, D.J., and Baily, P.H., "Digital Simulation of Agricultural Drier Performance," J.Ag.Eng.Res., 16(3), 1971, 223-244.

Osborn, D.E., Meinel, A.B., and Beauchamp, W.T., "A Solar Collector Modeling Technique for Grain Drying Applications," Proceedings of a joint conference of the American Section of the ISES and the Solar Energy Society of Canada, August 15-20, 1976, Winnipeg, Manitoba.

Paulsen, M.R., and Thompson, T.L., "Drying Analysis of Grain Sorghum," Trans ASAE, 16, 1973, 537-540.

Peart, R.M., and Barret, J.R., "Solar Grain Drying," AED-122, Agricultural Engineering Dept, Purdue University, Indiana, 1975.

Peart, R.M., and Foster, G.H., a Grain Drying with Solar Energy," paper presented at the 1975 ISES International Solar Energy Congress and Exposition, July 28-August 1, 1975, UCLA, L.A., California.

Peterson, W.H., "Drying Corn in South Dakota," Solar Age, 2(2), February 1977.

Peterson, W.H. and Hellickson, M.A., "Solar-Electric Drying of Corn in South Dakota," Trans ASAE, 19(2), February 1976, 349-353.

Roa, G. and Macedo, I.C., "Grain Drying in Stationary Bins with Solar Heated Air," Solar Energy, Volume 18, 1976, 445-449.

Roberts, D.E., and Brooker, D.B., "Grain Drying with a Recirculator, Trans ASAE, 18(1), January-February 1975, 181-184.

Saulnier, B., "Survey of Solar Agricultural Dryers," proceedings of a joint conference of the American Section of the ISES and the Solar Energy Society of Canada, August 15-20, 1976, Winnipeg, Manitoba.

Schlag, J.H., Ray, D.C., Sheppard, A.P., and Wood, J.M., "Improved Inexpensive Solar Collectors for Agricultural Requirements," proceedings of a joint conference of the American Section of the ISES and the Solar Energy Society of Canada, August 15-20, 1976, Winnipeg, Manitoba.

Schoenau, G.J., and Besant, R.W., "The Potential of Solar Energy for Grain Drying in Western Canada," proceedings of a joint conference of the American Section of the ISES and the Solar Energy Society of Canada, August 15-20, 1976, Winnipeg, Manitoba.

Schumann, T.E.W., "Heat Transfer: A Liquid Flowing through a Porous Prism," J. Franklin Inst., 208, 1929, 305-314.

Selcuk, M.K., Ersay, O., and Akyurt, M., "Development, Theoretical Analysis, and Performance Evaluation of Shelf Type Solar Driers," Solar Energy, 16(2), 1974, 81-88.

Shove, G.C., "Simultaneous Multilayer Grain Drying," Trans ASAE, 14(1), January-February 1971, 134-137.

Solar Energy Laboratory of the University of Wisconsin, "TRNSYS - A Transient Simulation Program," Engineering Experiment Station Report #38, Updated: October, 1977.

Spencer, H.B., "A Mathematical Simulation of Grain Drying," J.Ag.Eng.Res., 14(3), 1969, 226-235.

Spencer, H.B., "A Revised Model of the Wheat Drying Process," J.Ag.Eng.Res., 17(2), 1972, 189-194.

Sutherland, J.W., "Batch Grain Drier Design and Performance Prediction," J.Ag.Eng.Res., 20(4), December 1975, 423-432.

Sutherland, J.W., Banks, P.J., and Griffiths, "Equilibrium Heat and Mass Transfer in Air Flowing through Grain," J.Ag.Eng.Res., 16(4), December 1971, 368 +.

Thompson, T.L., "Temporary Storage of High Moisture Shelled Corn using Continuous Aeration," Trans ASAE, 15(2), February 1972, 333-337.

Thompson, T.L., Peart, R.M., and Foster, G.H., "Mathematical Simulation of Corn Drying - A New Model," Trans ASAE, 11(4), July-August 1968, 582-586.

Van Arsdel, W.B., "Simultaneous Heat and Mass Transfer in a Nonisothermal System: (Through-flow Drying in the Low Moisture Range)," CEP Symposium Series, 51(16), 1955, 47-58.

White, G.M., Ross, I.J., and Klaiber, J.D., "Moisture Equilibrium in Mixing of Shelled Corn," Trans. ASAE, 15(3), May-June 1972, 508-509, 514.

Woodforde, J., and Lawton, P.J., "Drying of Cereal Grain in Beds Six Inches Deep," J.Ag.Eng.Res., 10(2), 1965, 146-171.

Woodforde, J., and Osborne, L.E., "The Drying of Wheat in Beds One and Two Feet Deep," J.Ag.Eng.Res., 6(4), 1961, 300-314.

Young, J.H., and Dickens, J.W., "Evaluation of Costs for Drying Grain in Batch or Cross-flow Systems," Trans. ASAE, July-August 1975, 18(4), 734-739.